1918
TALLINNA TEHNIKAÜLIKOOL
EHITUSTEADUSKOND
Ehitiste projekteerimise instituut

PUITKONSTRUKTSIOONIDE TULETÕKESTUSVÕIME ARVUTUSMEETODI TÄIENDAMINE UUTE MATERJALIDEGA

IMPLEMENTATION OF NEW MATERIALS TO THE COMPONENT ADDITIVE METHOD FOR FIRE DESIGN OF TIMBER STRUCTURES

EEK 60LT

Üliõpilane: Katrin Nele Mäger

(allkiri)

Juhendaja: Dots. Alar Just

(allkiri)

Daniel Brandon

(allkiri)

Tallinn, 2016.a.

Olen koostanud lõputöö iseseisvalt.
Kõik töö koostamisel kasutatud teiste autorite
tööd, olulised seisukohad, kirjandusallikatest ja mujalt
pärinevad andmed on viidatud.

…………………………………………….. (töö autori allkiri ja kuupäev)

Üliõpilase kood: 105203

Töö vastab magistritööle esitatud nõuetele

……………………………………………… (juhendaja allkiri ja kuupäev)

Kaitsmisele lubatud …………………………….. (kuupäev)

Kaitsmiskomisjoni esimees …………………………….. (allkiri)

LÕPUTÖÖ ÜLESANNE

Üliõpilase kood	**105203EAEI**
Ehitustehnika õppesuuna üliõpilasele	**KATRIN NELE MÄGER**
Lõputöö kood:	**EEK 60LT**
Lõputöö juhendaja:	**ALAR JUST**
Lõputöö kaasjuhendaja:	**DANIEL BRANDON (SP)**
Lõputöö teema:	

IMPLEMENTATION OF NEW MATERIALS TO THE COMPONENT ADDITIVE METHOD FOR FIRE DESIGN OF TIMBER STRUCTURES

Puitkonstruktsioonide tuletõkestusvõime arvutusmeetodi täiendamine uute materjalidega

Lõputöö teema kehtivusaeg: **31.12.2016**

Lõputöö ülesanne:

Töötada välja metoodika uute materjalide lisamiseks ning selle alusel leida valemid Gyproc'i kipsplaatide Protect F ja Habito kaitsevõime arvutamiseks tulevase EN 1995-1-2 tuletõkestusvõime arvutusmeetodi jaoks.

Lõputöö sisu:

Euroopa tehnilises juhendis *Fire Safety in Timber Buildings* (peatükk 5) on esitatud uus arvutusmeetod konstruktsioonide tuletõkestusvõime leidmiseks, mis saab olema osaks tulevases projekteerimisstandardis EN 1995-1-2.
Lõputöö eesmärgiks on

1) välja töötada soovitused nimetatud arvutusmeetodisse lisatavate uute materjalide termiliste omaduste määramiseks.
2) leida nimetatud meetodi jaoks arvutusvalemid Gyproc kipsplaatide Protect F ja Habito.
3) rakendada välja töötatud protseduuri tselluvillast isolatsioonimaterjali termiliste omaduste kalibreerimisel.

Töös leida materjalide termilised omadused tulekatsete abil. Seejärel kalibreerida lähteandmed termilisteks simulatsioonideks. Simulatsioonid teostada programmiga SAFIR.

Töö kirjutada inglise keeles.

Resümee eesti keeles

Lõputöö konsultandid:

Töö osa nimetus	Konsultandi nimi	Konsultandi allkiri	Kuupäev

Lõputöö väljaandmise kuupäev: **20.09.2015**

Juhendaja: **Alar Just** ………………………..

Ülesande vastu võtnud: **Katrin Nele Mäger** ………………………..

Contents

1. Introduction

Wood is probably the most used building material throughout human history. It is still widely used today and has been gaining popularity again in more recent years. The biggest challenge surrounding timber buildings is how to make them more fire resistant. Nowadays there are many options – impregnation, protective claddings, sprinklers or other means of active fire protection. Probably the most common is to cover the timber member with non-combustible claddings.

For the engineers and officials, it is important to be able to show through accepted calculations that a structure will be safe in fire with acceptable probability. Therefore, calculation methods and suitable formulas are needed. This thesis focuses on the improved component additive method for calculation of fire resistance of timber structures.

New materials are developed constantly. The process of introducing a new material can be very long, especially due to the need for repeated testing and proving the properties. In order to determine the behaviour of a particular material in the fire scenario, numerous model- or full-scale tests are usually conducted. The need for abundant tests might be lessened with the development of computer technologies that can predict heat transfer quite accurately. Some testing is still going to be necessary in order to verify the computer models' accuracy. A few materials possibly used in timber frame assemblies are investigated from the fire safety point of view and simulated using the finite element method.

The improved component additive method provides general design equations for material groups. It is in the interest of producers and engineers alike to add product specific equations to the method. At the moment the method is very safe e.g. provides much shorter fire resistance times than seen in fire tests of the same structures. On the one hand, this is necessary to ensure the safety of life in most cases, but it can also be wasteful when members are dimensioned according to fire requirements.

In this thesis product specific thermal properties and design equations will be proposed and the methods used for development of these values are discussed. The first step is to conduct suitable model scale tests. The results of the fire tests then become the basis of simulations. The goal is for the results of the simulations to exactly mimic the results of the fire tests. Finally, specific simulations are conducted for the development of the equations.

This work is broadly divided into four main parts. Firstly, some background information is given about the current fire safety design of timber structures. Then, the model scale test procedure is described and the results presented to form a basis for the next part. Thirdly, the calibration of thermal properties and a short overview of the underlying theory is summarised. The last part deals with the development of product specific design equations that are developed with the input curves obtained from calibration. The design equations are compared to full scale test results as verification.

The main aim of this thesis is the addition of new materials to the improved component additive method. The new materials added are two specific gypsum plasterboard products made by Saint-Gobain Gyproc. The calibration procedure is tested on cellulose fibre insulation. This group of products was chosen as little is known about its behaviour in fire and also because of their fundamental difference from gypsum boards.

Acknowledgements

I would like to extend my most heartfelt gratitude to my supervisor Alar Just, who opened so many doors in front of me that I did not realise even existed. His unlimited support and encouragement is what made this thesis possible. It has been a pleasure working as a team.

Without my co-supervisor Daniel Brandon and his brilliant ideas, this work would have been much more tedious. I would like to thank him for all the kind words and the fruitful discussions we had which pushed me forward in great leaps every time. I am also very grateful for the courage to try the new and unfamiliar routes he has given me.

An exceptional opportunity for which I am deeply grateful was working with SP Technical Research Institute of Sweden in Stockholm. To the fire research group I owe so much knowledge gained during my stays there. I would especially like to thank Mattia Tiso for showing me the fun in research, Magdalena Sterley for giving me a glimpse of Swedish life and teaching me to be passionate about my work, and of course Birgit Östman who taught me that perseverance and connections will pay off in a grand way. I will forever cherish the support from everyone in SP.

It was an amazing experience to attend the Joint Conference of COST Actions FP1402 and FP1404 and to meet all the great people who took part in it. Many thanks for all the stimulating conversations and interesting presentations.

Last but not least, I would like to thank my nearest and dearest family and friends for all of the support and for keeping me 100% focused on completing this work.

2. Fire design of timber structures

Wood is a natural, combustible material that has a long history of being used as a construction material. That is due to its high strength-to-weight ratio and workability. During the last couple of decades, timber structures have been going through a renaissance in their popularity. The biggest factor in people's minds that is stopping the wider spread of timber as the main construction material is that it is perceived to be less safe in fire than, for example, concrete. This belief is starting to change, albeit slowly.

Fire safety regulations of timber structures are a national matter and thus, requirements vary greatly between countries. A study [1] showed and predicted an even further loosening of regulations regarding maximum allowed amount of storeys of timber buildings. The European standard EN 1995-1-2 [2] provides rules for the design of timber structures in fire. This standard also allows for fire design to be based on fire tests (may be in combination with calculations).

The graph below (see Figure 2.1) shows the main stages in the development of a typical fire. This is a generalised view of real fires, as there can be more flashover phases due to reignition caused by hot gasses and glowing of materials.

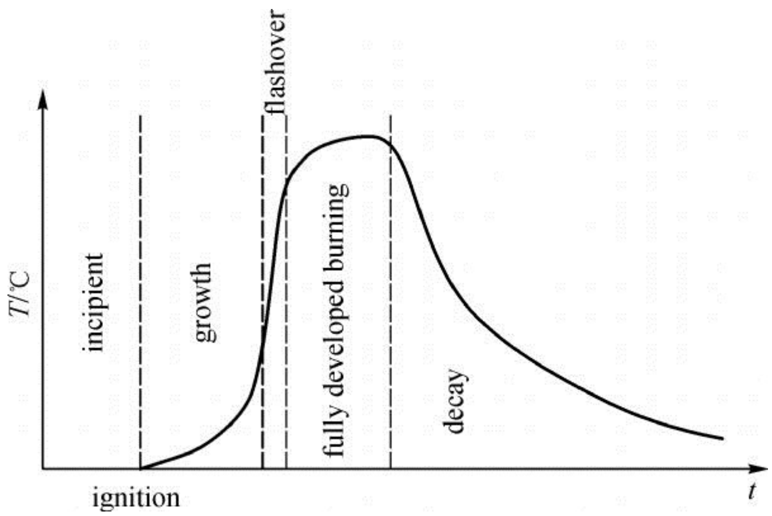

Figure 2.1 – Stages of development of a fire [3]

Currently there are two kinds of fire scenarios defined in the standard – nominal (standard) and parametric. The nominal fire curves are specified in EN 1991-1-2 [4] (see Figure 2.2).

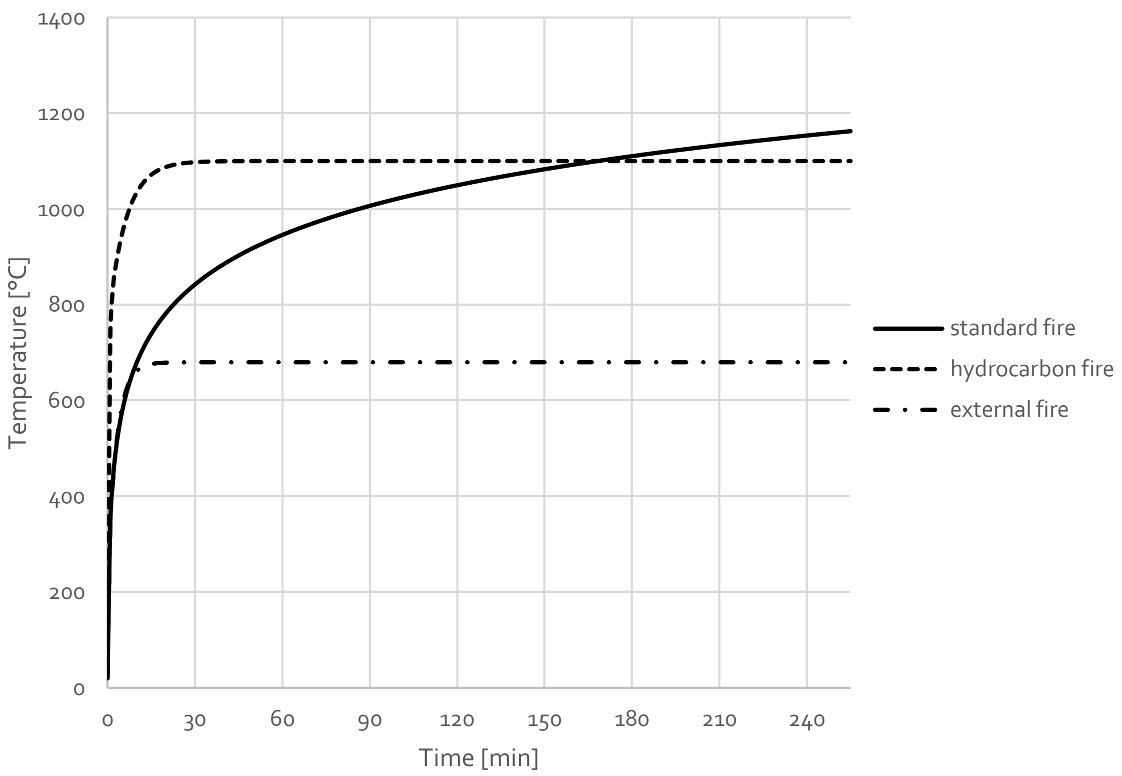

Figure 2.2 – Nominal time-temperature curves given in EN 1991-1-2 [4]

Of these curves the standard fire curve is most widely used. These fire curves present the temperatures of the gasses in the compartment without a cooling phase. They also only represent the fully developed fire phase. This means that the ignition phase, which can take a significant amount of time, is not taken into account.

The parametric fire scenario is a simplified method of describing real fires, where certain parameters are defined in order to have a good approximation of the natural fire load. Among these parameters can be fire load density, ventilation conditions, etc.

2.1. Design method by EN 1995-1-2

The main idea for calculating fire resistance of timber structures presented in [2] is to determine the depth of the char layer and reduce the cross-section of the member by the charring depth. Charring rates differ significantly before and after the protective cladding falls off, therefore the failure time of protection t_f is an important characteristic for the design of timber frame structures.

Figure 2.3 shows the variation of charring depth in time, when the cladding fails after the start of charring (t_{ch}). Line 1 on the graph represents the charring of unprotected timber members. Line 2a shows charring at a reduced rate when protection is in place. This is called the protection phase and it ends at t_f which is the failure (fall-off) time of protective cladding. Line 2b shows the post-protection phase, where charring occurs at a faster rate due to the lack of a fully developed charcoal layer acting as a thermal barrier. After the char layer reaches a thickness of 25 mm, charring slows to the same rate as seen in unprotected members.

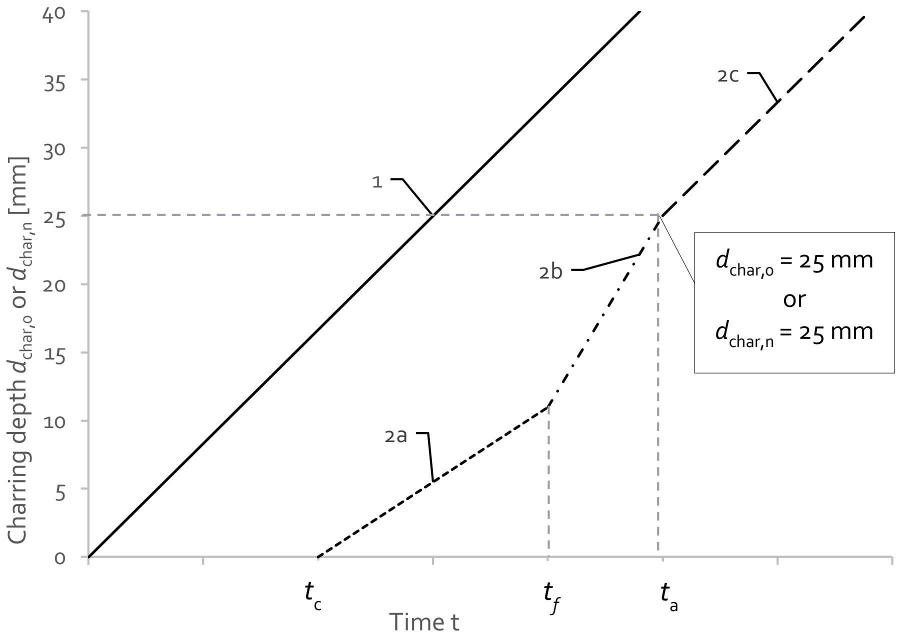

Figure 2.3 – Variation of charring depth with time when $t_{ch} < t_f$

When designing a timber member, the depth of charring that occurs during the required fire resistance time is calculated and the original cross-section is reduced by the charring depth. After that the load-bearing capacity of the timber member is calculated. This value represents the maximum load the member can resist after exposure to standard fire for the specified length of time. It is usually expressed in minutes - e.g. R30 describes a structure which will not collapse under the prescribed load after a 30-minute exposure to a standard fire.

2.2. Improved component additive method

To calculate the charring depth, it is necessary to correctly assess the protective effect of the material layers preceding and surrounding the timber element. This is most important when dealing with light timber frame structures where the timber members are quite slender. These structures, however, often have many different layers that can be combined in a wide variety of configurations.

The improved component additive method is based on summarising the contributions of each layer considering different heat transfer paths. This method is applicable to timber assemblies consisting of unlimited number of layers of gypsum plasterboards, wood panels, mineral wools and their combinations. A large amount of test data was studied [5] in order to develop the equations.

The total fire resistance of the assembly is the time between the start of the fire exposure and when the temperature on the unexposed side of the structure reaches a temperature rise of 140 K on average over the whole surface or 180 K in a single point. This temperature limitation prevents the ignition of nearby. Generally, the starting (ambient) temperature is 20°C, therefore the temperature criteria become 160°C and 200°C, respectively.

As the assembly can be multi-layered, an agreement on the naming of layers has been made. The symbols used for layer names are shown in Figure 2.4.

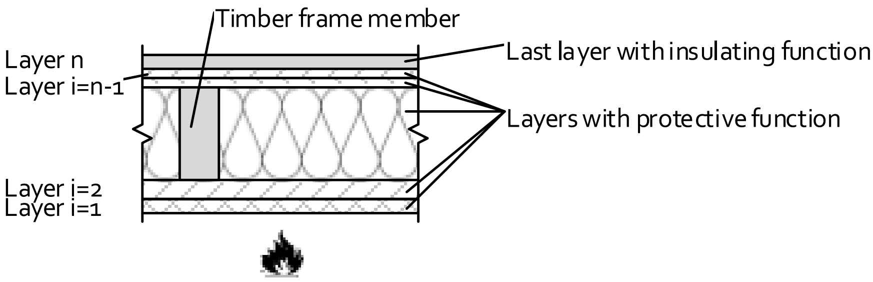

Figure 2.4 – Numbering and function of the layers in a timber frame structure

The insulation time is calculated as shown in (1).

$$t_{\mathrm{ins}} = \sum_{\mathrm{i=1}}^{\mathrm{i=n-1}} t_{\mathrm{prot,i}} + t_{\mathrm{ins,n}} \tag{1}$$

Where t_{ins} is the total fire resistance of the assembly [min];

$\sum_{\mathrm{i=1}}^{\mathrm{i=n-1}} \mathrm{t}_{\mathrm{prot,i}}$ is the sum of the protection times of the layers in the direction of the heat flux [min];

$t_{\mathrm{ins,n}}$ is the insulation time of the last layer of the assembly on the unexposed side [min].

The protection times of layers before the last layer can be calculated taking into account the basic values of the layers, the position coefficients and joint coefficients by equation (2).

$$t_{\mathrm{prot,i}} = \left(t_{\mathrm{prot,0,i}} \cdot k_{\mathrm{pos,exp,i}} \cdot k_{\mathrm{pos,unexp,i}} + \Delta t_{\mathrm{i}}\right) \cdot k_{\mathrm{i,j}} \tag{2}$$

Where
- $t_{\mathrm{prot,i}}$ is the protection time of the layer [min];
- $t_{\mathrm{prot,0,i}}$ is the basic protection value of layer i [min];
- $k_{\mathrm{pos,exp,i}}$ is the position coefficient that takes into account the influence of layers preceding the layer considered;
- $k_{\mathrm{pos,unexp,i}}$ is the position coefficient that takes into account the influence of layers backing the layer considered;
- Δt_{i} is the correction time for layers protected by Type F gypsum plasterboards or gypsum fibreboards [min];
- $k_{\mathrm{i,j}}$ is the joint coefficient.

Insulation time (3) of the last layer can be calculated taking into account the basic values of the layers, the position coefficients and joint coefficients.

$$t_{\mathrm{ins,n}} = \left(t_{\mathrm{ins,0,n}} \cdot k_{\mathrm{pos,exp,n}} + \Delta t_{\mathrm{n}}\right) \cdot k_{\mathrm{j,n}} \tag{3}$$

Where
- $t_{\mathrm{ins,n}}$ is the insulation time of the last layer of the assembly on the unexposed side [min];
- $t_{\mathrm{ins,0,n}}$ is the basic insulation time of the last layer n on the unexposed side [min];
- $k_{\mathrm{pos,exp,n}}$ is the position coefficient that takes into account the influence of layers preceding the layer considered;
- Δt_{n} is the correction time for layers protected by Type F gypsum plasterboards or gypsum fibreboards [min];
- $k_{\mathrm{j,n}}$ is the joint coefficient.

The coefficients and basic values are dependent on the material of the layer in question and the preceding and backing layers. These values are presented in [6] based on the work of Schleifer [5].

2.3. Gypsum boards

Gypsum plasterboard is a panel product that consists of a non-combustible core, composed primarily of gypsum, and paper surfacing on the face, back and long edges [7]. The facing can also be made of other materials. When a proper fastening system is used, the surface of the structure becomes continuous.

Gypsum is a naturally occurring mineral found in sedimentary rock formations. Its crystalline form is known as calcium sulphate dihydrate ($CaSO_4 \cdot 2H_2O$). Gypsum rock contains approximately 21% of chemically bound water by weight [8]. For the manufacturing of gypsum boards, the natural rock is ground and heated to drive off three-fourths of the chemically bound water, to create calcined gypsum or gypsum hemihydrate ($CaSO_4 \cdot \frac{1}{2}H_2O$). Chemically pure gypsum can be obtained from flue gasses released in electrical plants. Modern gypsum plasterboards contain a significant amount of recycled materials, both for the paper backing and gypsum.

When making the boards, natural and synthetic gypsum are mixed together with additives and water. Additives used include, but are not limited to, paper pulp, fibreglass, plasticisers, foaming agents, starch and waxes. The mixture is fed between continuous layers of paper which become chemically and mechanically bound to the gypsum core. The previously dehydrated gypsum rehydrates and reverts to its original rock state (regains chemically bound water to about 21% by weight). The board is made as a long strip which is cut to length after drying [8]. In normal room conditions, the boards absorb a small amount of free water (≤4%).

Due to the popularity and wide spread of gypsum plasterboards, many types have been developed to meet the needs of the construction industry. These types are defined in EN 520 [9] and presented in Table 2.1.

Table 2.1 – Types of gypsum plasterboards

Type	Defined performance
A	Plasterboard with a face to which suitable gypsum plasters or decoration may be applied
F	Fire protection board with improved core cohesion at high temperatures
H	Plasterboard with reduced water absorption rate
E	Boards specifically manufactured to be used as sheathing in external walls and are not intended to receive decoration
P	Boards, which have a face intended to receive gypsum plaster or to be combined by collage with other materials in form of boards of panels
D	Gypsum plasterboard with controlled density
R	Gypsum plasterboard with enhanced strength
I	Gypsum plasterboard with surface hardness

These classifications can be combined to some extent. In the scope of this thesis, the main focus will be on type A and type F boards. In North America, fire resistant gypsum plasterboards are classified as type X and they are analogous to type F in Europe.

As previously stated, gypsum is a non-combustible material. It also contains a significant amount of chemically bound water which has a retardant effect on the temperature rise in a fire scenario. Water evaporation is an endothermic reaction where heat is absorbed.

When the board is heated to 80-250°C dehydration (or calcination) of gypsum takes place. The range of temperatures is dependent on the way of heating and the composition of the board itself [10]. Gypsum dehydration is reported to have two steps. Firstly, about 75% of water is evaporated from the calcium sulphate dihydrate. Secondly, when heating continues, the hemi-hydrate loses the remaining water and becomes calcium sulphate anhydrite III. Some sources claim that this happens at once depending on the water vapour pressure (low pressure triggers a one-step process). Water evaporation is seen as a peak in the specific heat graph. The anhydrite has low thermal conductivity, which has a positive effect in the fire scenario by helping to sustain the temperature gradient across the thickness of the board.

At temperatures around 400°C a slightly exothermic reaction takes place where anhydrite III crystals reorganise to a lower energy state (anhydrite II). If the board contains magnesium and calcium carbonate, there is a mass loss observed at temperatures between 600-800°C. At temperatures near 1200°C the gypsum goes through another endothermic reaction and a mass reduction due to decomposition to calcium sulphate anhydrite I [10].

With most of the reactions happening in gypsum at elevated temperatures, loss in mass and shrinkage is involved. This causes cracking and strength loss of the board. Gypsum is also subject to ablation (flaking off of small layers of the material). This phenomenon is a greater issue with thinner boards as a relatively larger portion of the board may flake off [11]. Within the first couple of minutes the paper coating on the exposed face of the board burns off completely, therefore the board itself has to be able to stay in place. For this reason, type F boards are reinforced (usually) with glass fibres which do not allow the board to shrink and counteract the formation of big cracks (small, more abundant hair-like cracks tend to be unavoidable). Other additives (vermiculite, clay, fly ash) may be added to increase fire resistance.

2.4. Tested products

Four commercially available gypsum plasterboards – *Protect F*, *Storm*, *Normal* and *Habito* – made by Saint-Gobain Gyproc were tested in a model scale furnace.

Protect F is a type F gypsum plasterboard with a thickness of 15.4 mm. Its primary use is in structures with high fire resistance demands, as a stiffener in premade house modules. *Storm* is a thin (9 mm) type H sheathing board that is also applicable in modular house construction. It is the only board in this test group which does not have a paper coating. The other boards are classified as type A boards. *Normal* is the standard 12.5 mm board designed to be used in dry interior settings. *Habito* is a newer addition to the Gyproc product line. It is a 12.5 mm board with enhanced strength properties [12].

3. Literature survey

Gypsum as a widespread fire protection material for light timber (or steel stud) structures has been researched a lot. There is a growing interest in determining the thermal properties of gypsum plasterboards for computer simulations. In the following some examples of studies of thermal parameters at high temperatures are presented.

The thermal parameters of gypsum plasterboards are highly dependent on the chemical composition of the source material and therefore the board itself. This finding is presented by Wakili [13]. The thermo-physical properties (thermal conductivity, specific heat and density) of four gypsum plasterboards were investigated. The results are presented graphically in Figure 3.1 toFigure 3.3.

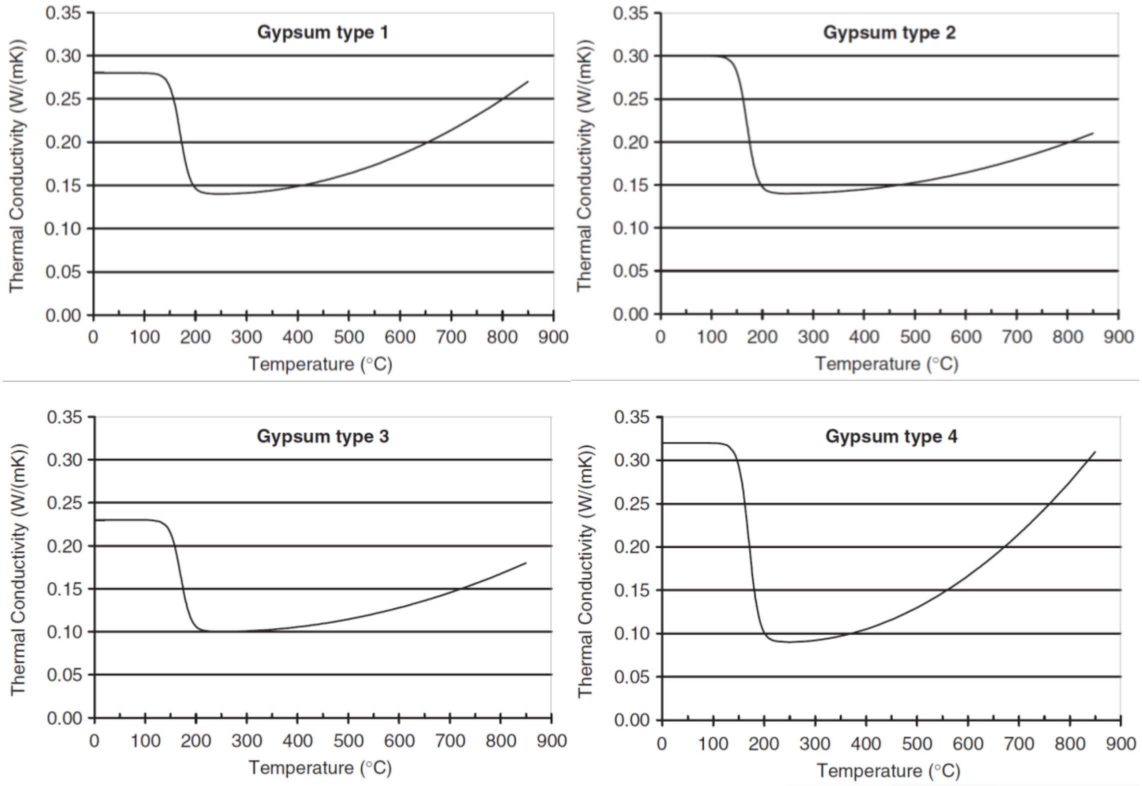

Figure 3.1 – Thermal conductivity curves presented in [13]

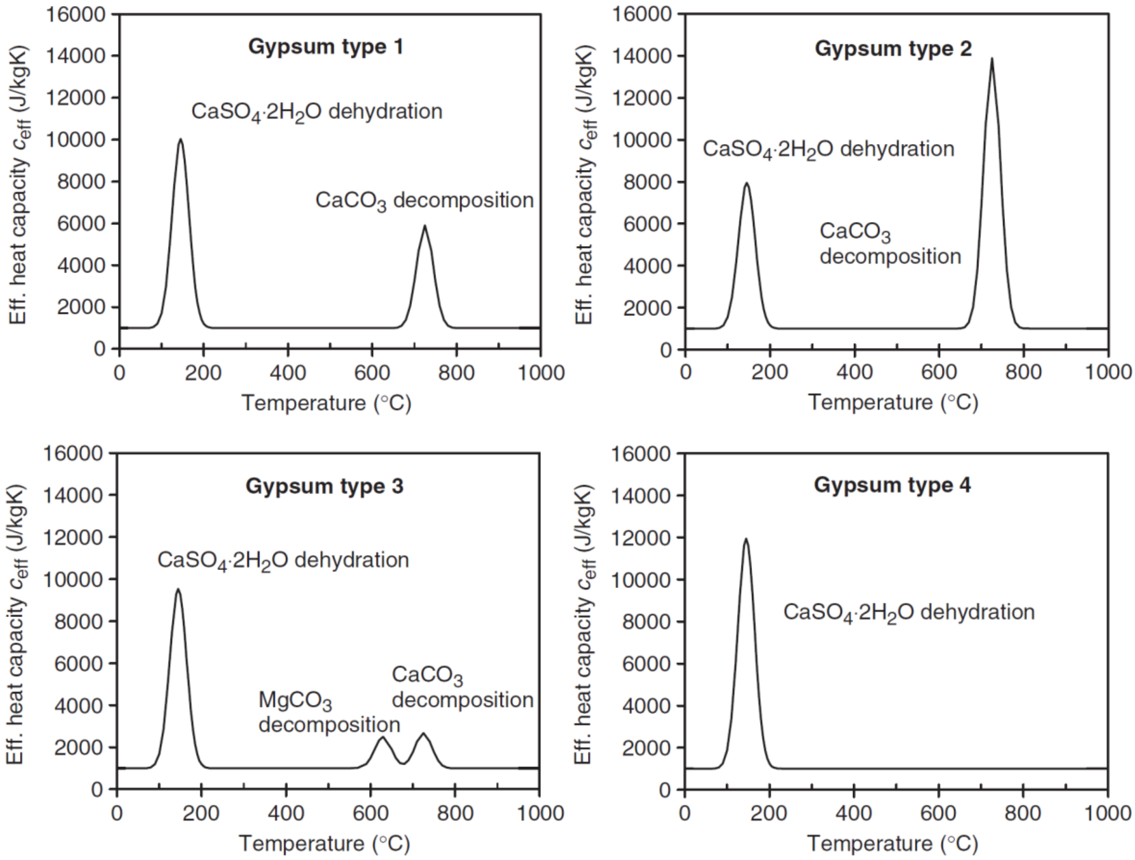

Figure 3.2 – Effective heat capacity curves presented in [13]

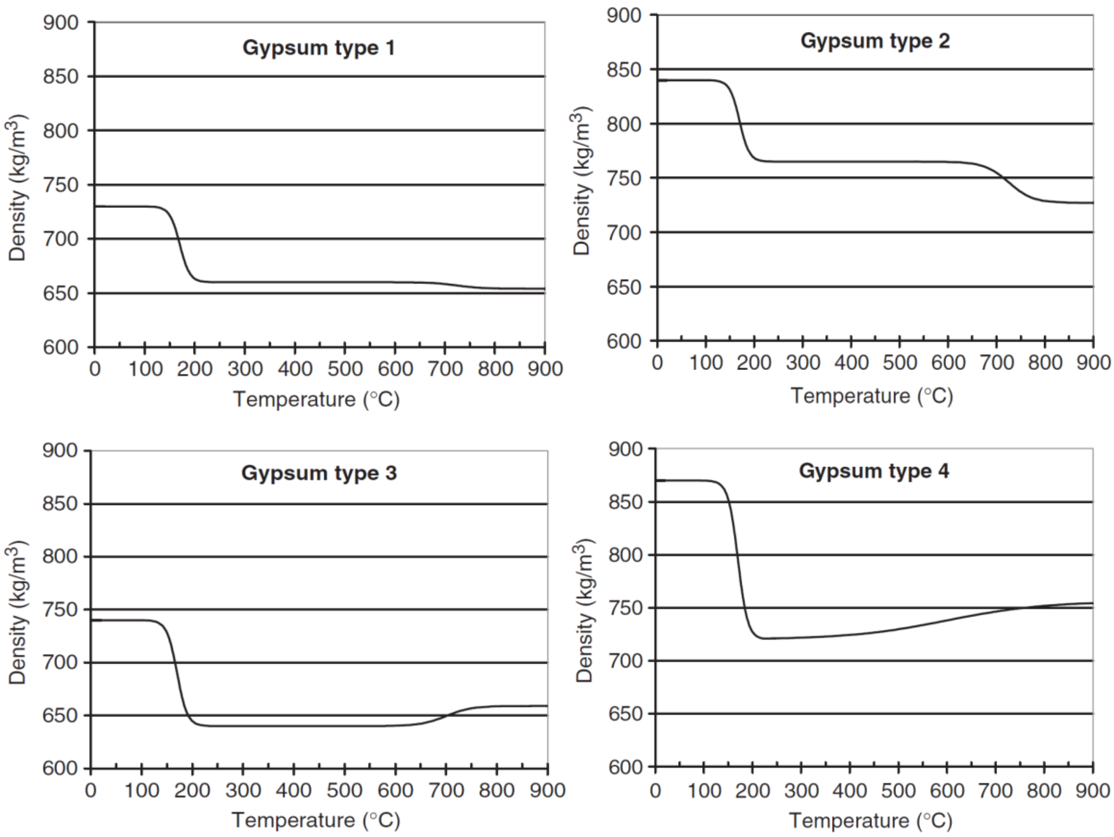

Figure 3.3 – Density curves presented in [13]

Even though some general observations can be made, it is clear that the thermal properties have a noticeable variation between boards which becomes apparent even with a selection of only four different products.

An extensive study was performed in Canada to determine the thermal properties of wood, gypsum and insulation materials [14]. The results are based on tests conducted during a 10-year period. The graphs showing the thermal parameter curves are shown in Figure 3.4 to Figure 3.6. The curves labelled Type X, FR and Regular are of particular interest for this thesis. Type X and FR are used as fire protective claddings and Regular could be compared to European type A gypsum plasterboards.

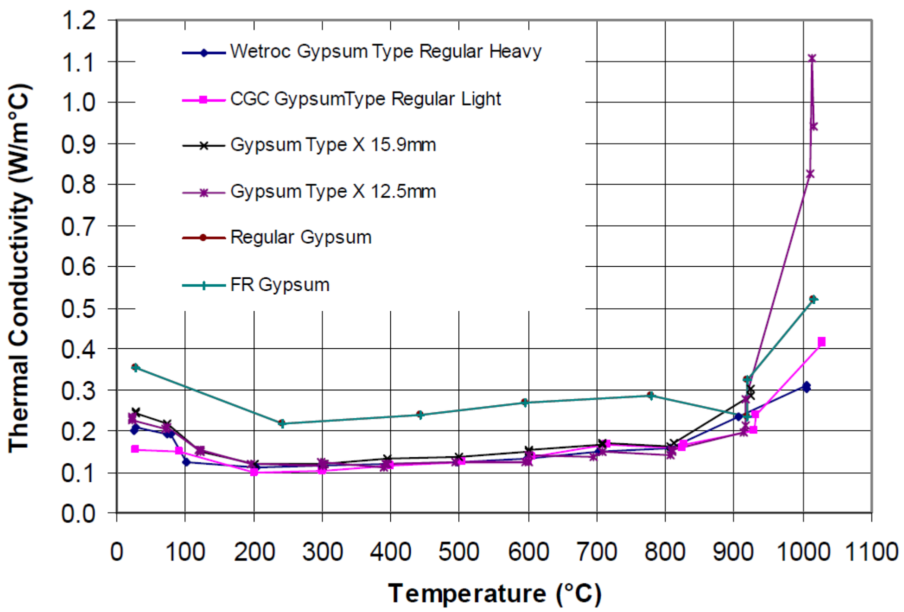

Figure 3.4 – Thermal conductivity curves from [14]

The authors of [14] have emphasised that the thermal conductivity curve can be roughly divided into three linear sections as can be seen from Figure 3.4. The peaks at temperatures above 900°C can be due to loss of integrity or formation of small cracks.

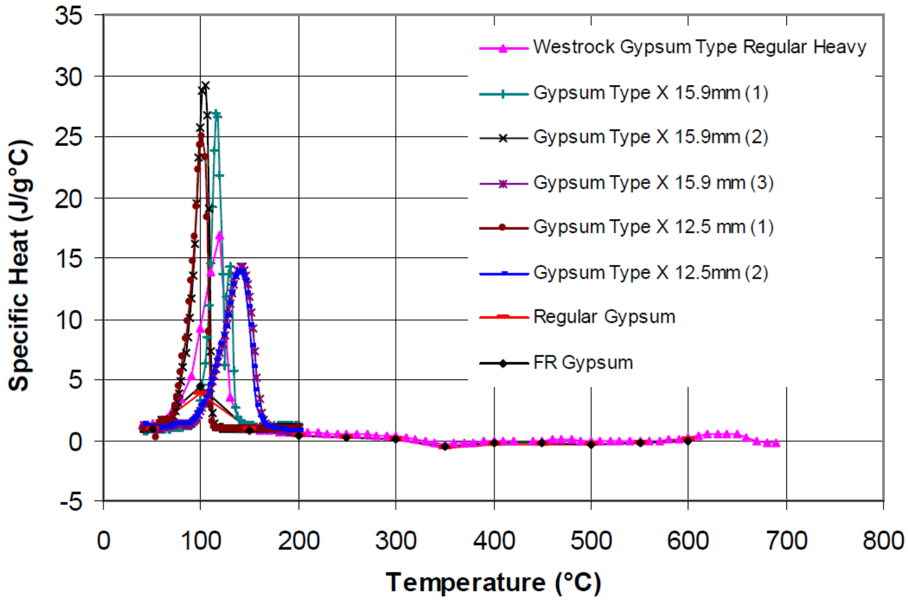

Figure 3.5 – Specific heat curves from [14]

The specific heat curves show an even larger scatter. The peaks observed around 100°C are attributable to the calcination reaction which has different energy requirements depending on the chemical composition of the boards. The results are obtained from differential scanning calorimeter tests done with different heating rates. It was observed that the higher the heating rate, the sharper the peaks are and they occur at higher temperatures.

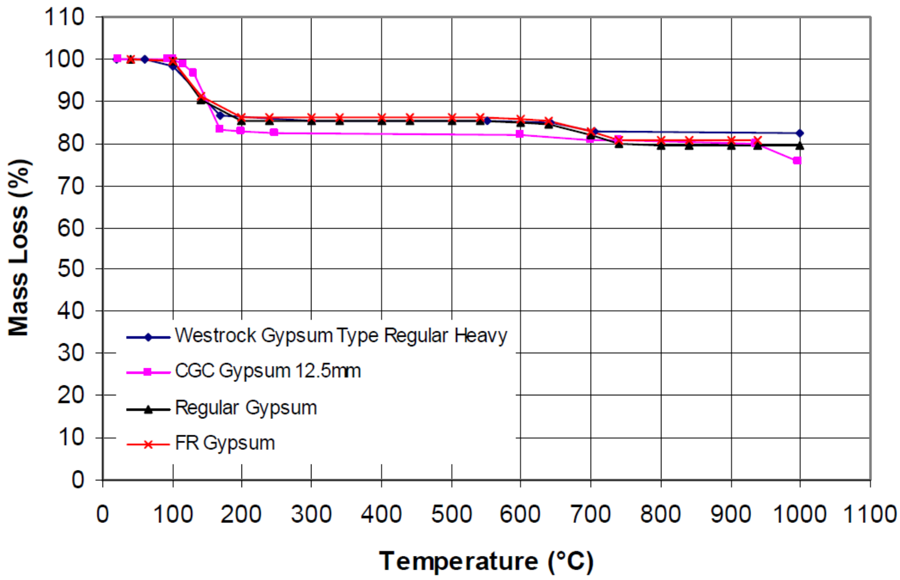

Figure 3.6 – Mass loss curves from [14]

The quite significant mass loss visible at temperatures around 100°C is due to the evaporation of water.

Another study was conducted by Semitelos et al to develop simplified correlations of thermal properties of gypsum for simulations [15]. A comprehensive research of previous tests was presented in the paper. The thermal conductivity results can be seen in Figure 3.7.

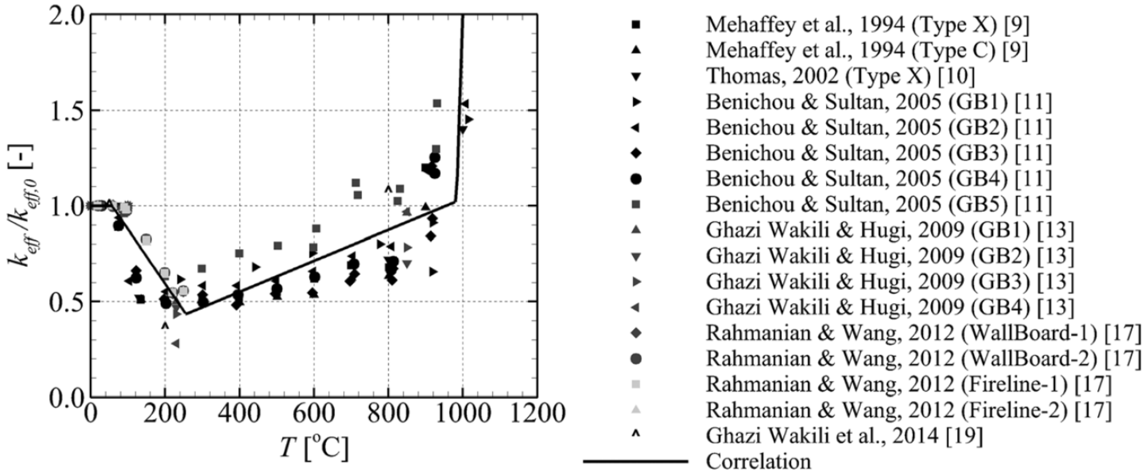

Figure 3.7 – Normalised thermal conductivity data from [15] (sources listed on graph correspond to the ones used for the article not this thesis)

A recent study in Spain [16] has been able to present the exothermic reaction happening in gypsum around 400°C as shown in the specific heat curve presented in Figure 3.8.

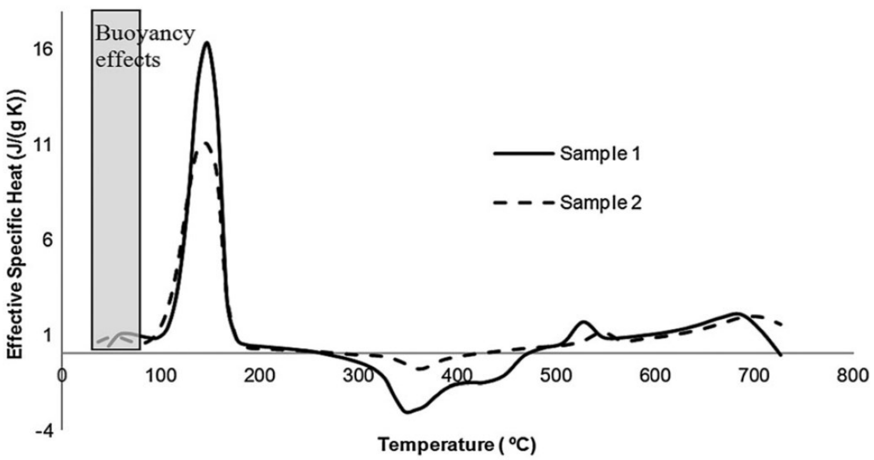

Figure 3.8 – Effective specific heat determined by simultaneous thermal analysis presented in [16]

The greyed out area on the graph marked as "Buoyancy effects" is an area of uncertainty in the results caused by the method used for determining mass loss. The effective specific heat was derived from the mass loss data and therefore also has a small area of unconfirmed accuracy.

4. Model scale fire tests

To form the basis for the calibration of thermal properties, test data is needed. Four non-loaded model scale furnace tests were conducted in SP Technical Research Institute of Sweden in Stockholm between December 2015 and April 2016. The results of the tests are presented in [17], [18] and [19].

4.1. Test description

The furnace has a volume of 1 m^3. It is fitted with 4 burners that use a mixture of propane and butane gasses as fuel. The temperature in the compartment for all tests followed the ISO 834 standard fire curve [20]. The temperature was controlled manually by changing the intensity of the burners.

All tests were conducted for horizontal (ceiling) structures. The specimens were built at SP Wood Technology and conditioned in a controlled climate chamber (20°C and 65% RH) before the fire tests. In all the tests four different gypsum boards were used (see Table 4.1). The exposed surface of the specimen was divided into equal quadrants (see Figure 4.1 for a picture of test specimen T1). The boards tested were Gyproc products [12], two of which (*Protect F* and *Habito*) are of concern of this thesis. Any gaps between the tested boards were covered with type F gypsum plasterboards and sealed with liquid sodium silicate based glue or aluminium tape.

The test specimens were equipped with type K thermocouples placed at different characteristic locations. Throughout the tests the temperatures were recorded every 5 seconds. This time step provides good accuracy without making the data so large that it becomes difficult to manage.

The first test specimen (T1) was built according to the configuration proposed by Schleifer [5]. The unexposed side was of wood particleboard (thickness 19 mm, density 630 kg/m^3). On the fire side were four gypsum plasterboards 0.4x0.4 m with varying thicknesses. See Figure 4.1 and Figure 4.2 for a picture and a drawing showing the configuration of test specimen T1. Locations of thermocouples for one board are shown in cross-section view in Figure 4.3.

Table 4.1 – Data of the gypsum plasterboards used in T1

Product	Dimensions			Before the fire test		After the fire test	
				Weight	Density	Weight	Density
	mm	mm	mm	kg	kg/m³	kg	kg/m³
Protect F	400	380	15	1,98	868,4	1,54	675,4
GHS Storm	397	397	9,5	1,18	788,1	1,12	748,0
GN Normal	390	400	12,5	1,36	697,4	-	-
GH Habito	398	400	12,5	1,94	974,9	1,42	713,6

The test duration was 40 minutes. During the test no cracks were visible, but *Protect F* board fell off during the dismounting of the specimen. The weight measurements after test were conducted on whole boards that had fallen off. *Normal* board had been extinguished with water which is the reason for no weighing.

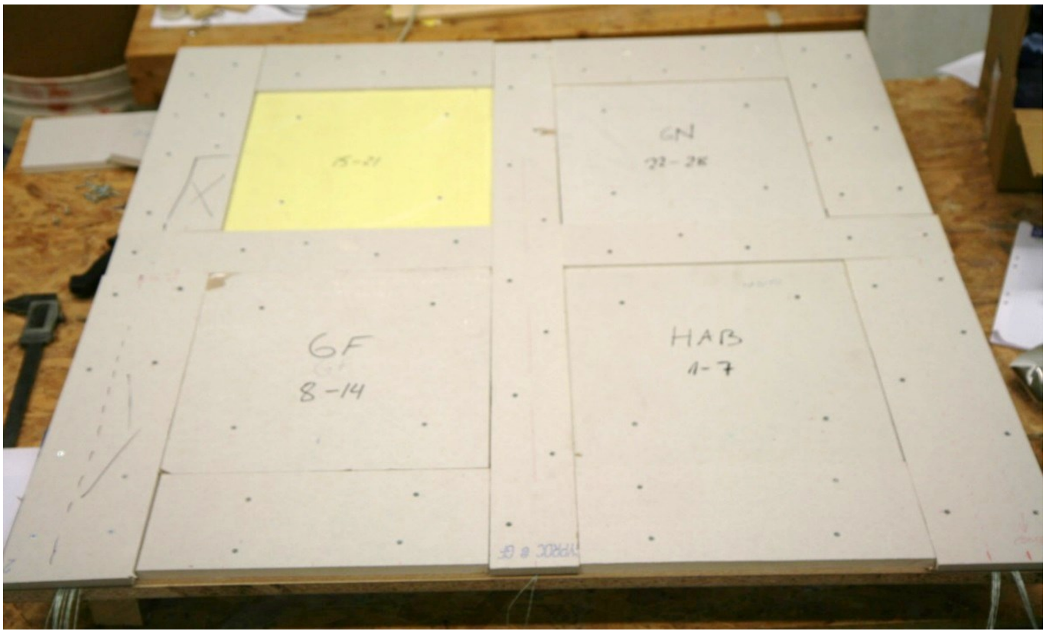

Figure 4.1 – View of the specimen T1 from the fire exposed side

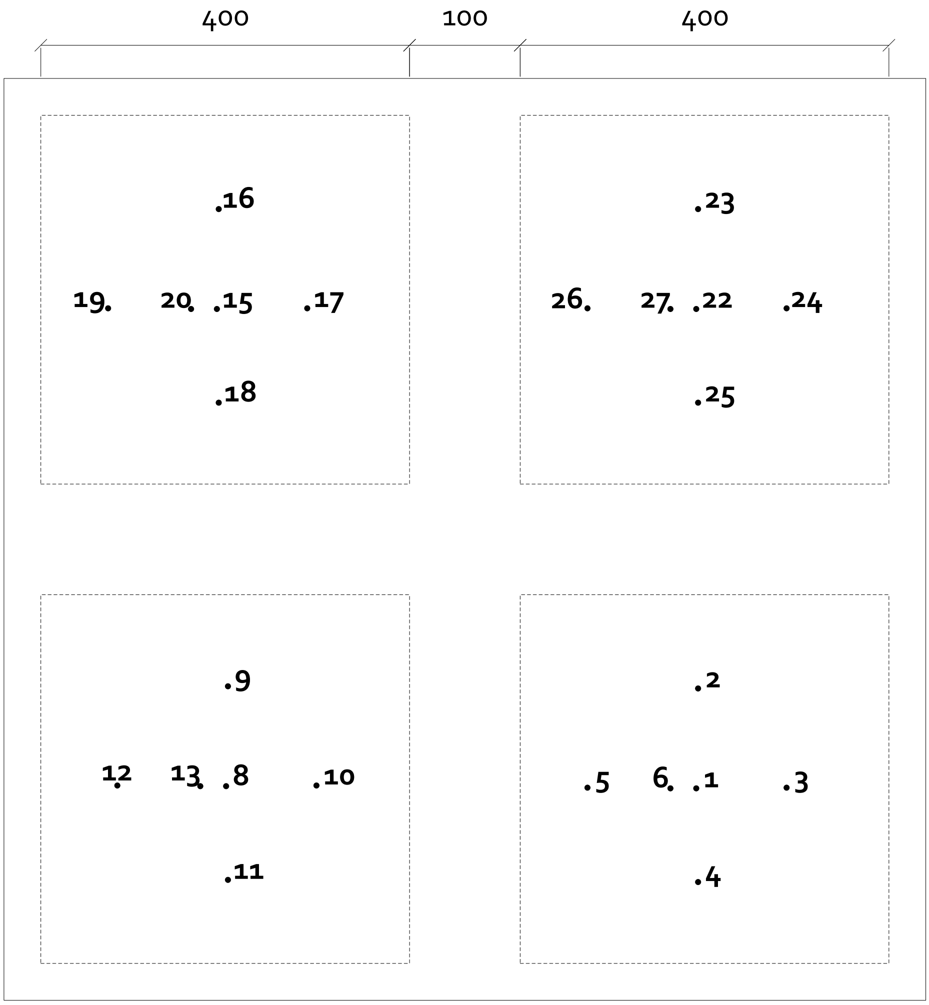

Figure 4.2 – Plan of test specimen T1 viewed from the fire exposed side

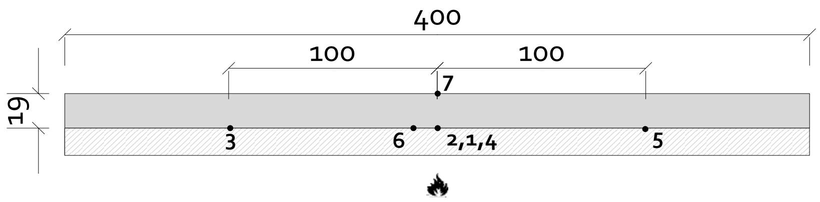

Figure 4.3 – Cross-section of one quadrant of test specimen T1

The second test specimen (T2) had 45x45 mm timber beams forming cavities that were fully filled with batt type stone wool (Paroc eXtra with density of 26 kg/m^3). On the unexposed side the same 19 mm wood particleboard was used. The fire exposed side was clad with the four kinds of gypsum plasterboards. See Figure 4.4 for a picture of specimen T3 during assembly with the quadrants filled with stone wool. In Figure 4.5 the gypsum boards have been attached to the same specimen. The aluminium tape used for achieving air-tightness is also visible. The finished specimen had all voids and cavities filled with stone wool.

Figure 4.4 – View of specimen T3 during assembly

Figure 4.5 – View of specimen T3 during assembly (gypsum boards attached)

Test three (T3) was otherwise like T2 with the exception that the beams used were 45x145 mm and therefore the thickness of insulation was 145 mm. See Figure 4.6 and Figure 4.7 for plan and cross-section views of test specimens T2 and T3 (specifically T3 is shown in cross-section for better readability).

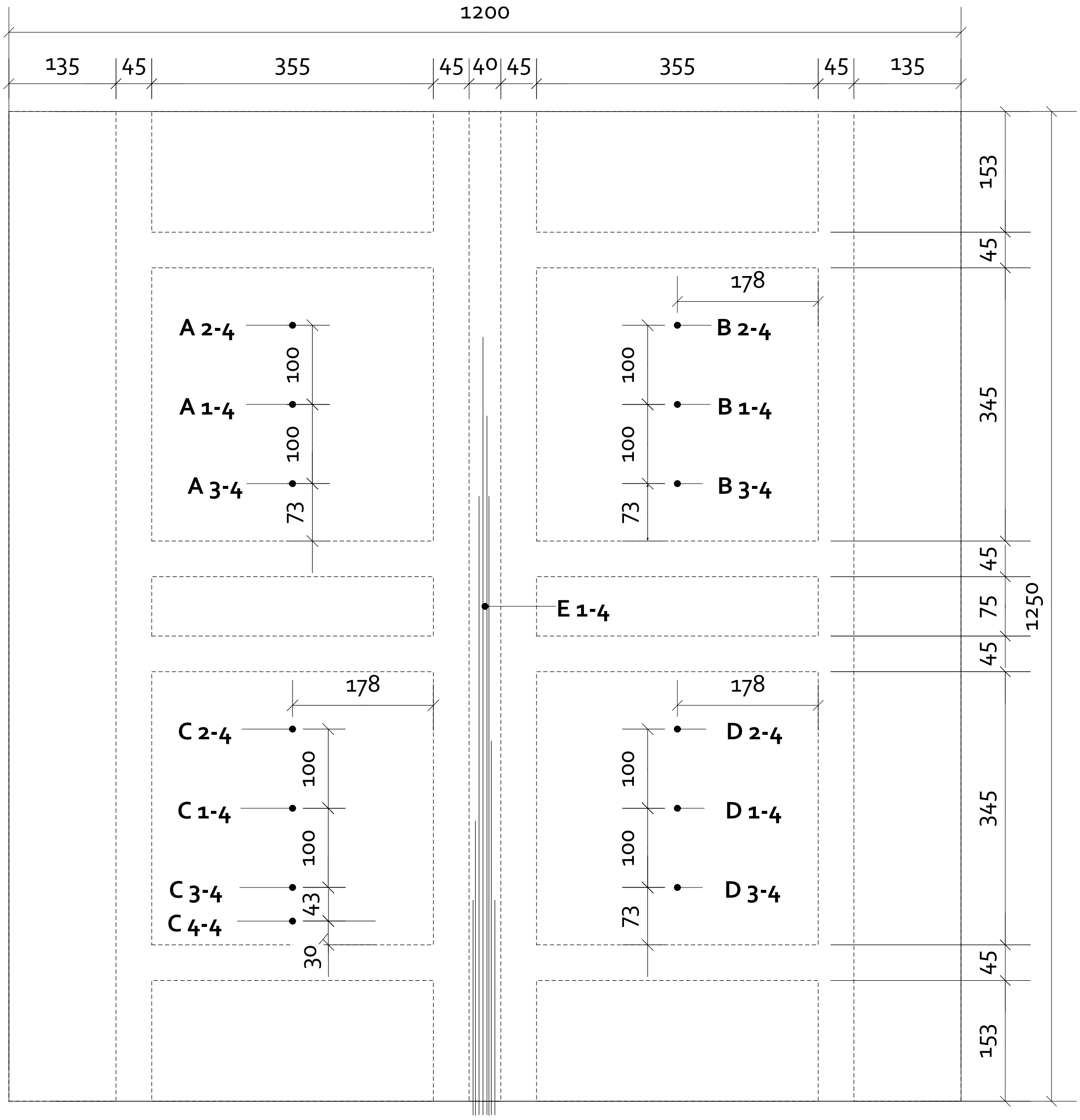

Figure 4.6 – Plan of test specimens T2 and T3 with thermocouples located behind insulation shown

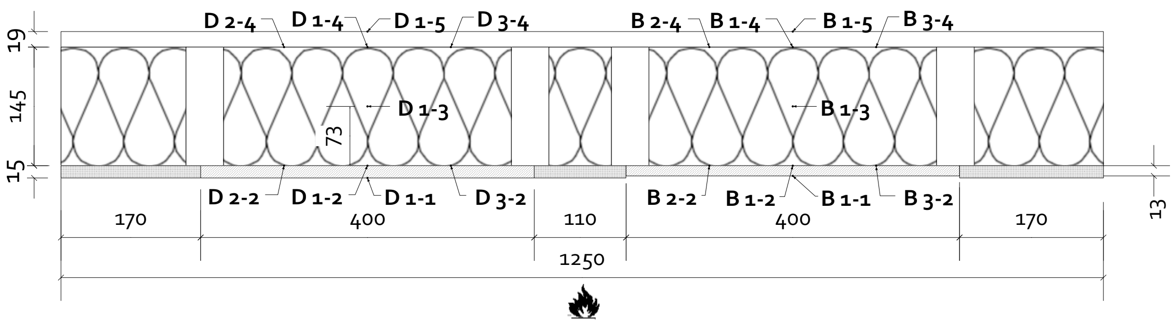

Figure 4.7 – Cross-section of test specimens T2 and T3

Test two was terminated after 45 minutes. At that time temperatures behind all boards had reached 600°C. The first crack appeared in *Normal* board after 22 minutes of fire exposure. After 41 minutes a part of the same board fell off. Other boards exhibited no cracks.

The duration of the third test was 75 minutes. The first cracks appeared after 26 minutes. At around 60 minutes a piece of *Storm* board fell off. After 73 minutes of standard fire exposure *Normal* board failed.

The fourth test (T4) was a setup conceived in order to get fair results where the temperature rise in the gypsum boards is unaltered by other materials. This test configuration had two layers of *Protect F* on the unexposed side and the tested boards (*Protect F* and *Habito*) were attached to the gypsum boards. See Figure 4.8 and Figure 4.9 for plan and cross-section views of test specimen T4.

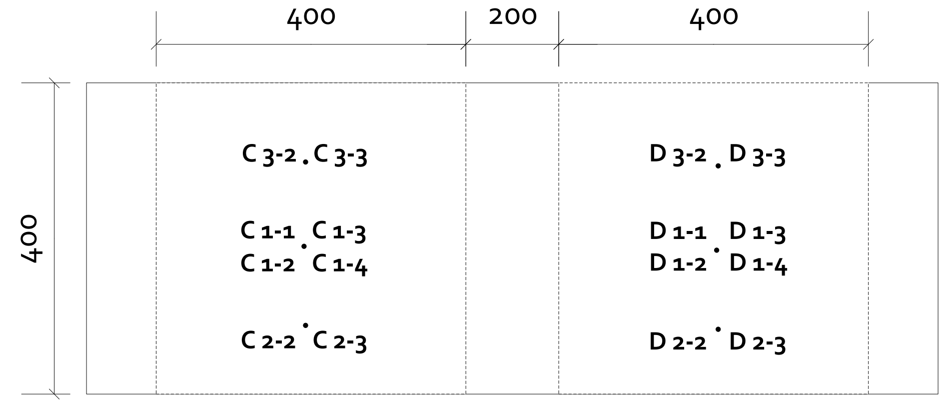

Figure 4.8 – Plan of test specimen T4

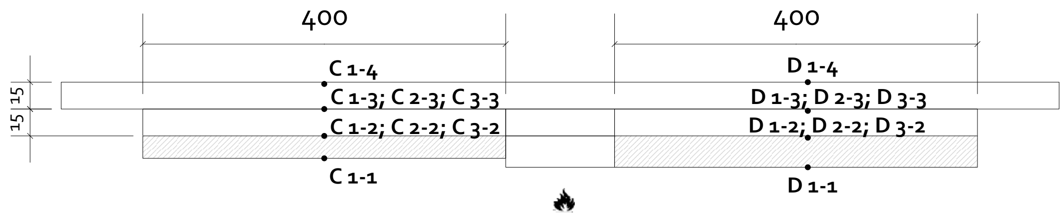

Figure 4.9 – Cross-section of test specimen T4

Pictures of specimens from the exposed side when mounted on the furnace and right after removal are presented in Figure 4.10 and Figure 4.11.

Figure 4.10 – Test specimen T3 mounted on the furnace (view of exposed side)

Figure 4.11 – Test specimen T2 after removal from furnace

4.2. Results

Thermocouple measurements during the tests are presented graphically in the following graphs (Figure 4.12 to Figure 4.15).

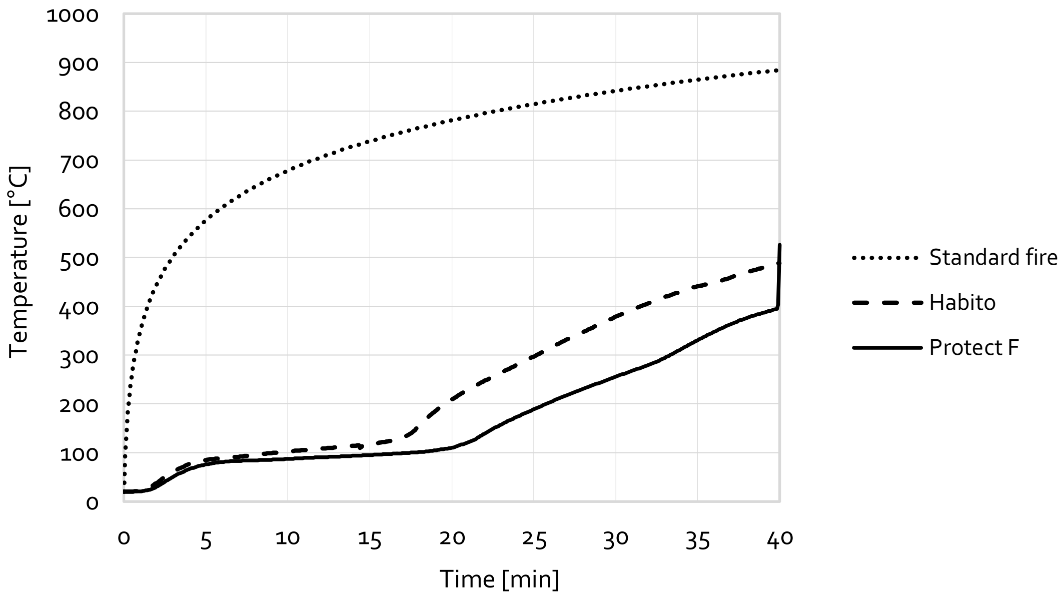

Figure 4.12 – Temperatures behind Habito and Protect F boards and furnace output curve of test T1

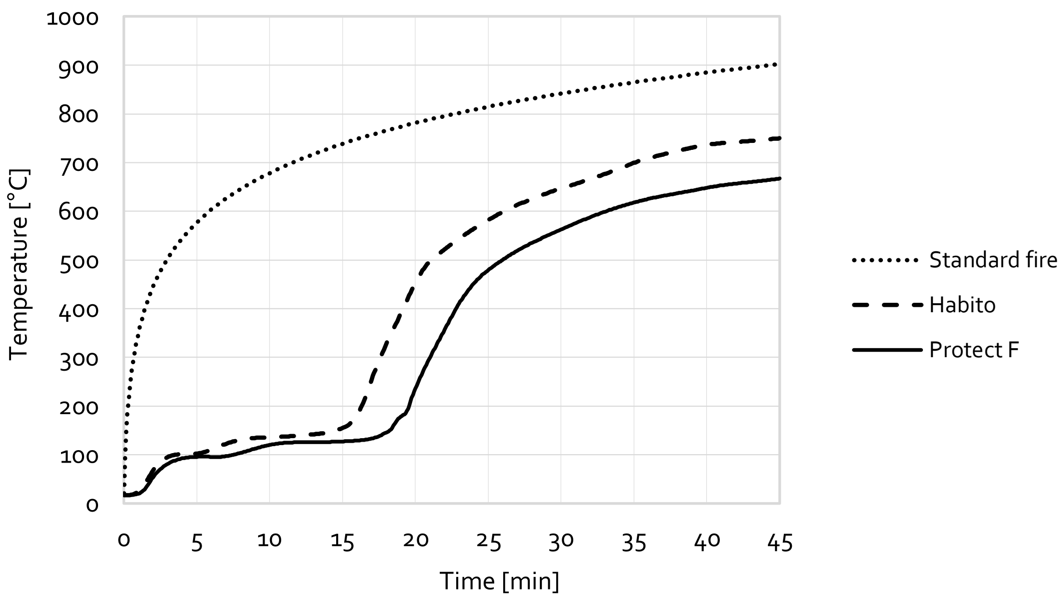

Figure 4.13 - Temperatures behind Habito and Protect F boards and on the exposed surface of test T2

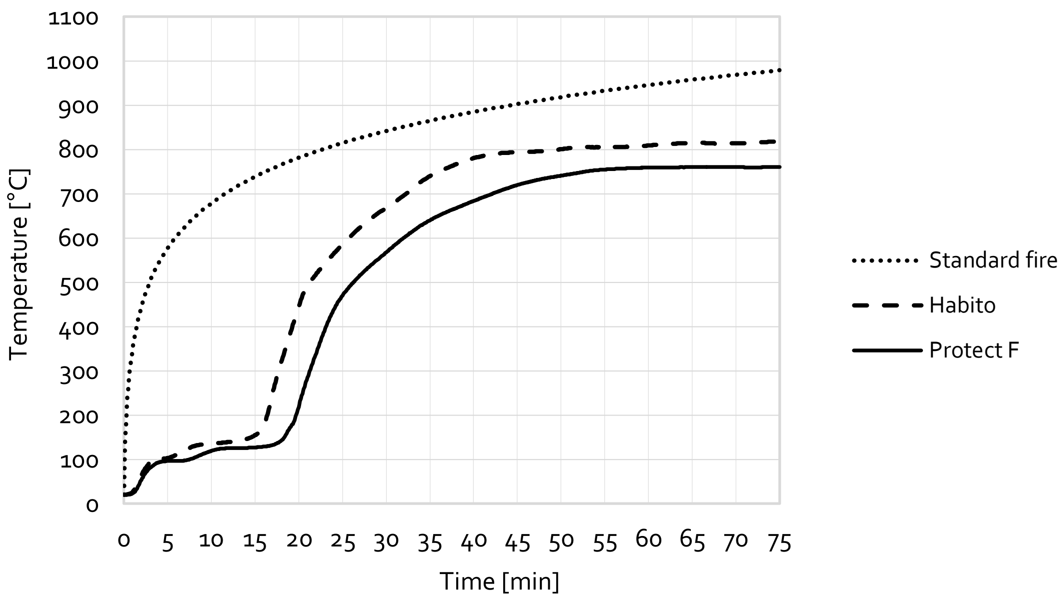

Figure 4.14 – Temperatures behind Habito and Protect F boards and on the exposed side of test T3

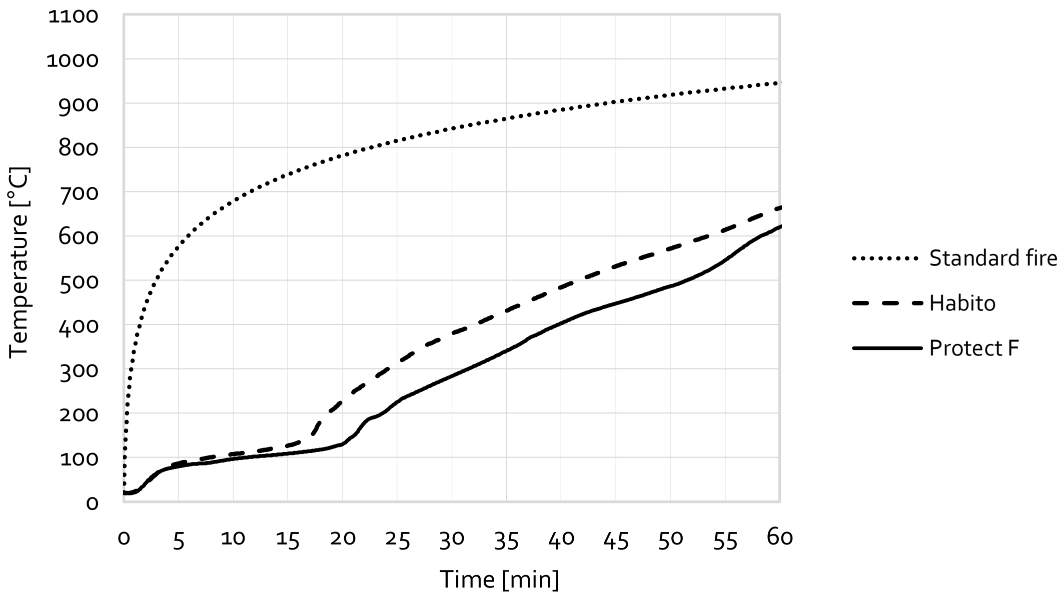

Figure 4.15 – Temperatures behind Habito and Protect F boards and on the exposed side of test T4

The graphs marked as *Habito* and *Protect F* are used as the basis for calibration in chapter 5.2.

5. Calibration of thermal properties

5.1. Simulation software

Within this thesis the software used for thermal simulations was SAFIR v2014a1. It is a commercial software developed in the University of Liège [21]. The program can be used to model the behaviour of building structures subjected to fire and to perform a mechanical analysis afterwards. It uses the finite element method (FEM) [22].

SAFIR calculates the field of temperatures that develops during a specified length of time of exposure to a particular fire scenario. Fires can be represented in different manners (time-temperature curves, imposed heat flux or local models) [23]. The structures can be analysed in 2D and also 3D. A two-dimensional approach has been used in this thesis.

The main concept for calculation in SAFIR is that heat is distributed in the structure by conduction since most construction elements are made of solid materials. This means that for some materials the calculation is an approximation. Such materials are, for example, fibrous insulation materials and wood. SAFIR does not take into account the migration of free water and its re-condensation nor heat transfer within the material via radiation between the fibres and air or by air convection. Such limitations mean that the thermal properties used in the conduction model have to be tuned.

On the surfaces heat is exchanged with the environment via convection and radiation. These phenomena are taken into account by specifying the appropriate coefficients. In the scope of this thesis the coefficient of convection on the heated surface is $\alpha_{c,exp}$=25 W/(m²·K) and on the unheated surface – $\alpha_{c,unexp}$=4 W/(m²·K) as suggested in [4]. The formulas describing heat transfer at the surface and in internal cavities are presented in the technical reference [23].

Calculation within solid materials is based on the Fourier equation (for its representation in Cartesian coordinate system, see (4)).

$$\frac{\partial}{\partial x}\left(k\frac{\partial T}{\partial x}\right)+\frac{\partial}{\partial y}\left(k\frac{\partial T}{\partial y}\right)+\frac{\partial}{\partial z}\left(k\frac{\partial T}{\partial z}\right)+Q=c\rho\frac{\partial T}{\partial t} \qquad (4)$$

Where $\{x, y, z\}$ is the vector of Cartesian coordinates [m];

T is the temperature [K];

k	is the thermal conductivity [W/(m·K)];
Q	is a term that accounts for internal generation of heat [W/m^3];
ρ	is the density [kg/m^3];
c	is the specific heat [J/(kg·K)];
t	is time [s].

Formula (4) can be simplified further to express one-dimensional conduction without internal heat generation. This is presented in equation (5).

$$k\frac{\partial^2 T}{\partial^2 x} = c\rho\frac{\partial T}{\partial t} \Rightarrow \frac{\partial T}{\partial t} = \frac{k}{c\rho}\cdot\frac{\partial^2 T}{\partial^2 x} \tag{5}$$

From equation (5) it can be seen that thermal conductivity is divided by the product of specific heat and density. This means that theoretically only one of these values needs to be calibrated to fit test data if there is sufficient certainty in the values of the other. Generally it is simpler to determine the mass loss and therefore the decrease in density. In the scope of this thesis, thermal conductivity and specific heat have been calibrated and density values acquired from separate tests. For gypsum plasterboards, the density change follows the correlation presented in Fire Safety in Timber Buildings [6].

5.2. Calibration procedure

This chapter will be focusing on developing the procedure of calibrating the thermal properties for the simulations run with SAFIR software. Different methods were used for conducting this work, starting from guesses, followed by literature surveys and mathematical approximations. This part concerns Gyproc Protect F gypsum plasterboard.

The first thermal simulations were conducted for test configuration T1 with the thermal properties of gypsum plasterboard published in the European technical guideline Fire Safety in Timber Buildings [6]. These properties are based on the results of Vanessa Schleifer's PhD thesis [5]. However, after running the simulations, it was discovered that the temperature curves were quite different from test results (see Figure 5.1).

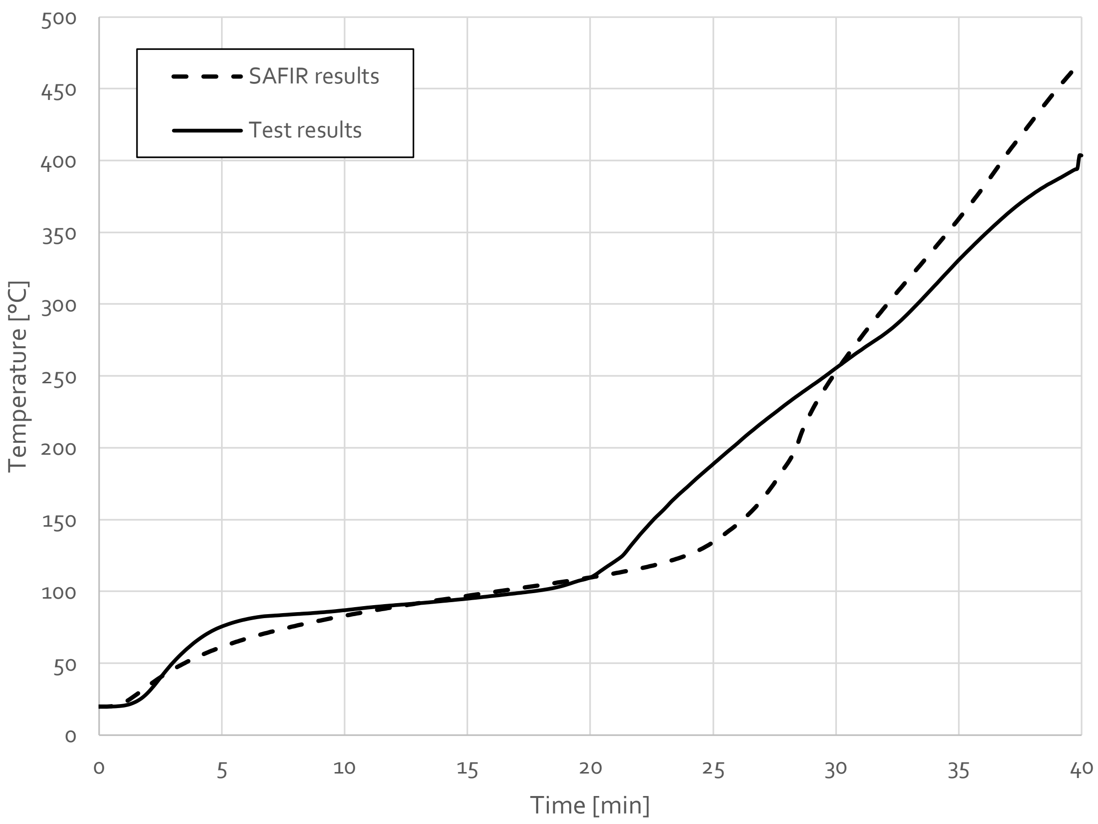

Figure 5.1 – Comparison of test results and first simulation (using input parameters from FSITB [6])

As seen from the graph, the first ~20 minutes show good correlation. After that the difference between the simulated temperature curve and the test data becomes rather large.

The simulated curve indicates that the first dehydration phase of gypsum (nearly horizontal part of the curve around 100°C) lasts more about 5 minutes longer than it did in real test environment. In terms of timber safety engineering, the most important is to know the time when temperature behind the protective layers reaches 270°C. Interestingly, it is at about that temperature where the simulated curve crosses the test results and becomes safer. The end temperature, however, is about 470°C compared to the test in which the temperature behind the gypsum board reached 400°C right before the fall off of the board. That was deemed too large a difference for the simulations to be trustworthy in other setups.

This showed that some of the input parameters were not in correlation with the actual material tested. Hence, better thermal properties had to be found. This idea is supported also in the SAFIR technical documentation [23]. A combination of methods was used to determine more accurate properties.

Form the literature survey, the range in which the thermal properties could change was found. There was quite a large scatter in the results of studies conducted over the world as described in chapter 3. That meant a great uncertainty in modifying the input for the setup in hand.

The first test simulations were run with input parameters that were changed incrementally to see the correlations between the change in the curve and the change in the input parameters. This connection shortly proved to be rather complex. That was due to the author's limited knowledge of the chemical and thermal reactions happening in the material at different temperatures. Even though there is no phase change in the material, gypsum goes through many reactions that change either the chemical composition of the material or its integrity overall.

Simplified correlations for simulation tools were presented in [15]. The general idea would be to use the properties at ambient temperatures, as declared by the manufacturer, as the starting point for the thermal properties' curves. This approach proved to be effective with thermal conductivity, see Figure 5.2. The method for calculating specific heat presented in the same paper is too complex for the scope of this thesis as it involves calculating the energy released or absorbed in each of the reactions that are represented as peaks or valleys on the specific heat curve.

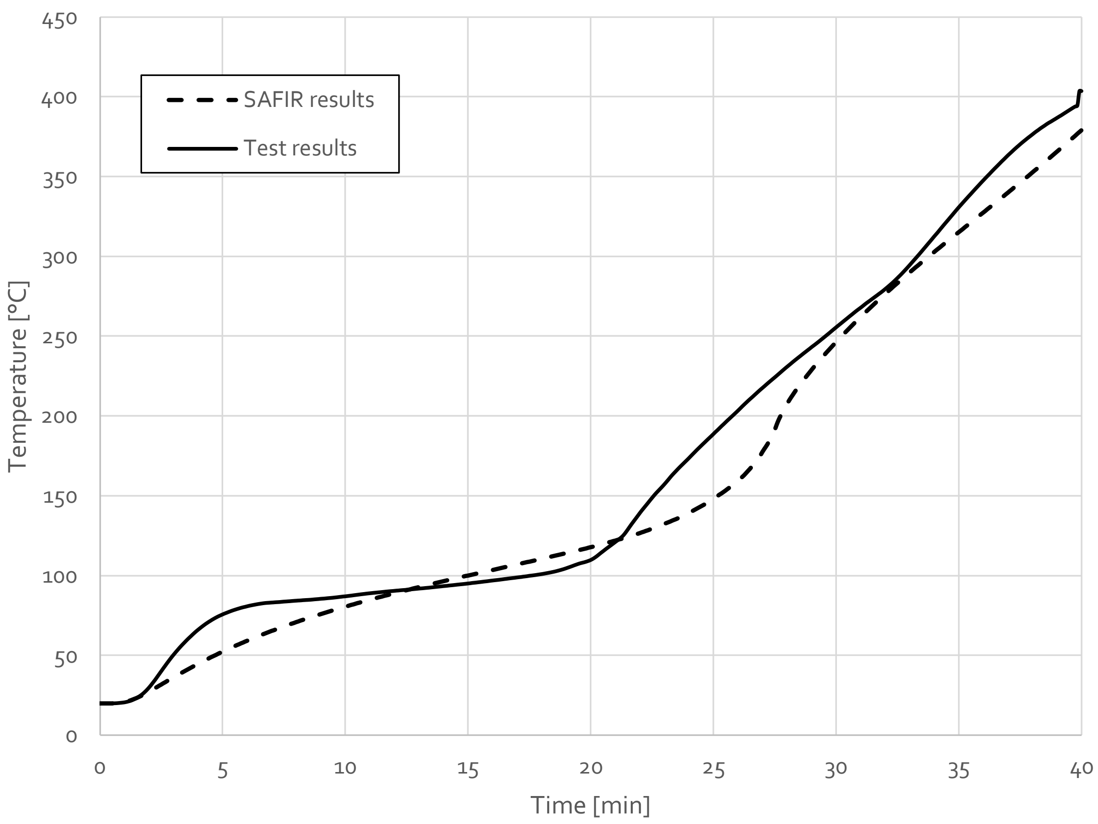

Figure 5.2 – Comparison of test results and simulations using modified thermal conductivity values from [15]

As can be seen from Figure 5.2, the simulated and test curves show quite good similarity, however, the simulation results are unsafe throughout almost the whole test. The dashed curve shown in Figure 5.2 could be precise enough for simulating other test configurations. See Figure 5.3 for a comparison of test results and simulations of the second test configuration.

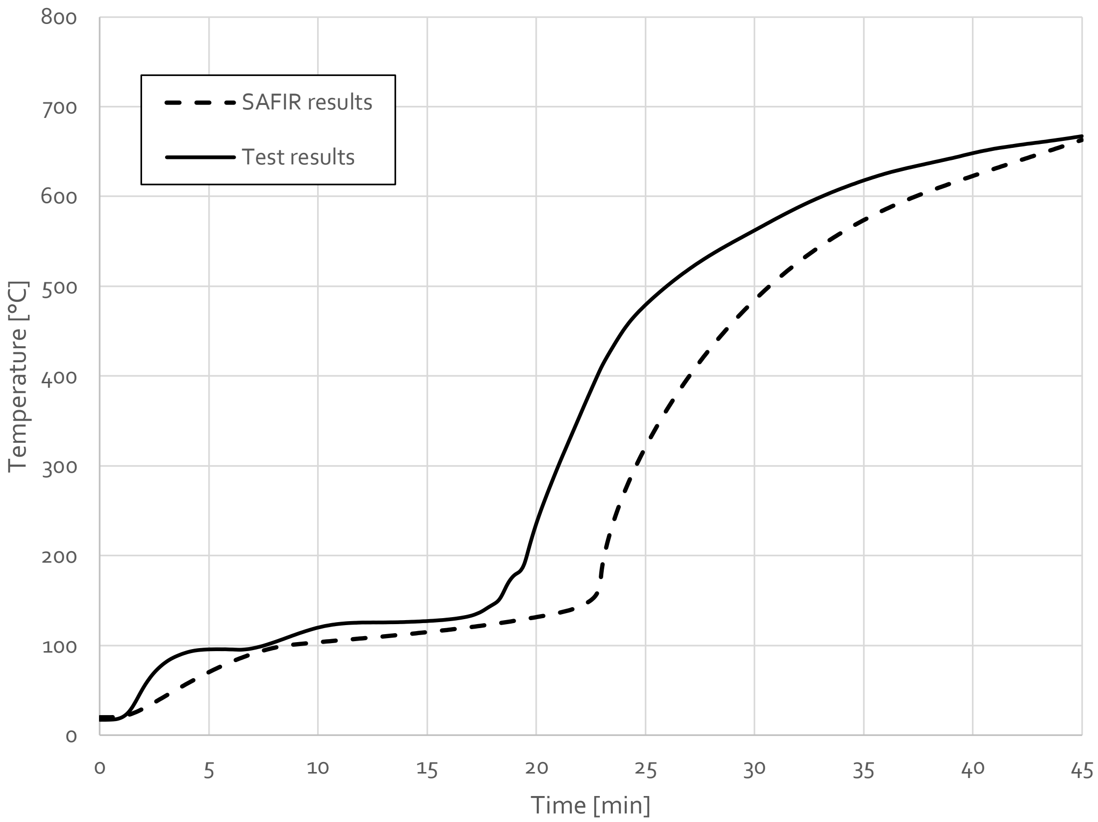

Figure 5.3 – Comparison of test results and simulations of the second test configuration

Simulations of the second test configuration (T2) do not have acceptable results. The SAFIR curve shown in a dashed line is unsafe for the whole duration of the test. The character of the curves is quite similar but the simulations show a longer horizontal part in the beginning. That means the evaporation of water takes too long and the specific heat curve should have a lower and/or shorter peak.

Test methods are available for measuring specific heat, however, this parameter is dependent on the way of heating. Currently available test equipment allows for either a constant heat flux or a constant temperature rise in the specimen. Both of these methods do not correlate well with the standard fire curve and therefore the results cannot be applied directly. A solution to this problem was to find the necessary input by way of a MATLAB code.

The idea to use computing software to look for the input parameters was put forward by Daniel Brandon, PhD, in a meeting held at SP Technical Research Institute in Stockholm. That was a turning point in the whole thesis as it was realised that with such an approach the implementation of any number of new materials could be unified. A detailed schematic of the code progression written in MATLAB R2015a is presented in Appendix A. The same method can be used to calibrate other properties as well.

The code for finding the input curve is based on rather simple principles. The software changes one value by a set percentage and then calculates the difference between the simulated and test result curves. This is done in loops the number of which can be different. It was found that executing three consecutive loops with different increments yielded good results without taking too much time.

The temperature curve of T1 resulting from calibration of specific heat to fit the same test data and the modified thermal conductivity from [15] is presented in Figure 5.4.

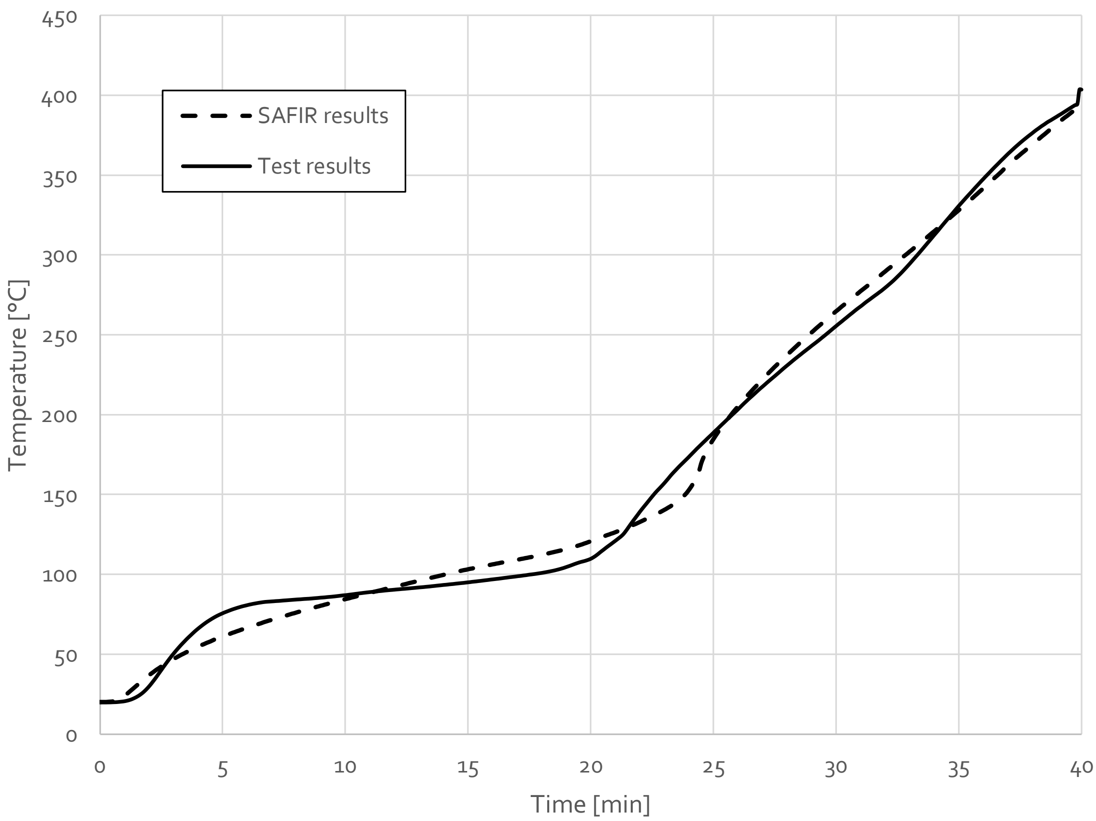

Figure 5.4 – Comparison of test results and simulation of T1 with thermal conductivity from [15] and specific heat calibrated to fit T1

The curves show rather good correlation, especially at and after the 200°C mark. In order to determine if these input parameters are suitable for other simulations, configuration

T2 was simulated. The comparison of test results and SAFIR curve is presented in Figure 5.5.

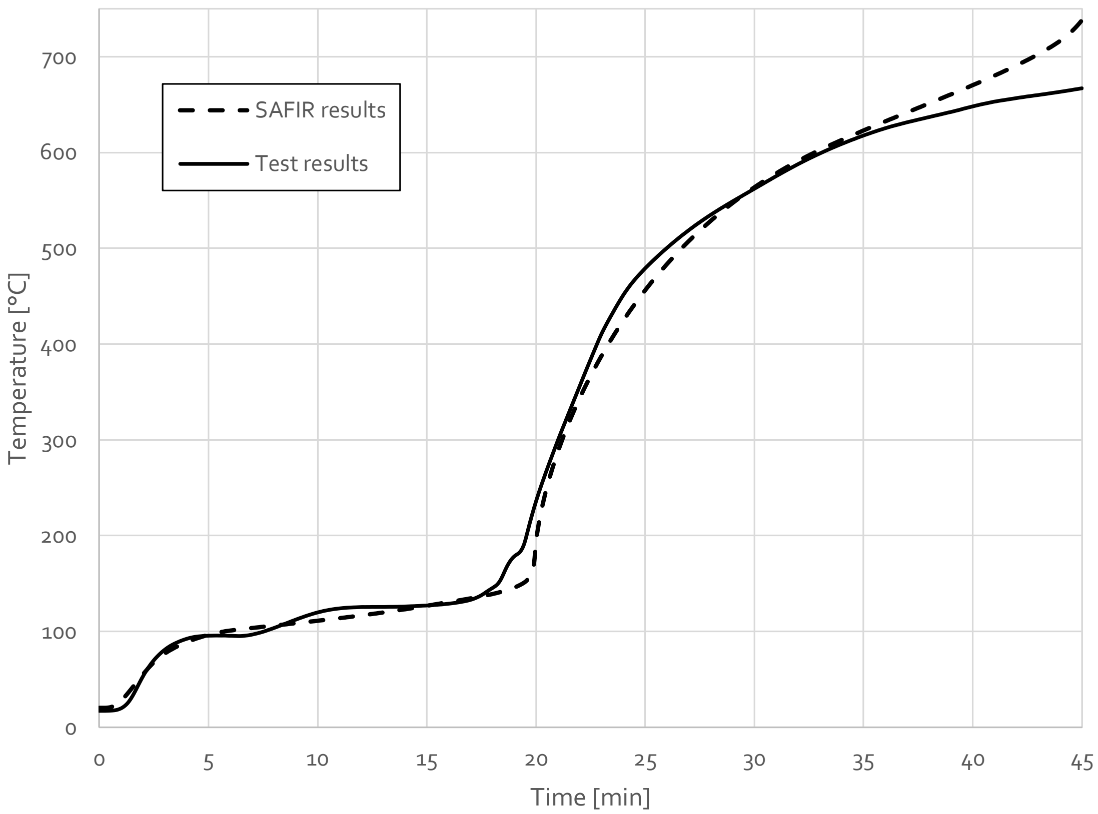

Figure 5.5 – Comparison of test results and simulation of T2 with thermal conductivity from [15] and specific heat calibrated to fit T1

The curves above show good similarity even though the simulations are slightly on the unsafe side. To evaluate the effectiveness of these input parameters used in the last two graphs, another test configuration – T3 – was simulated, see Figure 5.6.

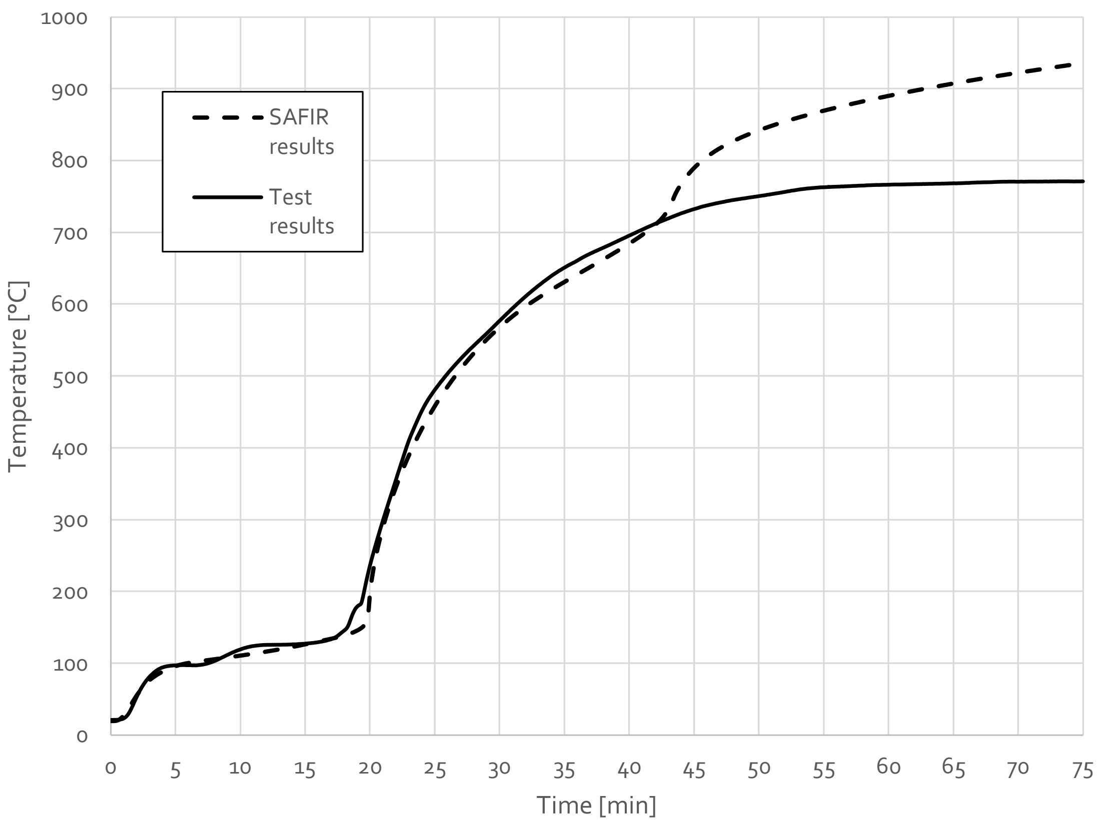

Figure 5.6 – Comparison of test results and simulation of T3 with thermal conductivity from [15] and specific heat calibrated to fit T1

As can be seen form the graph above, the calibration of specific heat and thermal conductivity from [15] provide rather good results. The difference is large at temperatures above 700°C. This could be caused by the approximate nature of the simulations where solely conductive heat transfer is taken into account inside the material. Such high temperatures are really not much of a concern in the scope of this thesis because the charring of timber starts at approximately 300°C.

In order to validate the thermal properties of *Protect F*, test configuration T4 was simulated with the input parameters used in the previous three graphs (see results in Figure 5.7).

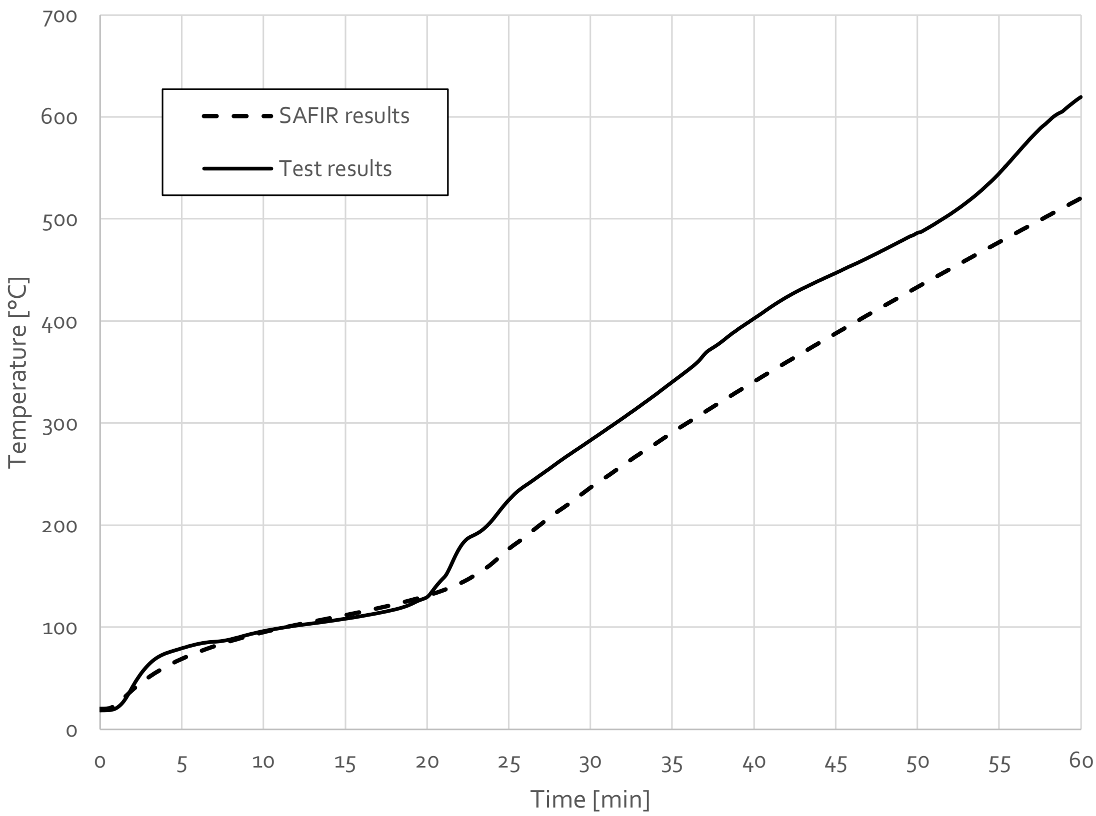

Figure 5.7 – Comparison of test results and simulation of T4 with thermal conductivity from [15] and specific heat calibrated to fit T1

The simulated curve is much too unsafe during most of the test. This means that in the previously simulated tests (T1…3) the combination of the backing layers is similar enough to counteract the incorrectness of the modified thermal properties of gypsum plasterboard.

As test T4 consisted of only gypsum plasterboards, it should provide the most accurate results to describe the particular material. Therefore, the thermal properties were calibrated to fit the results of test four. It was decided to calibrate thermal conductivity first and then specific heat. The results are presented in Table 5.1 which shows a table of graphs where a comparison between all the results can be made.

Table 5.1 – Comparison of time-temperature curves of tests T1…T4 with different thermal properties

<table>
<tr><th>Thermal conductivity from [15] and specific heat calibrated to T1</th><th>Thermal conductivity and specific heat calibrated to fit T1</th><th></th></tr>
<tr><td>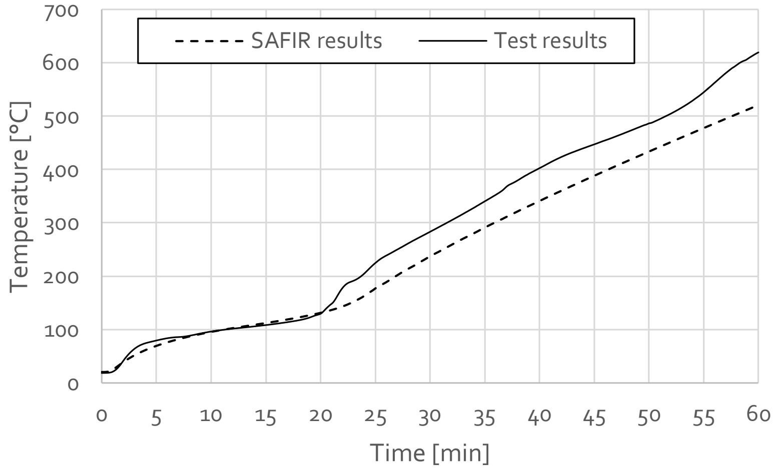
</td><td>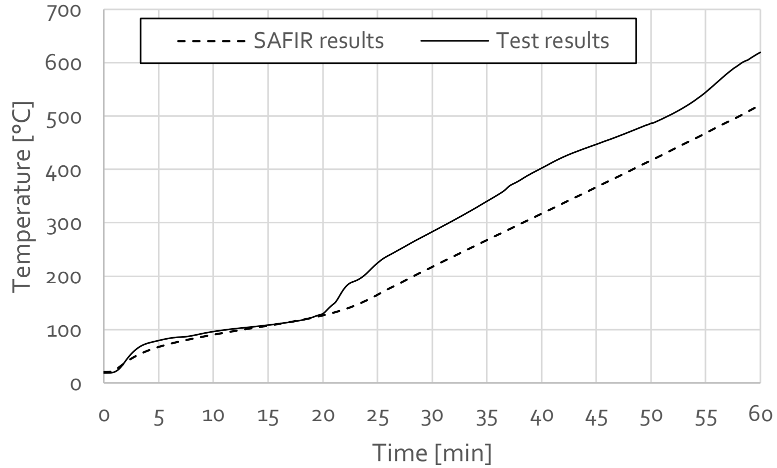
</td><td>Comparison of test results and simulations of test T4</td></tr>
<tr><td>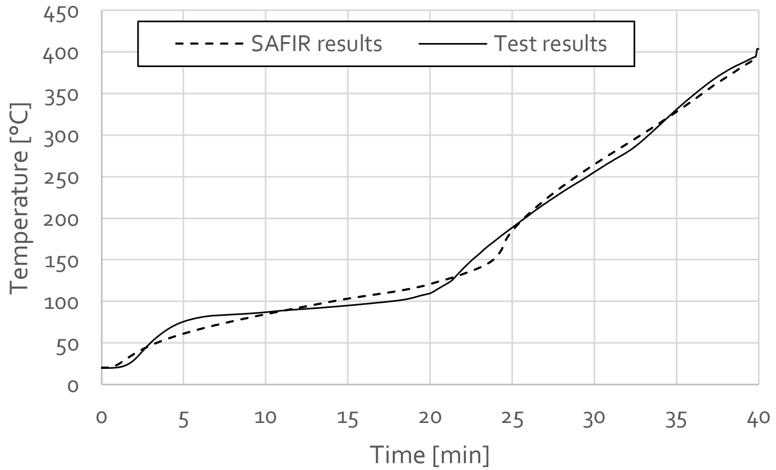
</td><td>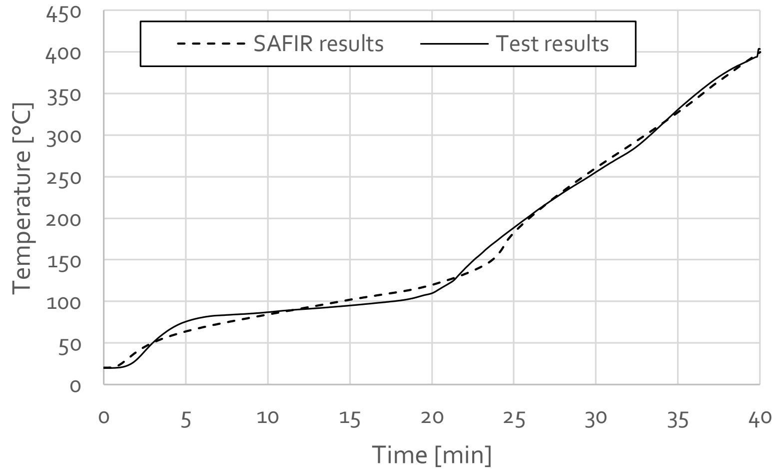
</td><td>Comparison of test results and simulations of test T1</td></tr>
</table>

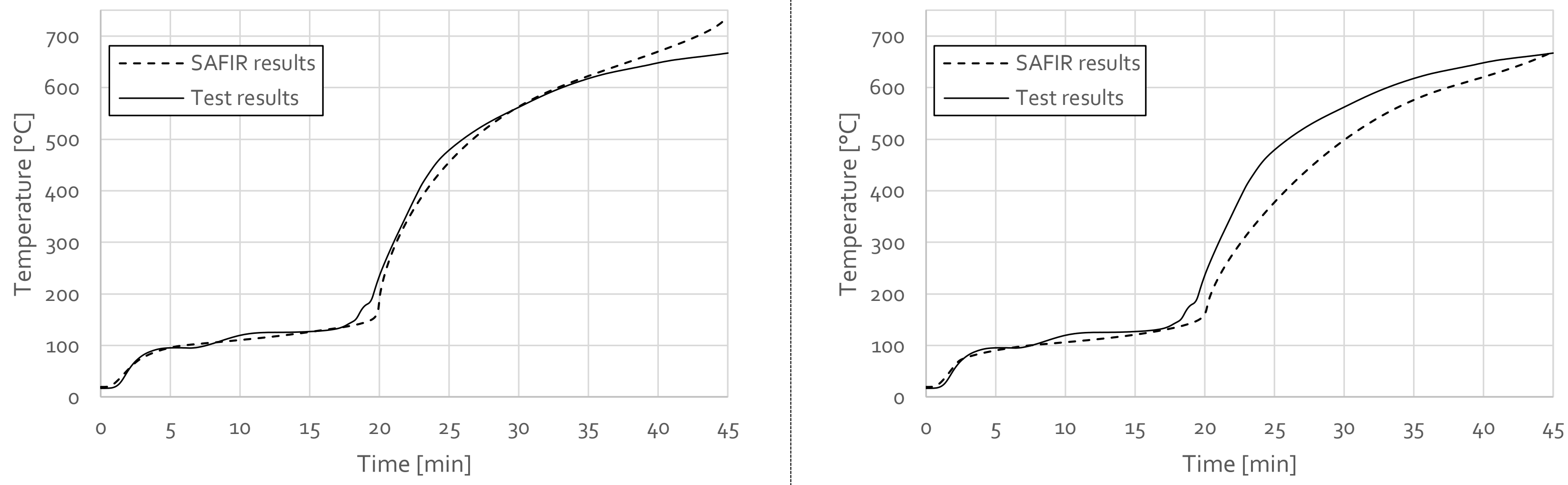

Comparison of test results and simulations of test T2

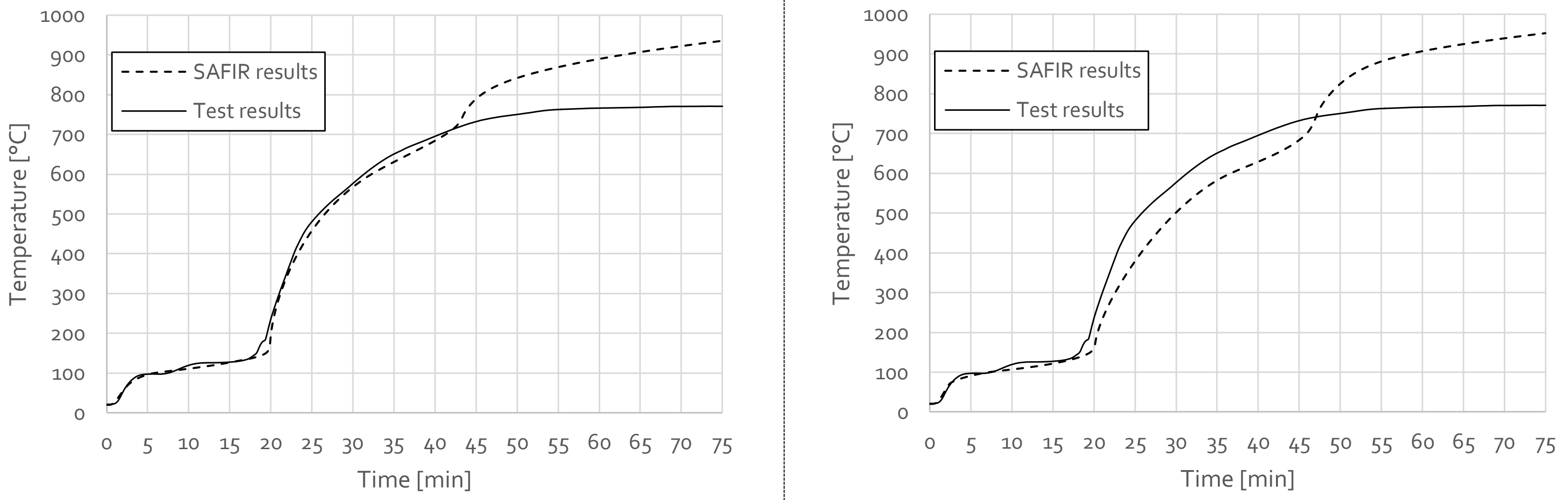

Comparison of test results and simulations of test T3

<table>
<tr><th>Thermal conductivity from [15] and specific heat calibrated to T4</th><th>Thermal conductivity and specific heat calibrated to fit T4</th><th></th></tr>
<tr><td>
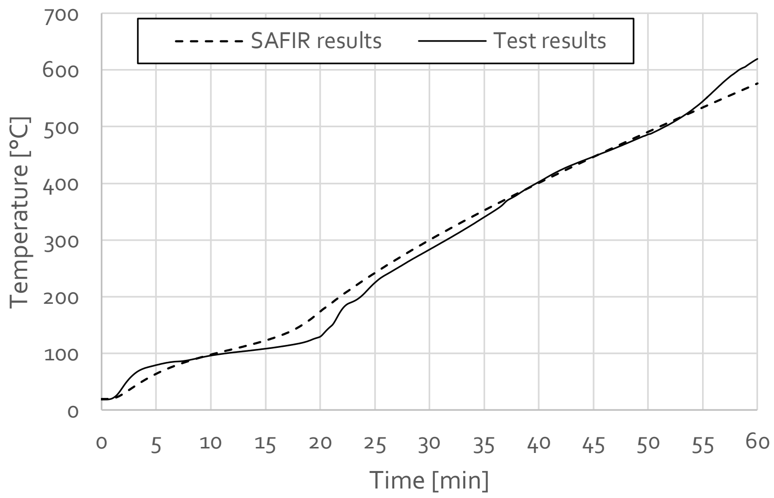

</td><td>
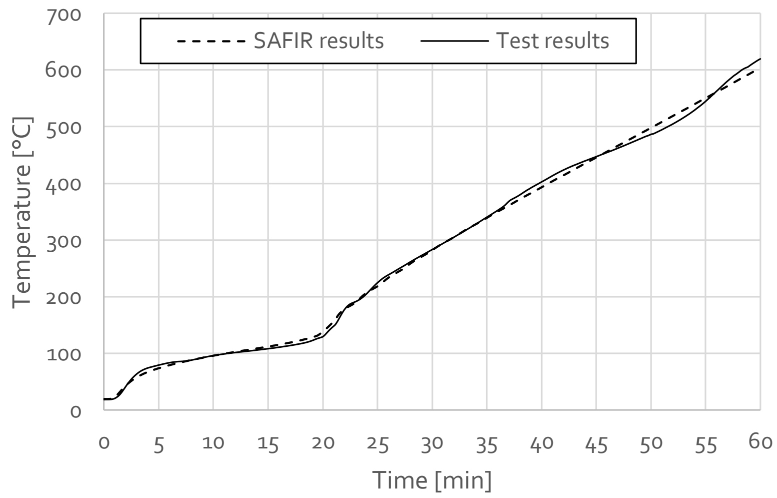

</td><td>Comparison of test results and simulations of test T4</td></tr>
<tr><td>
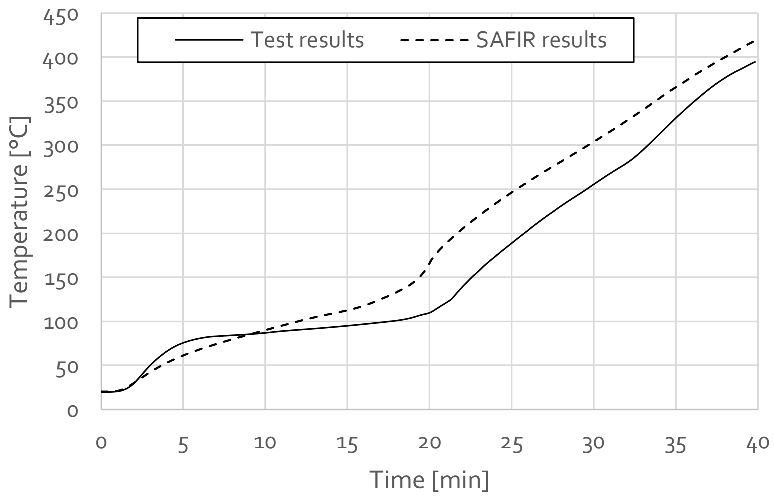

</td><td>
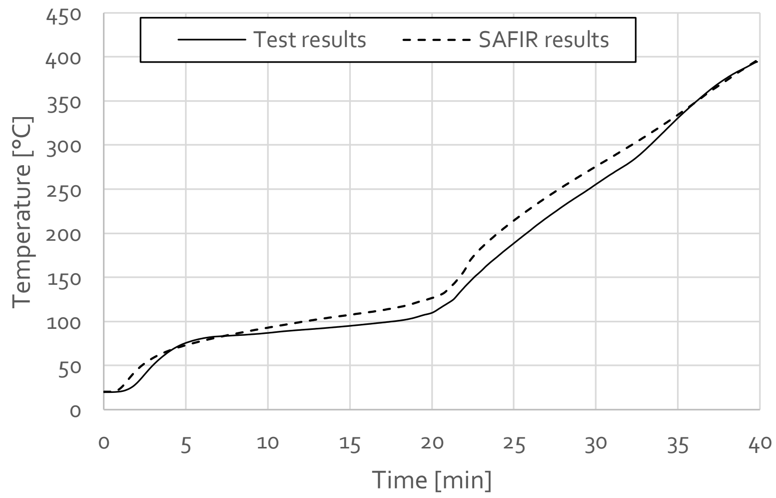

</td><td>Comparison of test results and simulations of test T1</td></tr>
</table>

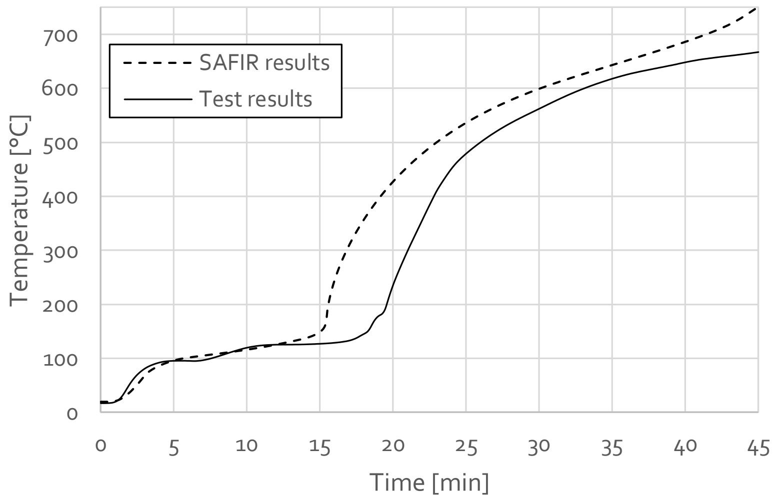

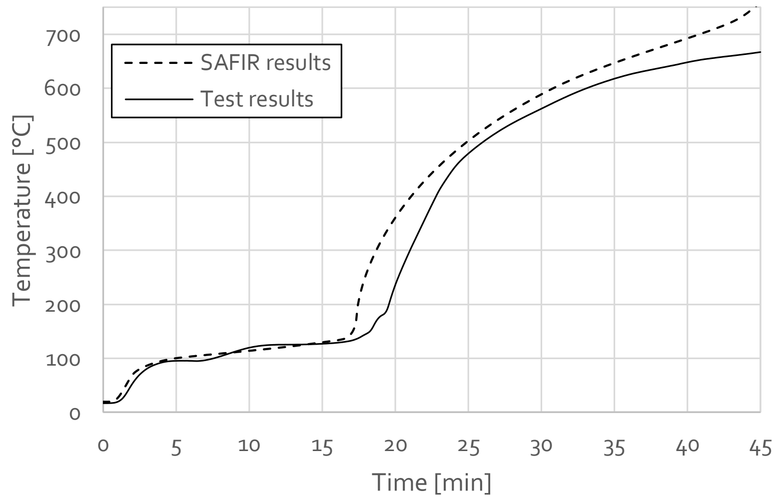

Comparison of test results and simulations of test T2

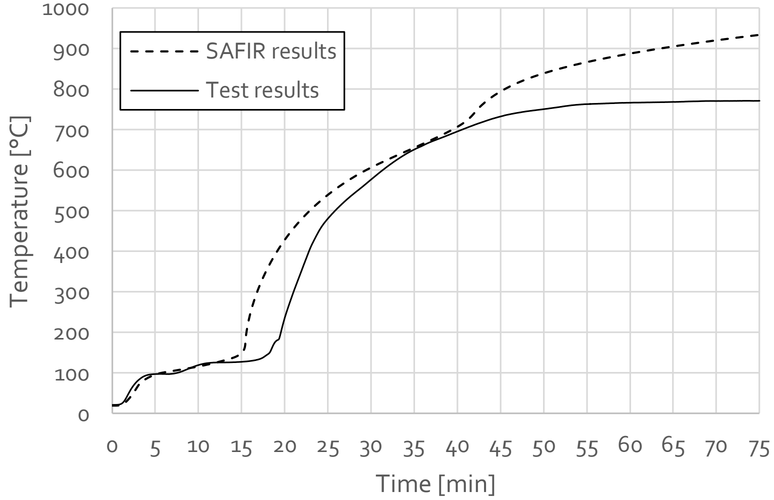

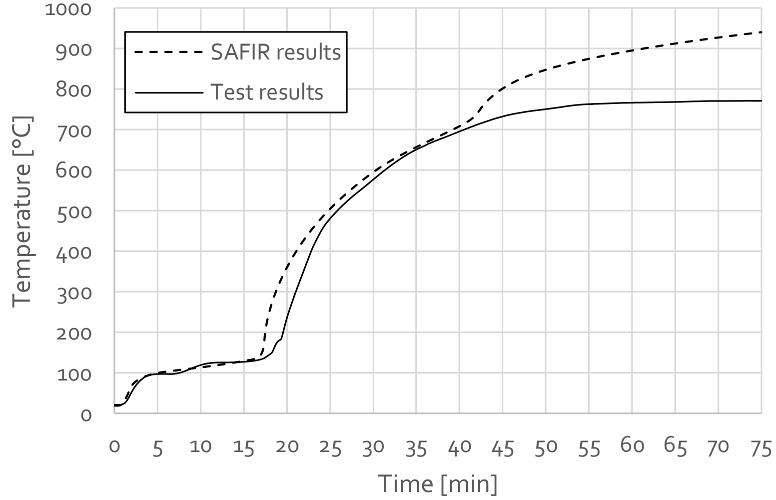

Comparison of test results and simulations of test T3

The results presented in Table 5.1 are rather interesting. In one column are graphs obtained from simulations with thermal conductivity from [15] and specific heat calibrated to fit either test one or test four. As can be seen, the thermal parameters from T1 show very good results in all tests with exception to test four, which is unsafely simulated. This shows that the configuration used for calibration is extremely important. Also interestingly, calibrated thermal conductivity and specific heat curves provide worse results.

In the second half of the table are results with parameters fitted to test four. Across the different tests, the simulations done with calibrated thermal conductivity and specific heat show safe and acceptable results. Therefore, based on this investigation, these thermal properties shall be declared as effective for *Protect F*.

5.3. Effective thermal properties for *Protect F*

In the following the graphs of effective thermal properties obtained from calibration to fit test four are presented in comparison with the curves proposed in [6]. See Figure 5.8 and Figure 5.9 for comparisons of thermal conductivity and specific heat curves.

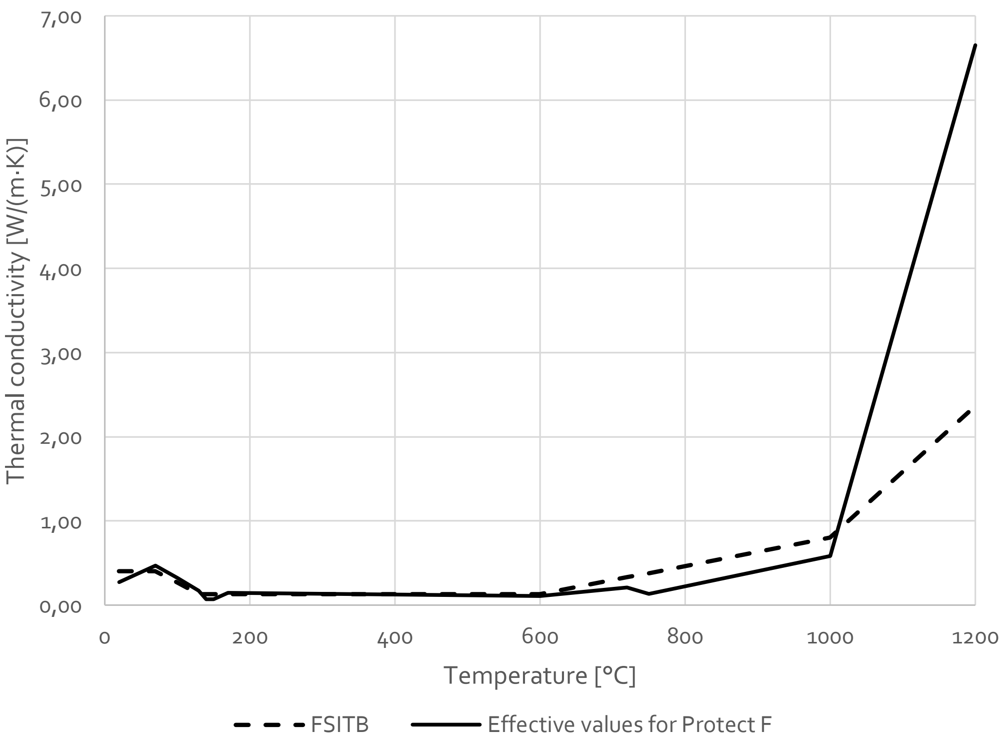

Figure 5.8 – Comparison of thermal conductivity curves

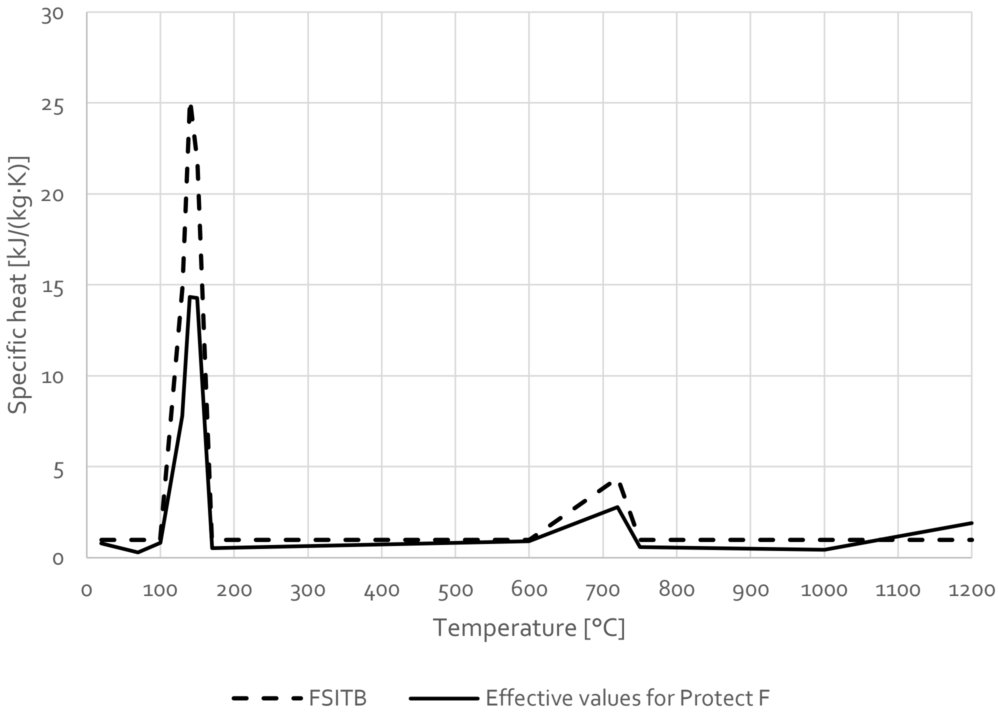

Figure 5.9 – Comparison of specific heat curves

These curves yielded the best results in the simulated configurations (see comparisons in Table 5.1). As shown in chapter 3 there can be significant differences in the thermal properties' curves. Such is the case in this study. Both the thermal conductivity and specific heat curves are lower than proposed in [6] throughout almost all of the temperatures.

In the thermal conductivity graph a high peak can be observed at 1200°C. It must be pointed out that these calibrated thermal properties are generated to provide good results in simulations which unfortunately do not take into account the physical changes in the material. Therefore, even if there is no particular reaction happening in the material at that temperature, there might be hair-like micro cracks forming, which increase the effective thermal conductivity needed as input for the simulations.

6. Model for implementation of new materials

This chapter outlines the procedure for implementation of new materials described at length in the previous chapter. The procedure is applied on a gypsum plasterboard and cellulose fibre insulation.

Stage	Deliverable(s)
• Literature survey	– Material properties and chemical composition – Thermo-chemical reactions – Thermal properties' curves
• Choosing of test setups for model scale tests	
• Model scale tests	– Thermocouple readings of temperatures at different characteristic locations – Input for calibration of thermal properties
• Choice of calibration procedure	– Which parameters to calibrate – Which method to use for calibration (guesses, iterative mathematical method, etc.)
• Calibration of thermal properties	– Input curves of thermal parameters
• Simulations of other test setups	– Temperature curves with the same input parameters but different setups
• Comparisons of results	– Graphic comparisons of results of simulations of different setups
• Choosing and declaring effective thermal properties	– Effective thermal properties' curves for thermal simulations

6.1. Application of the model on Habito gypsum plasterboard

Habito is classified as a type A gypsum plasterboard. In small scale fire tests, it showed nearly as good fire resistance as *Protect F* which is classified as a type F board. Therefore, the calibration procedure was started from the *Protect F* effective values. After calibration, the simulated curve approached the fire test results nearly perfectly as shown in Figure 6.1. Test configuration T4 (only gypsum plasterboards, as shown in Figure 4.8 and Figure 4.9) was used for calibration.

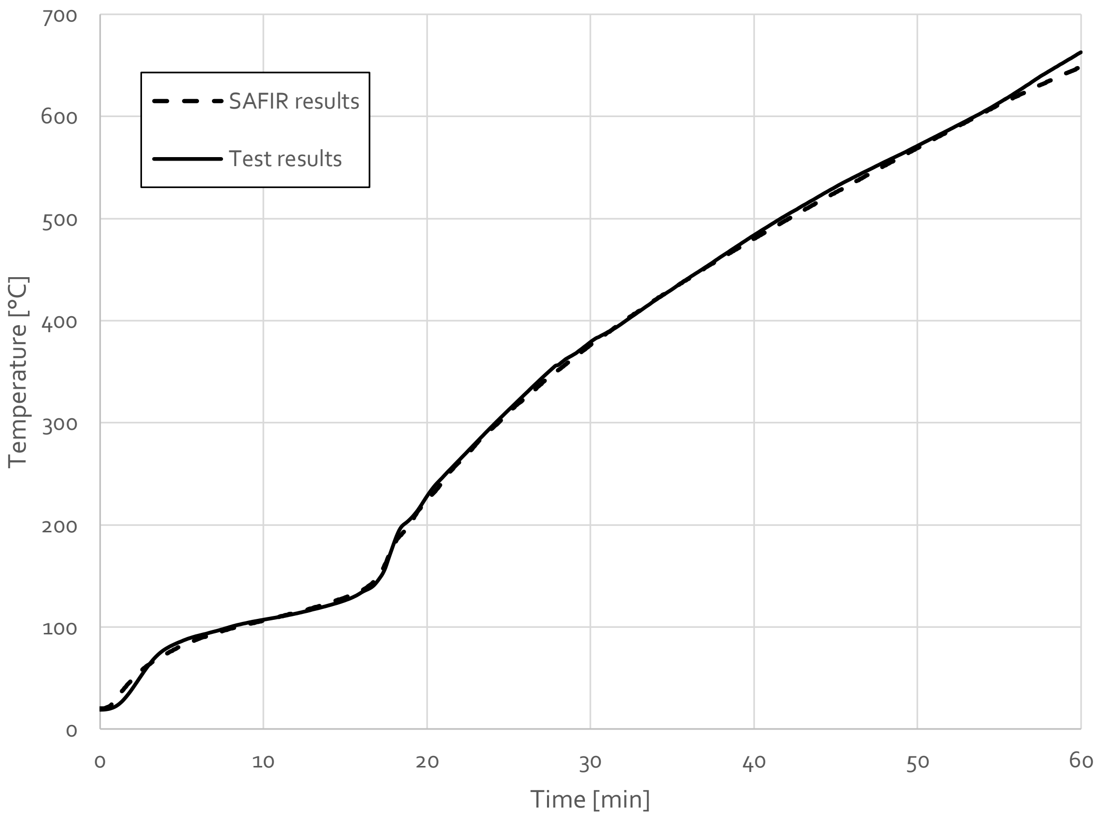

Figure 6.1 – Comparison of temperatures on the unexposed side of Habito board in test T4

The thermal properties used for the simulation presented in the figure above, are shown in Figure 6.2 and Figure 6.3.

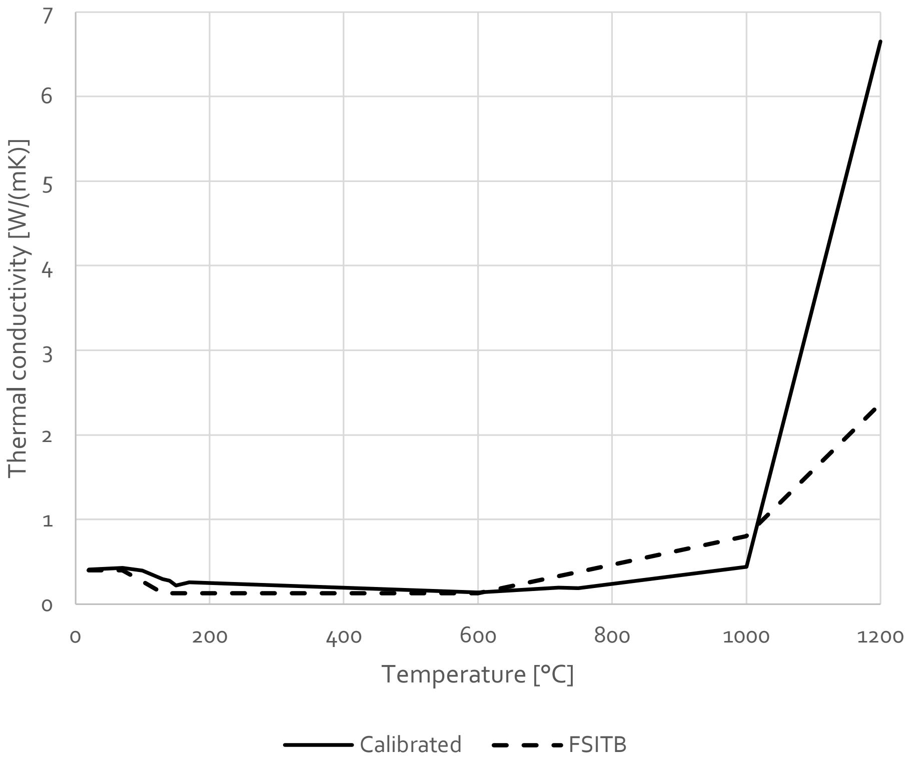

Figure 6.2 – Comparison of thermal conductivity calibrated to fit Habito in T_4, and presented in [6]

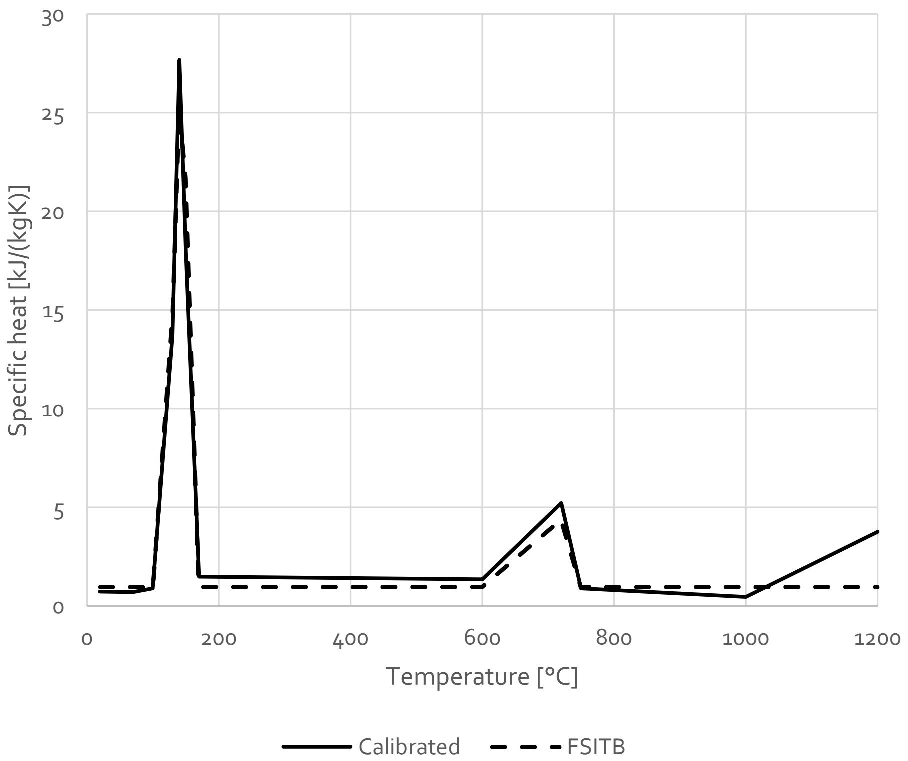

Figure 6.3 – Comparison of specific heat calibrated to fit Habito in T_4, and presented in [6]

6.2. Application of the model on cellulose fibre insulations

As previously stated, using such a code for calibrating the thermal properties could be applicable to other materials. This hypothesis is tested in this subchapter considering cellulose fibre insulations both in loose fill and batt types. This material was chosen because it is completely different from gypsum plasterboards and it is gaining popularity in the industry as a green building material.

Initially a literature survey was attempted to find at least some starting points to calibration. Results were non-existent considering the behaviour of the material at higher temperatures. It seems that there is interest in showing that cellulose fibre insulations can be used safely in the fire scenario but very little is being shown by way of actual results. Therefore, it was decided that this class of materials would be interesting to try the developed model on.

Results of thermo-gravimetric analysis and transient plane source test [24] were used as the starting point for the curves of thermal conductivity, specific heat and loss in mass. The missing points on the curves were filled in using analogy with mineral wools. As discussed earlier, loss in mass is not calibrated. It was also useful that the test data showed a full curve for density loss.

Eight model scale test results with different types of cellulose fibre insulation were available to the author. Of these tests, two were conducted without protective cladding and two more with *Protect F*. The types of cellulose fibre insulation were loose fill insulation in the original composition (OF) and fire improved loose fill (FF). The third was a batt type material (BF).

As seen with gypsum plasterboards, the most universal thermal properties are found with calibrating the setups with the least amount of uncertain materials. Therefore, for cellulose fibre insulation, the input parameters found with simulations of unprotected test results were declared effective. However, these are preliminary results, since so few tests have been conducted with these materials. Also, the thermo-chemical behaviour of cellulose fibre insulations is little researched.

The test configurations used for calibration both had a 19 mm wood fibreboard on the unexposed side, 45x145 mm timber members surrounded by the insulation which was held in place by chicken net. The cavities were filled completely with the insulation materials.

The graphs shown in Figure 6.4 to Figure 6.6 present the time-temperature curves obtained with the thermal properties shown in Figure 6.7 to Figure 6.9.

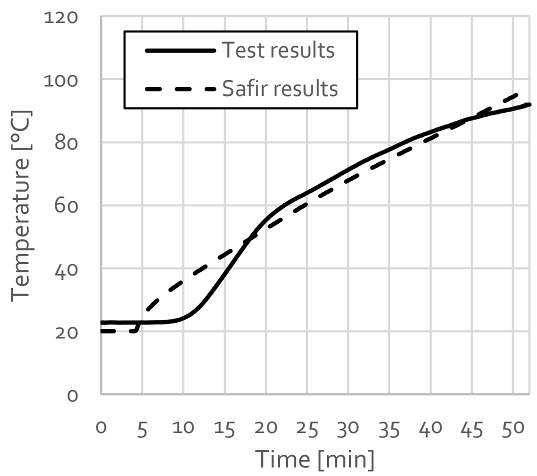

Figure 6.4 – Comparison of test results and simulated temperature curves for batt type cellulose fibre insulation (BF)

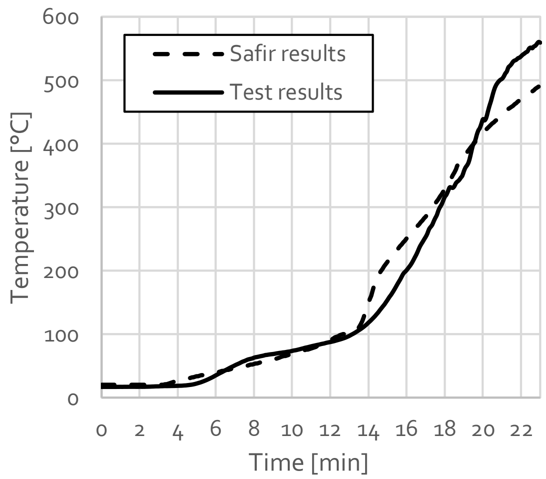

Figure 6.5 – Comparison of test results and simulated temperature curves for original loose fill cellulose insulation (OF)

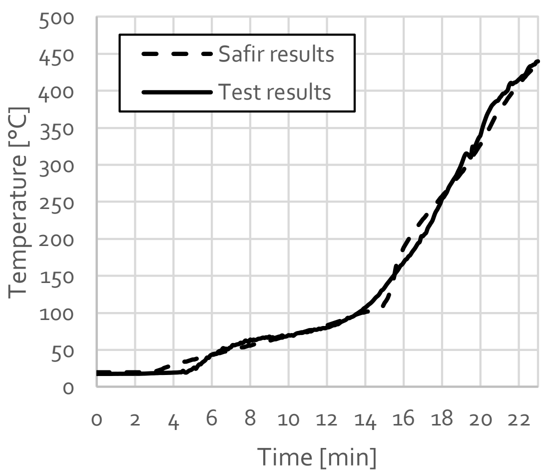

Figure 6.6 – Comparison of test results and simulated temperature curves for fire improved loose fill cellulose fibre insulation (FF)

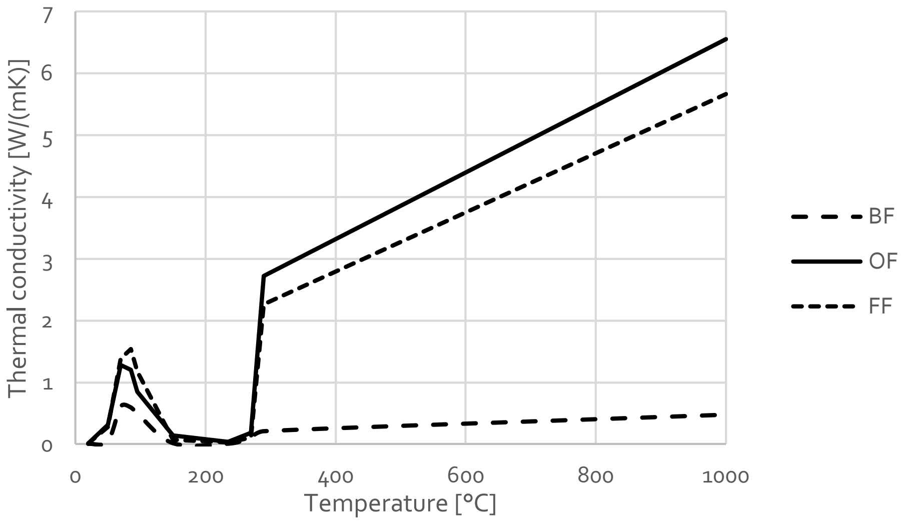

Figure 6.7 – Calibrated effective thermal conductivity curves of cellulose fibre insulations

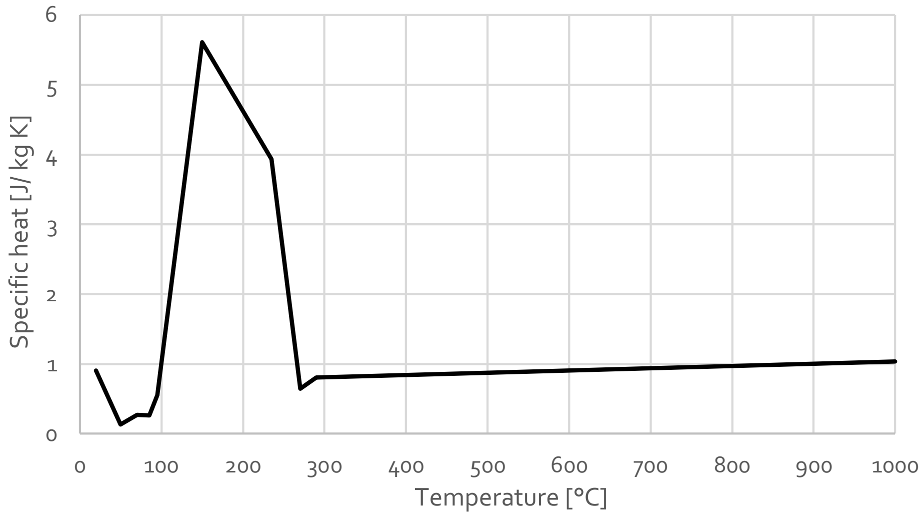

Figure 6.8 – Calibrated effective specific heat curve for cellulose fibre insulations

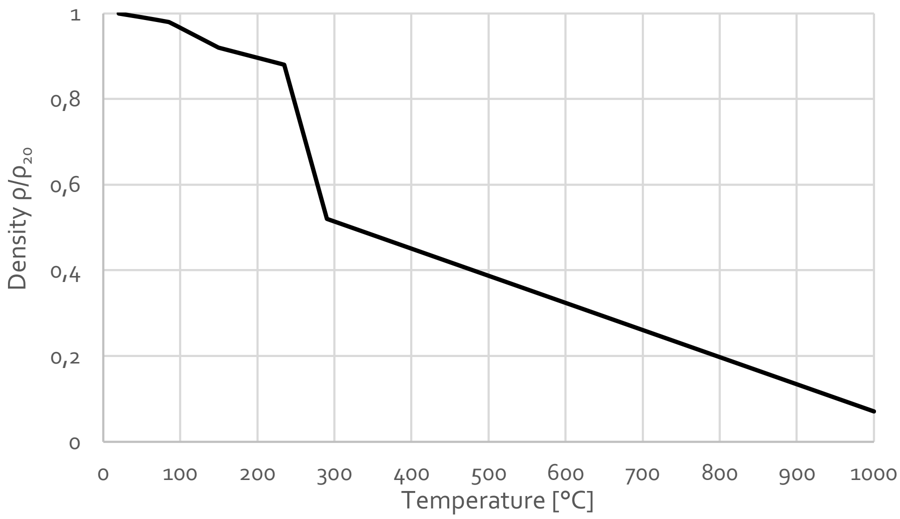

Figure 6.9 – Effective mass loss curve for cellulose fibre insulations

7. Design equations

In this chapter design equations are developed for two gypsum plasterboards.

7.1. Protect F

The procedure used for developing the design equations is based on the work of Schleifer [5] and it is used for all the materials in view of this thesis. It is described in more detail for *Protect F* board.

As shown in chapter 2.2 there are multiple components to be specified for a material to be added to the improved component additive method. These are basic insulation and protection times, position coefficients and for type F gypsum boards also the correction times. All of these values are based on specific simulations conducted with the calibrated thermal properties obtained in previous chapters.

The basic insulation time is the time of standard fire exposure during which the temperature rise on the unexposed side is equal to 140 K on average over the area of the structure and 180 K in one single point. In the simulations, the single point criterion is not taken into account. In this work the starting temperature is taken to be 20°C and therefore the average temperature on the unexposed side is limited to 160°C.

The basic protection time is the time until the temperature rise behind the layer in question is 250 K on average and 270 K in a single point. This work focuses on the average temperature rise up to 270°C (initial temperature of 20°C with the temperature rise of 250°C added).

The simulation configurations for obtaining the basic insulation time and basic protection time are presented in Figure 7.1.

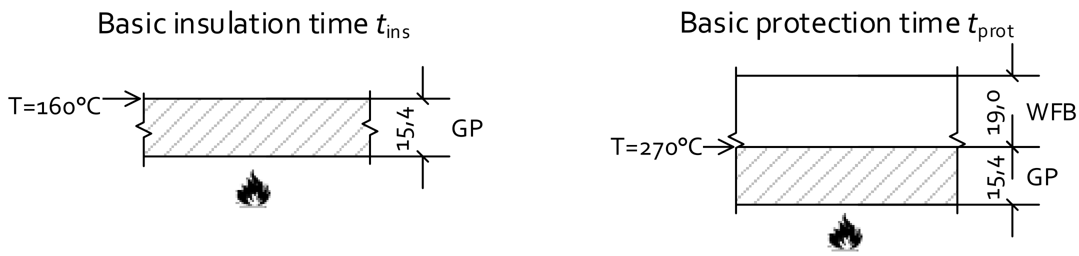

Figure 7.1 – FE simulations for Basic insulation time and Basic protection time (GP - gypsum plasterboard, WFB - wood fibreboard)

The equations for calculating the basic insulation and protection times given in [6] are presented depending on the thickness of the material. In the case of *Protect F* only one board with a set thickness of 15.4 mm is available. Therefore, the basic insulation and protection times are proposed in this thesis as one number representing the time in minutes it takes for the temperature on the unexposed side to reach the set criteria.

Resulting from a simulation of the configuration presented in Figure 7.1 on the left, the basic insulation time $t_{ins,0,n}$ is proposed as:

$$t_{\text{ins,0,n}} = 20 \text{ [min]} \tag{6}$$

The basic protection time $t_{prot,0,i}$ according to the FE simulation of the configuration presented on the right-hand side of Figure 7.1 is:

$$t_{\text{prot,0,i}} = 31 \text{ [min]} \tag{7}$$

For the development of position coefficients, a more elaborate system of FE simulations and configurations was needed.

The position coefficient $k_{pos,exp}$ takes into account the effect the preceding layer (in the direction of heat flow) has on the layer in question. For gypsum plasterboards the preceding layer could be either a cladding or some type of insulation. This is simplified to some extent in the simulations which are narrowed down to two configurations presented in Figure 7.2.

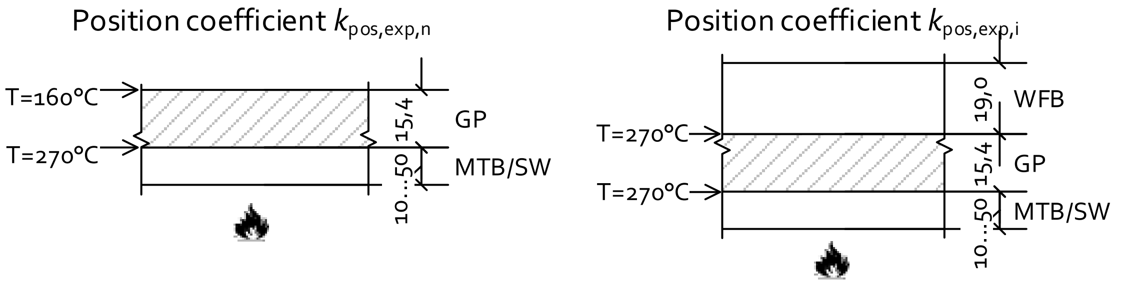

Figure 7.2 – FE simulations for position coefficients $k_{pos,exp,n}$ and $k_{pos,exp,i}$ (GP gypsum plasterboard, WFB – wood fibreboard, MTB – massive timber board, SW – stone wool)

Position coefficient $k_{pos,exp,n}$ is used when the investigated layer n is the last layer counting from the exposed side. The temperature criteria for the last layer is 160°C average over the whole area of the unexposed side. This is represented by the left-hand side drawing in Figure 7.2. The investigated layer (gypsum plasterboard) is initially protected by a layer of either massive timber or stone wool with a thickness of 10-50 mm varied in 10 mm increments. The time when the temperature behind the protection layer reaches 270°C is recorded (t_1=$t_{\text{prot,n-1}}$) and the simulation is continued without the protection layer which is considered to have fallen off. When the temperature on the unexposed side of GP reaches 160°C the simulation is ended and the time recorded (t_2).

The position coefficient $k_{\text{pos,exp,n}}$ is calculated as shown in equation (8):

$$k_{\text{pos,exp,n}} = \frac{t_{\text{ins,n}}}{t_{\text{ins,0,n}}} \tag{8}$$

Where $t_{\text{ins,n}}$ is the insulation time of the layer n, calculated as $t_2 - t_1$ [min];

$t_{\text{ins,0,n}}$ is the basic insulation time of layer n [min].

Due to the different thicknesses of the preceding layer, the fall-off of the preceding layer happens at different points in time. The position coefficients can be represented graphically in order to provide a formula for the coefficient. The graphs for timber and stone wool as preceding layers are presented in Figure 7.3 and Figure 7.4. Comparisons of the proposed curves and the ones presented in [6] are also shown.

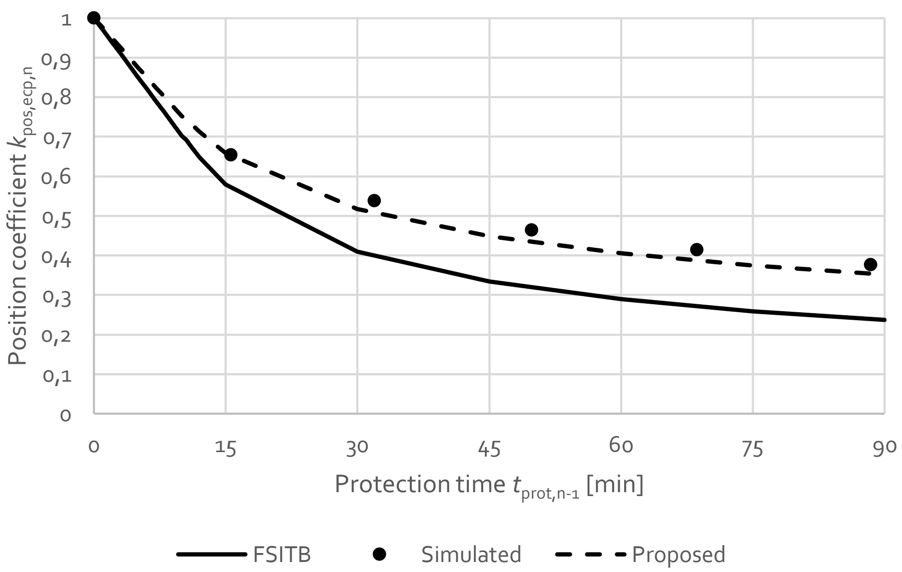

Figure 7.3 – Graphs of $k_{pos,exp,n}$ *vs.* $t_{prot,o,n-1}$ *with solid timber panel as the preceding layer*

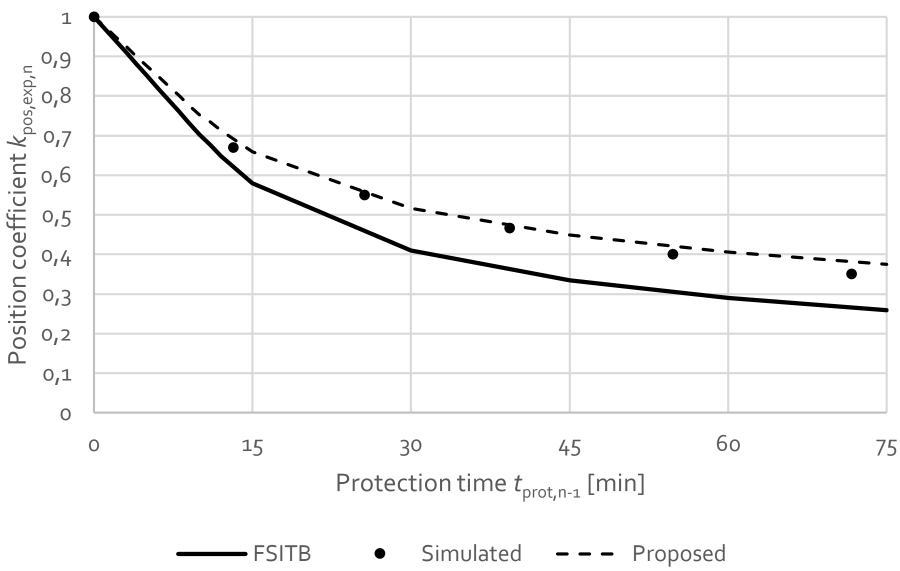

Figure 7.4 – Graphs of $k_{pos,exp,n}$ *vs.* $t_{prot,n-1}$ *with stone wool as the preceding layer*

The position coefficient $k_{pos,exp,n}$ for *Protect F* for $t_{ins,n}$ is proposed in equation (9):

$$k_{\text{pos,exp,n}} = \begin{cases} 1 - 0{,}5 \cdot \dfrac{\sum_{\text{p}=1}^{\text{n}-1} t_{\text{prot,p}}}{t_{\text{ins,0,n}}}, & \text{if} \sum_{\text{p}=1}^{\text{n}-1} t_{\text{prot,p}} \leq \dfrac{t_{\text{ins,0,n}}}{2} \\ 1{,}7 \cdot \left(\sum_{\text{p}=1}^{\text{n}-1} t_{\text{prot,p}} \right)^{-0{,}35}, & \text{if} \sum_{\text{p}=1}^{\text{n}-1} t_{\text{prot,p}} > \dfrac{t_{\text{ins,0,n}}}{2} \end{cases} \quad (9)$$

Where $\sum_{\text{p}=1}^{\text{n}-1} t_{\text{prot,p}}$ is the sum of protection times of the preceding layer(s) [min];

$t_{\text{ins,0,n}}$ is the basic insulation time of layer n [min];

The position coefficient $k_{pos,exp,i}$ was developed from the right-hand side configuration in Figure 7.2. Initially, the setup shown was simulated until the temperature between the preceding layer (massive timber panel or stone wool) and the gypsum plasterboard reached 270°C and the time was recorded as t_1. After that, the preceding layer was removed and the simulation continued. When the temperature behind the gypsum plasterboard reached 270°C the simulation was stopped and the time recorded as t_2.The formula for calculating the position coefficient is similar to (8):

$$k_{\text{pos,exp,i}} = \frac{t_{\text{prot,i}}}{t_{\text{prot,0,i}}} \quad (10)$$

Where $t_{\text{prot,i}}$ is the protection time of the layer i, calculated as $t_2 - t_1$ [min];

$t_{\text{prot,0,i}}$ is the basic protection time of layer i [min].

After simulating the setup with different thicknesses of the preceding layer, a graph was compiled of the results versus the basic protection times shown in Figure 7.5 and Figure 7.6.

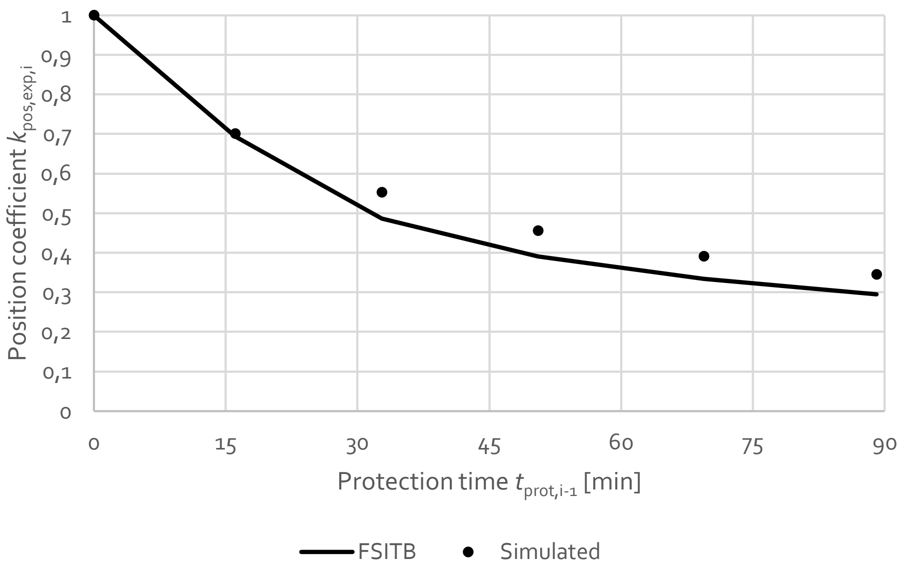

Figure 7.5 - Graphs of $k_{pos,exp,i}$ *vs.* $t_{prot,i-1}$ *with timber as the preceding layer*

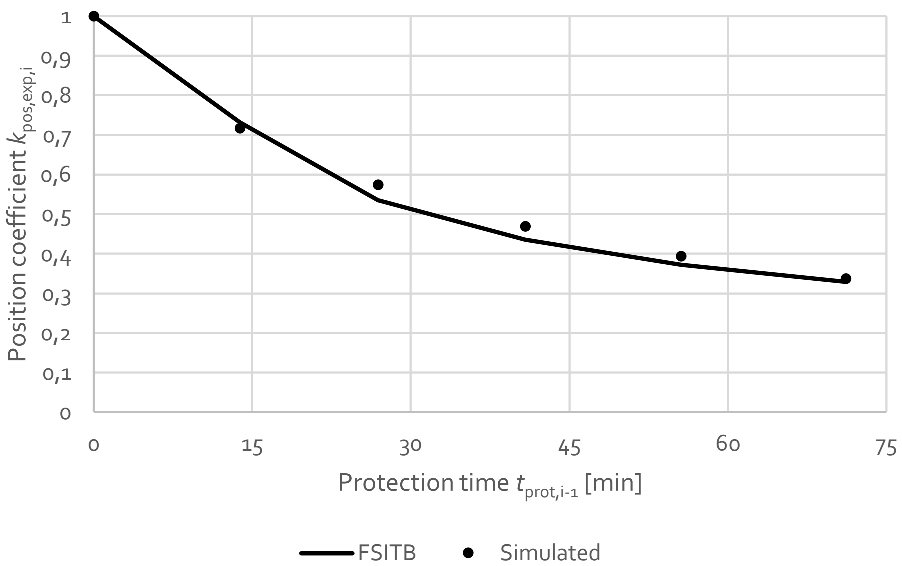

Figure 7.6 - Graphs of $k_{pos,exp,i}$ *vs.* $t_{prot,i-1}$ *with stone wool as the preceding layer*

As can be seen from the previous two graphs, the formulas presented in [6] show rather good similarity to the results of the simulations of this thesis. Therefore, the same formulas shall be used.

In the next step, the position coefficient $k_{\mathrm{pos,unexp,i}}$ was developed. This coefficient takes into account the effect the backing layer has on the layer under investigation. In [6] the values provided for different materials backed by timber or gypsum are given as 1.0. The work of this thesis confirms this finding as the results of the tests conducted with wood fibreboard or gypsum as a backing layer showed similar results. Based on this, a simulation of the setup presented in Figure 7.7 is needed.

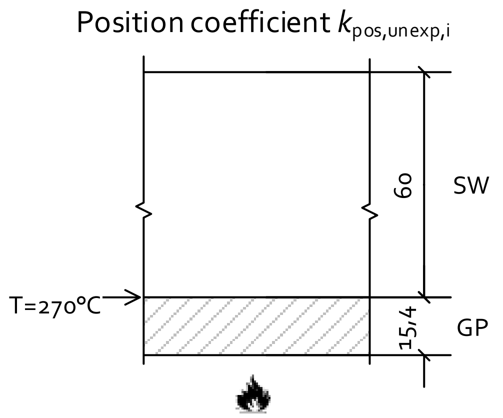

Figure 7.7 – FE simulation for position coefficient $k_{pos,unexp,i}$ *(GP – gypsum plasterboard, SW – stone wool)*

A layer of 60 mm stone wool insulation is simulated behind a layer of *Protect F*. The time required for the temperature to reach 270°C between the materials is recorded as $t_{\mathrm{prot,i}}$. Position coefficient $k_{\mathrm{pos,unexp,i}}$ is calculated according to (11):

$$k_{\mathrm{pos,unexp,i}} = \frac{t_{\mathrm{prot,i}}}{t_{\mathrm{prot,0,i}}} \tag{11}$$

For a layer of *Protect F* gypsum plasterboard backed by insulation, the position coefficient $k_{\mathrm{pos,unexp,i}}$ is proposed in (12).

$$k_{\mathrm{pos,unexp,i}} = 1{,}223 \cdot \frac{h_{\mathrm{i}}}{t_{\mathrm{prot,0,i}}} \approx 0{,}609 \tag{12}$$

For type F gypsum plasterboards it has been observed that the boards stay in place longer. To account for this in the calculation of insulation time of the structure, a correction time is added to the layer preceded by fire resistant gypsum plasterboard.

When the layer preceded by gypsum plasterboard is the last layer on the unexposed side of the structure, the correction time Δt_{n} is added to the insulation time $t_{\mathrm{ins,n}}$. It is derived from simulations of the configurations shown in Figure 7.8.

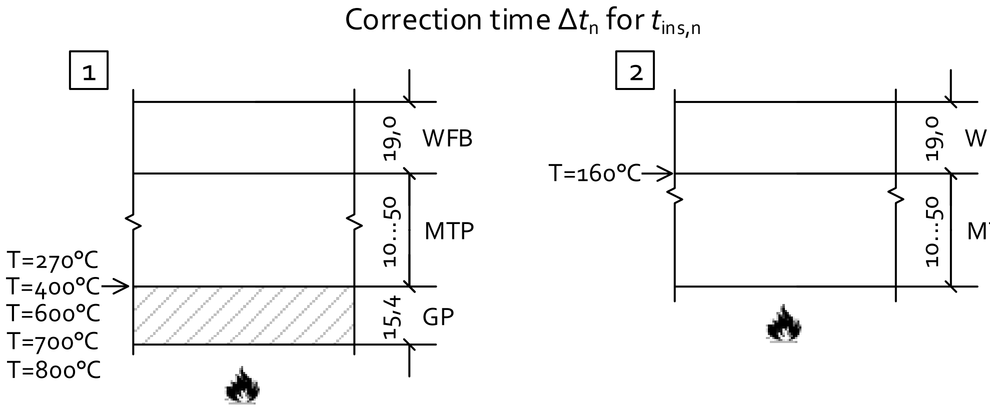

Figure 7.8 – FE simulations for correction time Δt_n *for* $t_{ins,n}$ *(GP – gypsum plasterboard, WFB – wood fibreboard, MTP – massive timber panel)*

The correction time Δt_{n} is developed only for solid panels (timber, gypsum, etc.) as the simulation tools available severely underestimate the temperature rise on the unexposed side of insulation materials when these are not backed by a cladding. This is due to the limitations created by the underlying assumption that within the material, heat is transferred only through conduction. At high temperatures and without backing, there is a significant heat transfer through fibrous insulation materials by convection which is not taken into account in the simulations. Therefore, any attempts to provide a value of correction time for insulation materials as the last layer are futile.

Firstly, the simulation is run until the temperature behind the gypsum layer reaches 270/400/600/700/800°C (shown in Figure 7.8-1) and the times are recorded as t_{270}/ t_{400}/ t_{600}/ t_{700}/t_{800}. These temperatures are chosen based on the observations of tests, where the fall-off of the boards can happen at higher temperatures behind the board [25]. When such a temperature is reached, the board is removed and the simulation continued until the temperature behind the timber panel reaches 160°C (Figure 7.8-2). The thickness of the timber panel is varied between 10-50 mm in 10 mm increments and new simulations conducted.

To develop the formulas the results are plotted on a graph with the axes being the correction time and the basic insulation time. The correction times Δt_{n} for graphs are calculated as shown in equation (13).

$$\Delta t_{\mathrm{n}} = \begin{cases} t_{400} - t_{270} \\ t_{600} - t_{270} \\ t_{700} - t_{270} \\ t_{800} - t_{270} \end{cases} \qquad (13)$$

The resulting graphs are presented below after a description of the development of the correction times Δt_i for protection times $t_{prot,i}$. The necessary simulations are shown in Figure 7.9.

Correction time Δt_i for $t_{prot,i}$

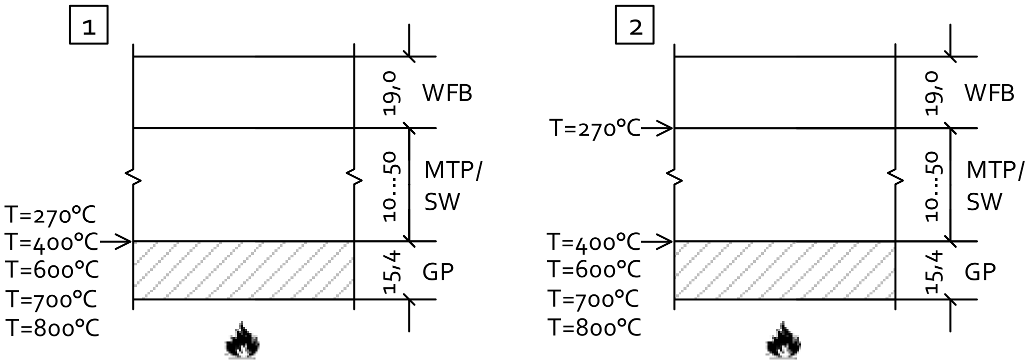

Figure 7.9 – FE simulations for correction time Δt_i *for* $t_{prot,i}$ *(GP - gypsum plasterboard, WFB – wood fibreboard, MTP – massive timber panel, SW – stone wool)*

The procedure is largely similar to the one used for developing Δt_n equations but the layer behind gypsum can be either timber or stone wool. For the sake of consistency in the results, both of the correction times' simulations have a backing layer of wood fibreboard on the unexposed side of the assembly.

For the correction time Δt_i the temperature criterion for the unexposed side of the backing layer (MTP or SW) is 270°C. In the following the graphs comparing the simulated, proposed and calculated (according to [6]) correction times are presented in Figure 7.10-Figure 7.21.

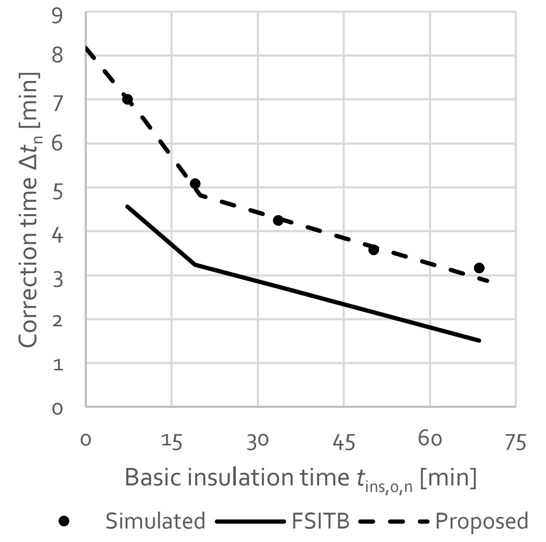

Figure 7.10 – Comparison of simulated, proposed and calculated correction times Δt_n *for timber backing when failure temperature is 400°C*

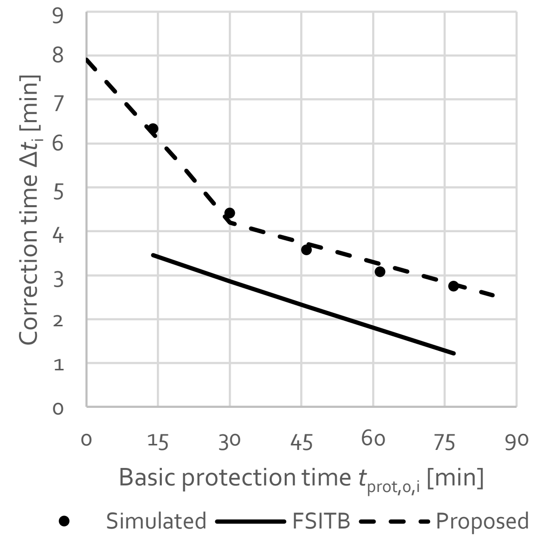

Figure 7.11 – Comparison of simulated, proposed and calculated correction times Δt_i *for timber backing when failure temperature is 400°C*

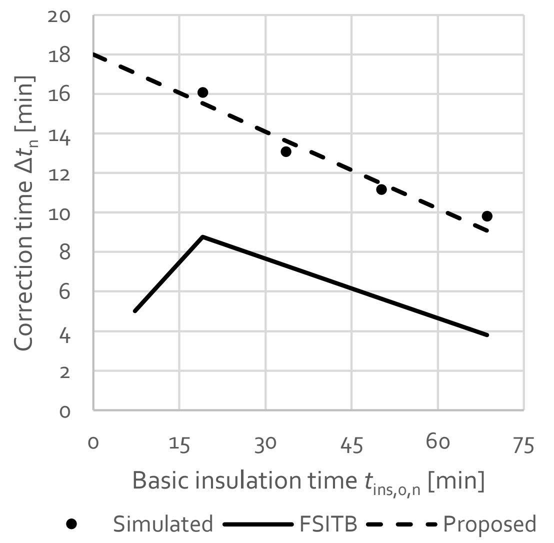

Figure 7.12 – Comparison of simulated, proposed and calculated correction times Δt_n *for timber backing when failure temperature is 600°C*

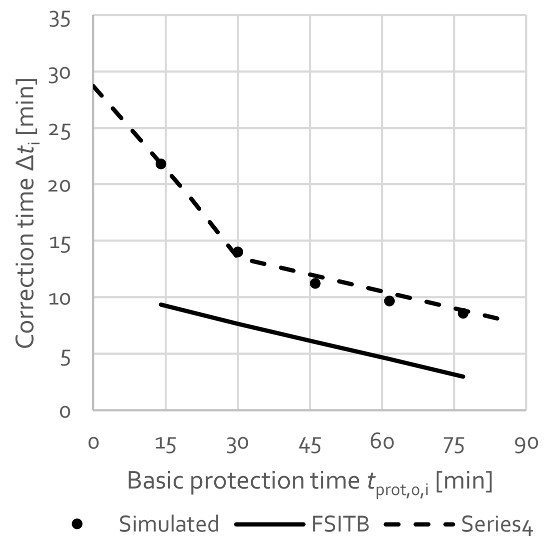

Figure 7.13 – Comparison of simulated, proposed and calculated correction times Δt_i *for timber backing when failure temperature is 600°C*

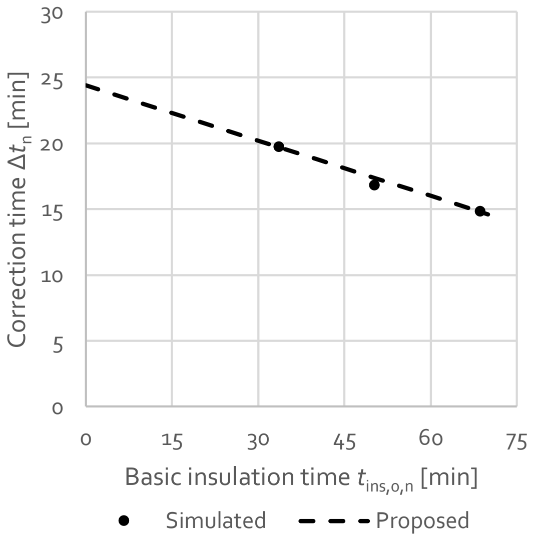

Figure 7.14 – Comparison of simulated, proposed and calculated correction times Δt*ₙ* *for timber backing when failure temperature is 700°C*

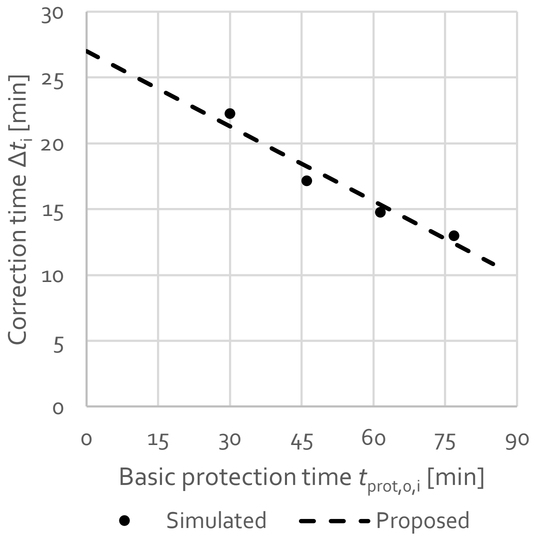

Figure 7.15 – Comparison of simulated, proposed and calculated correction times Δt_i *for timber backing when failure temperature is 700°C*

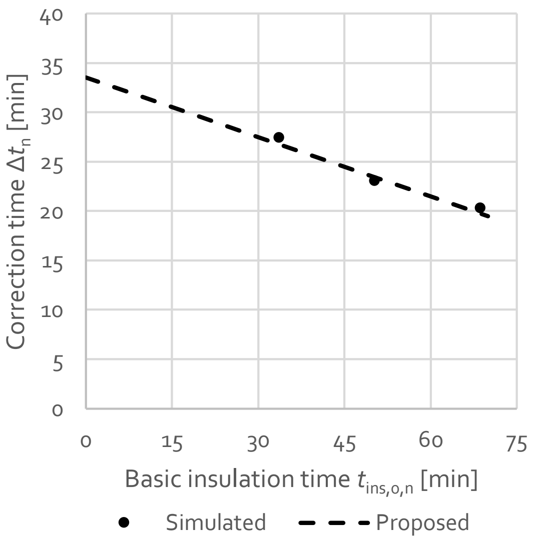

Figure 7.16 – Comparison of simulated, proposed and calculated correction times Δt_n *for timber backing when failure temperature is 800°C*

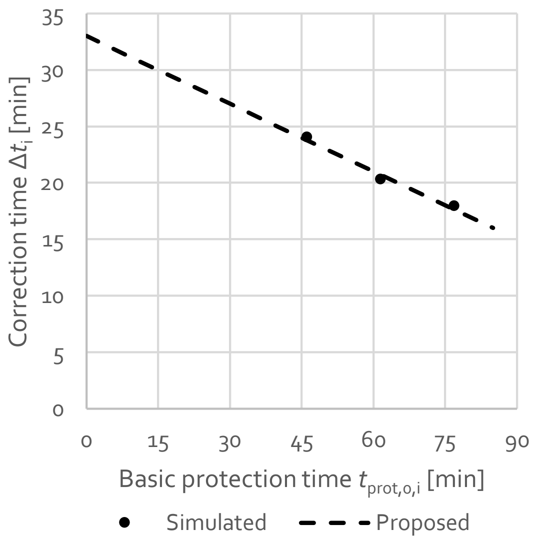

Figure 7.17 – Comparison of simulated, proposed and calculated correction times Δt_i *for timber backing when failure temperature is 800°C*

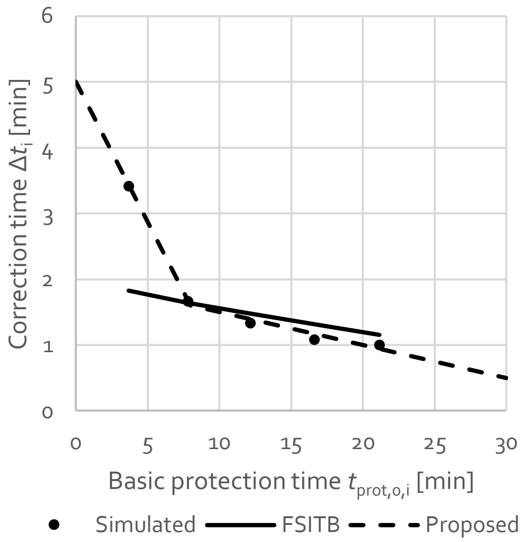

Figure 7.18 – Comparison of simulated, proposed and calculated correction times Δt_i *for stone wool backing when failure temperature is 400°C*

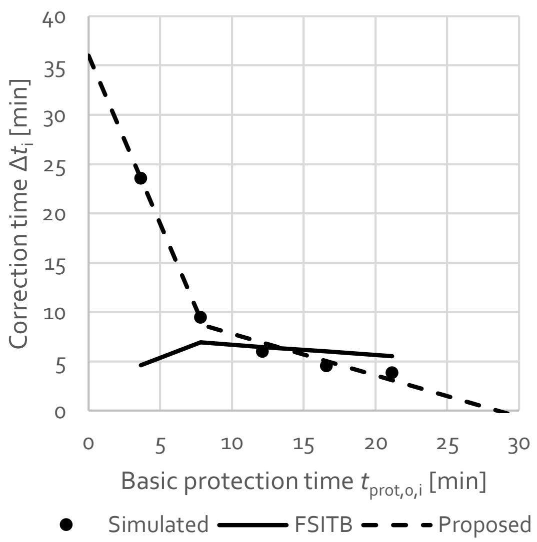

Figure 7.19 – Comparison of simulated, proposed and calculated correction times Δt_i *for stone wool backing when failure temperature is 600°C*

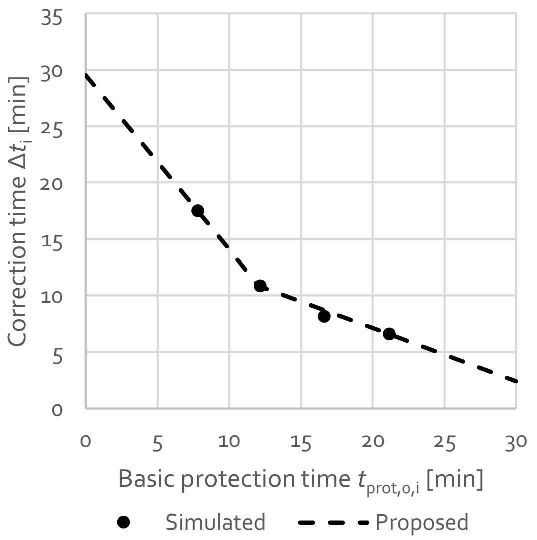

Figure 7.20 – Comparison of simulated, proposed and calculated correction times Δt_i *for stone wool backing when failure temperature is 700°C*

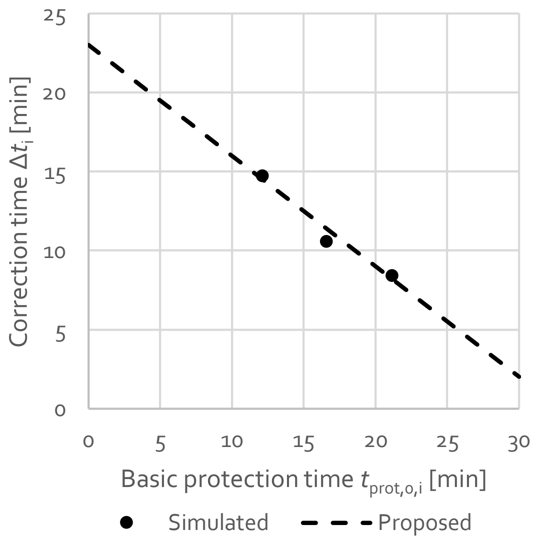

Figure 7.21 – Comparison of simulated, proposed and calculated correction times Δt_i *for stone wool backing when failure temperature is 800°C*

The formulas of the proposed curves shown in previous graphs are presented in Table 7.1.

Table 7.1 – Formulas for correction times Δt_n and Δt_i

Material	**Failure temperature**	**$t_{ins,n}$ correction time Δt_n**
Cladding (timber, gypsum plasterboard)	400°C	$8{,}17 - 0{,}16 \cdot t_{\mathrm{ins,0,n}}$ if $t_{\mathrm{ins,0,n}} < 19$ $5{,}6 - 0{,}039 \cdot t_{\mathrm{ins,0,n}}$ if $t_{\mathrm{ins,0,n}} \geq 19$
	600°C	$18 - 0{,}13 \cdot t_{\mathrm{ins,0,n}}$
	700°C	$24{,}4 - 0{,}14 \cdot t_{\mathrm{ins,0,n}}$
	800°C	$33{,}5 - 0{,}2 \cdot t_{\mathrm{ins,0,n}}$
	$t_{prot,i}$ correction time Δt_i	
	400°C	$7{,}9 - 0{,}12 \cdot t_{\mathrm{prot,0,i}}$ if $t_{\mathrm{prot,0,i}} < 30$ $5{,}1 - 0{,}03 \cdot t_{\mathrm{prot,0,i}}$ if $t_{\mathrm{prot,0,i}} \geq 30$
	600°C	$28{,}7 - 0{,}49 \cdot t_{\mathrm{prot,0,i}}$ if $t_{\mathrm{prot,0,i}} < 30$ $16{,}5 - 0{,}1 \cdot t_{\mathrm{prot,0,i}}$ if $t_{\mathrm{prot,0,i}} \geq 30$
	700°C	$27 - 0{,}19 \cdot t_{\mathrm{prot,0,i}}$
	800°C	$33 - 0{,}2 \cdot t_{\mathrm{prot,0,i}}$
Mineral wool	400°C	$5 - 0{,}4 \cdot t_{\mathrm{prot,0,i}}$ if $t_{\mathrm{prot,0,i}} < 8$ $2 - 0{,}05 \cdot t_{\mathrm{prot,0,i}}$ if $t_{\mathrm{prot,0,i}} \geq 8$
	600°C	$36 - 3{,}4 \cdot t_{\mathrm{prot,0,i}}$ if $t_{\mathrm{prot,0,i}} < 8$ $12 - 0{,}42 \cdot t_{\mathrm{prot,0,i}}$ if $t_{\mathrm{prot,0,i}} \geq 8$
	700°C	$29{,}5 - 1{,}54 \cdot t_{\mathrm{prot,0,i}}$ if $t_{\mathrm{prot,0,i}} < 12$ $16{,}5 - 0{,}47 \cdot t_{\mathrm{prot,0,i}}$ if $t_{\mathrm{prot,0,i}} \geq 12$
	800°C	$23 - 0{,}7 \cdot t_{\mathrm{prot,0,i}}$

7.2. Habito

The procedure used for obtaining the design equations for *Habito* is the same as described in chapter 7.1. The results are presented briefly in the following.

The basic insulation and protection times are shown in equations (14) and (15).

$$t_{\mathrm{ins,0,n}} = 16\ [\mathrm{min}] \quad (14)$$

$$t_{\mathrm{prot,0,i}} = 23\ [\mathrm{min}] \quad (15)$$

The simulations for obtaining position coefficient $k_{pos,exp}$ were done with configurations shown in Figure 7.2. The graphs in Figure 7.22-Figure 7.25 represent the results. The equations for the proposed curves are shown with the graphs where applicable.

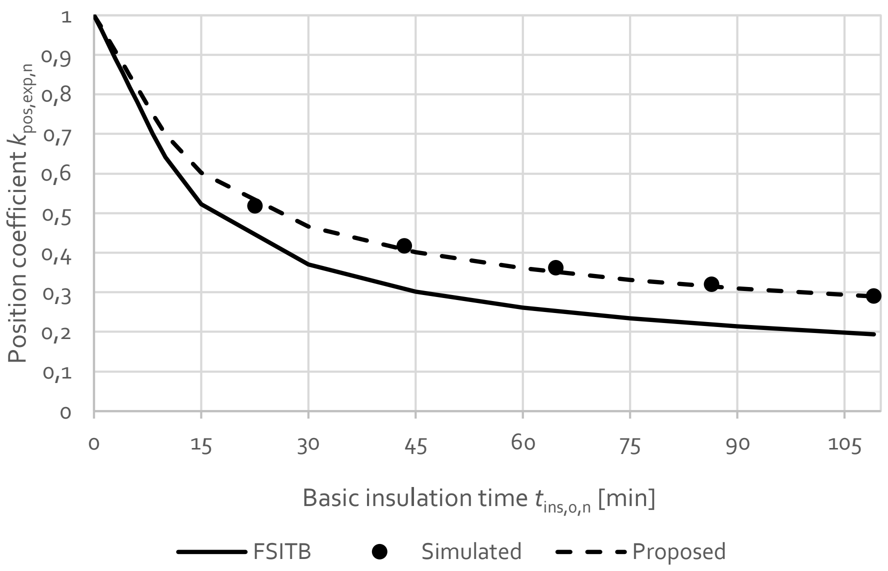

Figure 7.22 – Graphs of $k_{pos,exp,n}$ *vs.* $t_{ins,o,n}$ *with timber as the preceding layer*

Equation (16) presents the proposed formula for calculation of the position coefficient $k_{pos,exp,n}$ if *Habito* board is backed by cladding.

$$k_{\mathrm{pos,exp,n}} = \begin{cases} 1 - 0{,}5 \cdot \dfrac{\sum_{\mathrm{p}=1}^{\mathrm{n}-1} t_{\mathrm{prot,p}}}{t_{\mathrm{ins,0,n}}}, & \text{if } \displaystyle\sum_{\mathrm{p}=1}^{\mathrm{n}-1} t_{\mathrm{prot,p}} \leq \dfrac{t_{\mathrm{ins,0,n}}}{2} \\ 1{,}64 \cdot \left(\displaystyle\sum_{\mathrm{p}=1}^{\mathrm{n}-1} t_{\mathrm{prot,p}}\right)^{-0{,}37}, & \text{if } \displaystyle\sum_{\mathrm{p}=1}^{\mathrm{n}-1} t_{\mathrm{prot,p}} > \dfrac{t_{\mathrm{ins,0,n}}}{2} \end{cases} \quad (16)$$

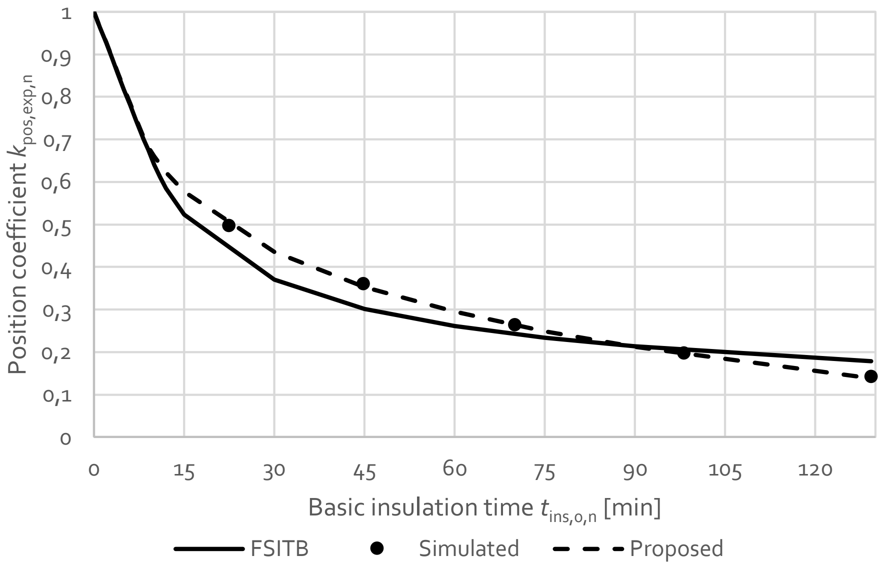

Figure 7.23 – Graphs of $k_{pos,exp,n}$ *vs.* $t_{ins,o,n}$ *with stone wool as the preceding layer*

Equation (17) presents the proposed formula for calculation of the position coefficient $k_{\text{pos,exp,n}}$ if *Habito* board is backed by stone wool.

$$k_{\text{pos,exp,n}} = \begin{cases} 1 - 0{,}59 \cdot \dfrac{\sum_{\text{p}=1}^{\text{n}-1} t_{\text{prot,p}}}{t_{\text{ins,0,n}}}, & \text{if } \sum\limits_{\text{p}=1}^{\text{n}-1} t_{\text{prot,p}} \leq \dfrac{t_{\text{ins,0,n}}}{2} \\ 1{,}13 - 0{,}204 \cdot \ln\left(\sum\limits_{\text{p}=1}^{\text{n}-1} t_{\text{prot,p}}\right), & \text{if } \sum\limits_{\text{p}=1}^{\text{n}-1} t_{\text{prot,p}} > \dfrac{t_{\text{ins,0,n}}}{2} \end{cases} \quad (17)$$

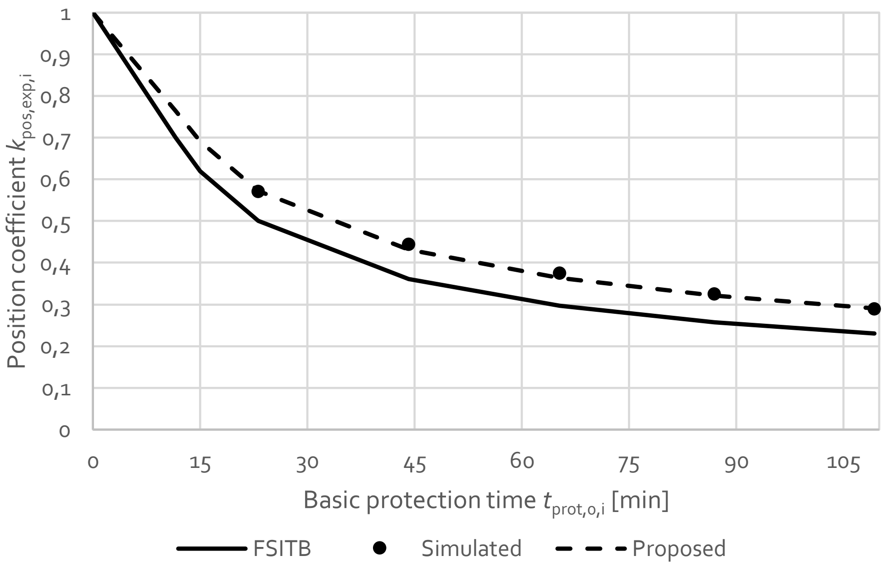

Figure 7.24 - Graphs of $k_{pos,exp,i}$ *vs.* $t_{prot,o,i}$ *with timber as the preceding layer*

Equation (18) describes the proposed correlation shown in Figure 7.24.

$$k_{\mathrm{pos,exp,i}} = \begin{cases} 1 - 0{,}47 \cdot \dfrac{\sum_{\mathrm{p}=1}^{\mathrm{n}-1} t_{\mathrm{prot,p}}}{t_{\mathrm{prot,0,i}}}, & \text{if } \sum\limits_{\mathrm{p}=1}^{\mathrm{n}-1} t_{\mathrm{prot,p}} \leq \dfrac{t_{\mathrm{prot,0,i}}}{2} \\ 2{,}25 \cdot \left(\sum\limits_{\mathrm{p}=1}^{\mathrm{n}-1} t_{\mathrm{prot,p}} \right)^{-0{,}436}, & \text{if } \sum\limits_{\mathrm{p}=1}^{\mathrm{n}-1} t_{\mathrm{prot,p}} > \dfrac{t_{\mathrm{prot,0,i}}}{2} \end{cases} \quad (18)$$

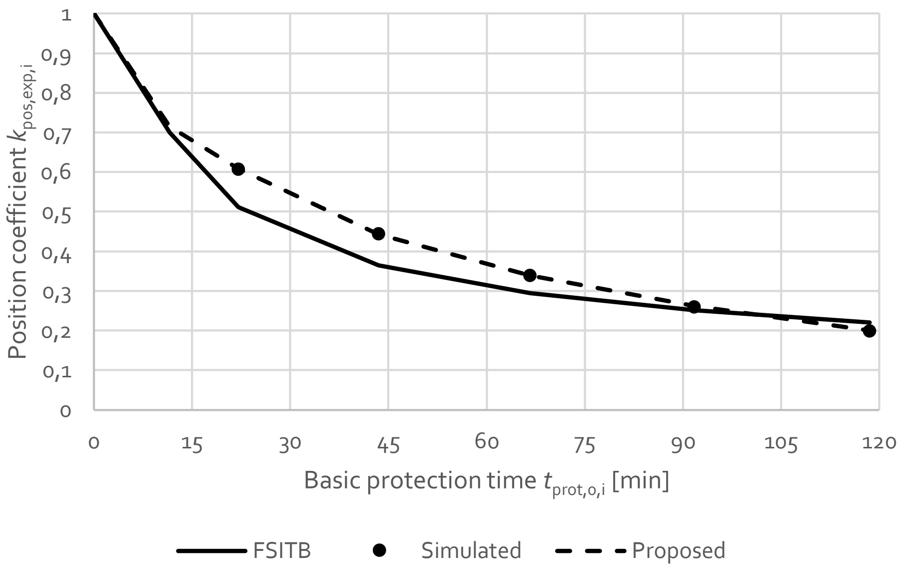

Figure 7.25 – Graphs of $k_{pos,exp,i}$ *vs.* $t_{prot,o,i}$ *with stone wool as the preceding layer*

Equation (19) describes the proposed curve shown in Figure 7.25.

$$k_{\mathrm{pos,exp,i}} = \begin{cases} 1 - 0{,}47 \cdot \dfrac{\sum_{\mathrm{p}=1}^{\mathrm{n}-1} t_{\mathrm{prot,p}}}{t_{\mathrm{prot,0,i}}}, & \text{if } \sum\limits_{\mathrm{p}=1}^{\mathrm{n}-1} t_{\mathrm{prot,p}} \leq \dfrac{t_{\mathrm{prot,0,i}}}{2} \\ 1{,}36 - 0{,}243 \cdot \ln \left(\sum\limits_{\mathrm{p}=1}^{\mathrm{n}-1} t_{\mathrm{prot,p}} \right), & \text{if } \sum\limits_{\mathrm{p}=1}^{\mathrm{n}-1} t_{\mathrm{prot,p}} > \dfrac{t_{\mathrm{prot,0,i}}}{2} \end{cases} \quad (19)$$

The position coefficient $k_{\mathrm{pos,unexp,i}}$ is presented in equation (20).

$$k_{\mathrm{pos,unexp,i}} = 1{,}32 \cdot \frac{h_{\mathrm{i}}}{t_{\mathrm{prot,0,i}}} \approx 0{,}715 \quad (20)$$

Even though *Habito* is not a type F board, it has exhibited a good ability to stay in place for longer than *Normal* the type A board used in the tests. Hence, correction times are proposed in Table 7.2. The graphic comparisons of the simulated, proposed and [6] curves are shown in Figure 7.26 to Figure 7.37.

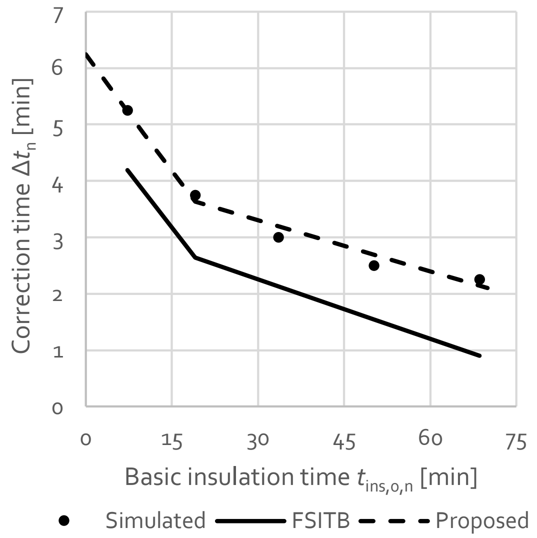

Figure 7.26 – Comparison of simulated, proposed and calculated correction times Δt_n *for timber backing when failure temperature is 400°C*

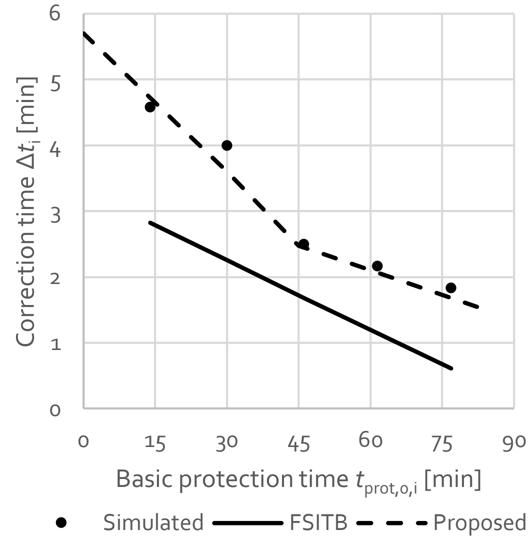

Figure 7.27 – Comparison of simulated, proposed and calculated correction times Δt_i *for timber backing when failure temperature is 400°C*

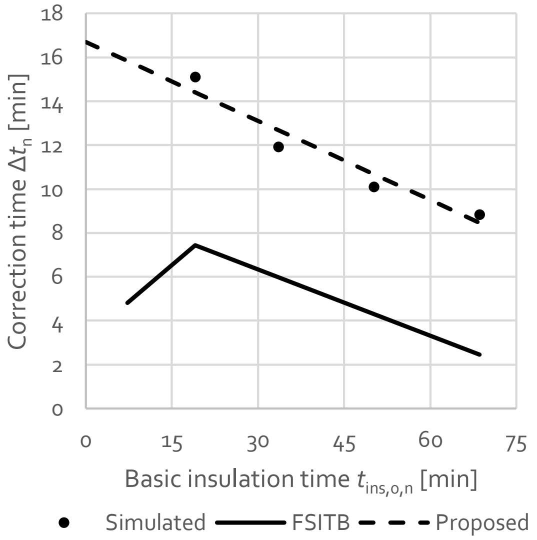

Figure 7.28 – Comparison of simulated, proposed and calculated correction times Δt_n *for timber backing when failure temperature is 600°C*

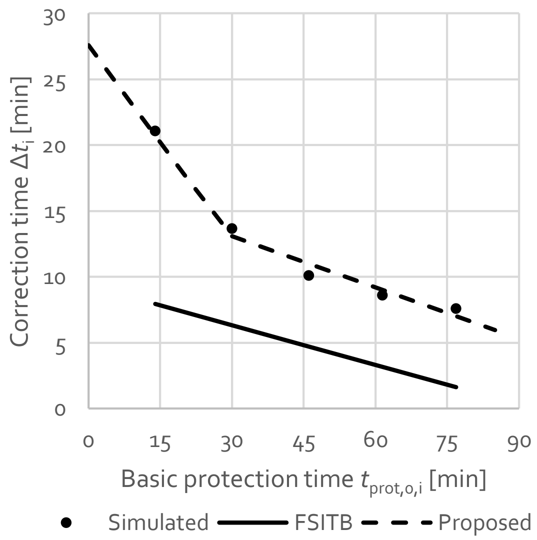

Figure 7.29 – Comparison of simulated, proposed and calculated correction times Δt_i *for timber backing when failure temperature is 600°C*

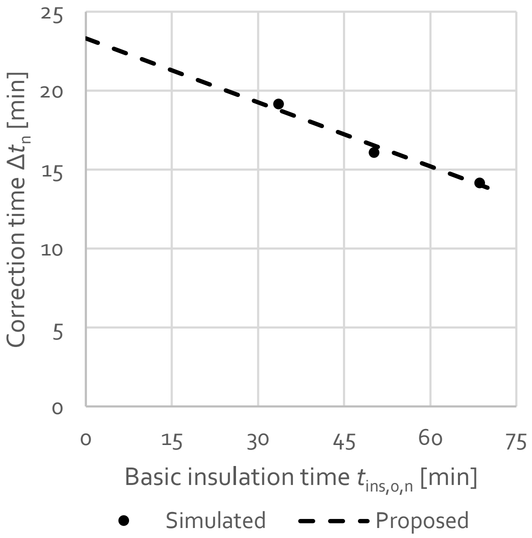

Figure 7.30 – Comparison of simulated, proposed and calculated correction times Δt*ₙ for timber backing when failure temperature is 700°C*

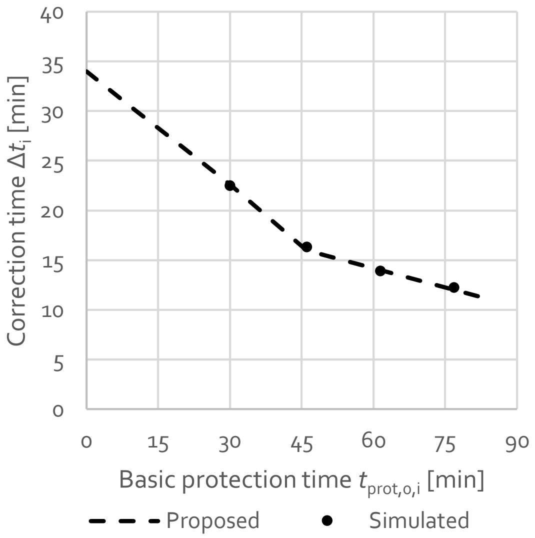

Figure 7.31 – Comparison of simulated, proposed and calculated correction times Δt_i *for timber backing when failure temperature is 700°C*

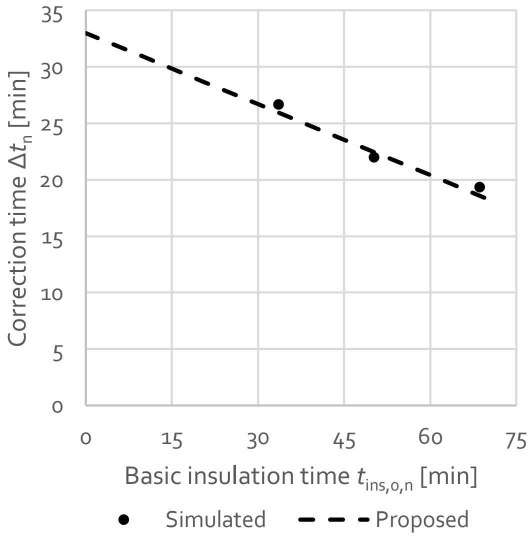

Figure 7.32 – Comparison of simulated, proposed and calculated correction times Δt_n *for timber backing when failure temperature is 800°C*

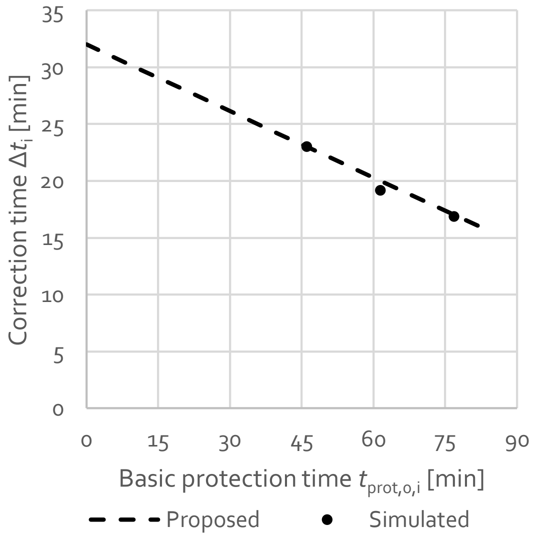

Figure 7.33 – Comparison of simulated, proposed and calculated correction times Δt_i *for timber backing when failure temperature is 800°C*

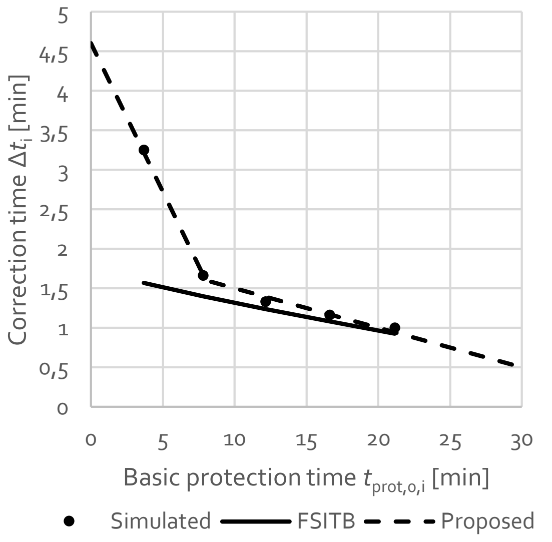

Figure 7.34 – Comparison of simulated, proposed and calculated correction times Δt*ᵢ for stone wool backing when failure temperature is 400°C*

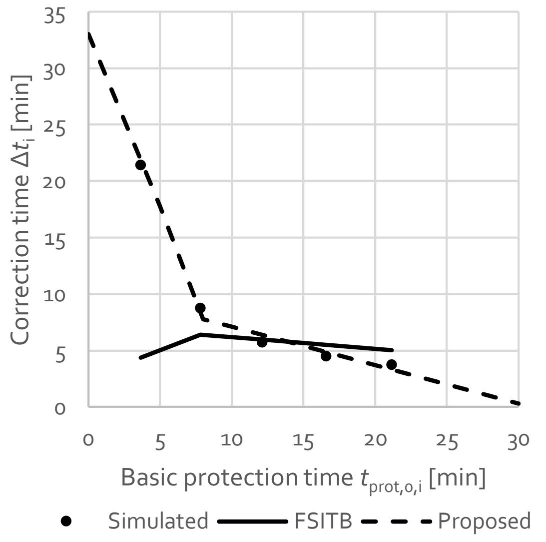

Figure 7.35 – Comparison of simulated, proposed and calculated correction times Δt*ᵢ for stone wool backing when failure temperature is 600°C*

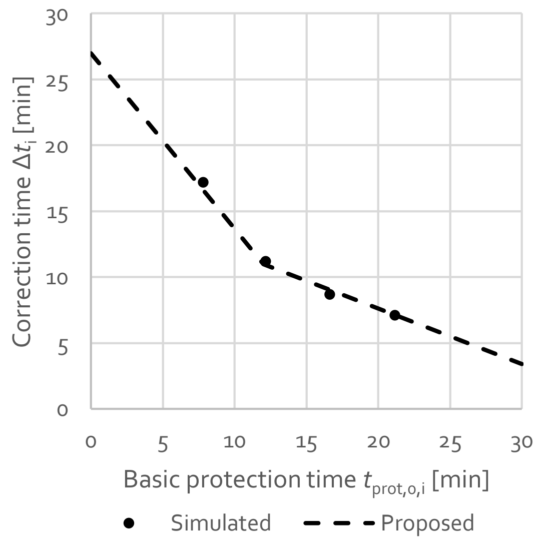

Figure 7.36 – Comparison of simulated, proposed and calculated correction times Δt_i *for stone wool backing when failure temperature is 400°C*

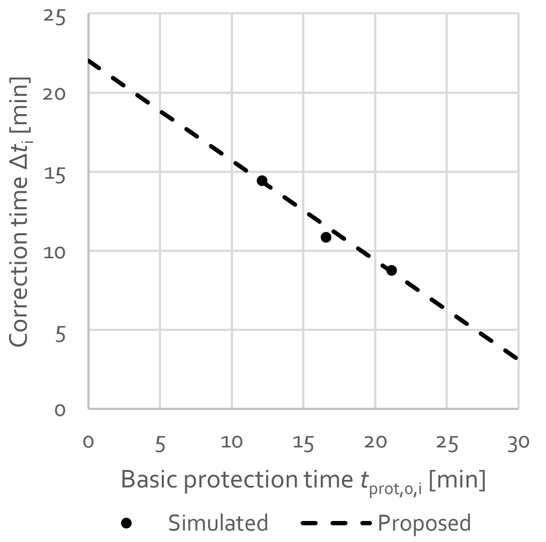

Figure 7.37 – Comparison of simulated, proposed and calculated correction times Δt_i *for stone wool backing when failure temperature is 600°C*

Table 7.2 – Formulas for correction times Δt_n *and* Δt_i

Material	**Failure temperature**	$t_{ins,n}$ **correction time** Δt_n
Cladding (timber, gypsum plasterboard)	400°C	$6{,}24 - 0{,}14 \cdot t_{\mathrm{ins,0,n}}$ if $t_{\mathrm{ins,0,n}} < 19$ $4{,}2 - 0{,}03 \cdot t_{\mathrm{ins,0,n}}$ if $t_{\mathrm{ins,0,n}} \geq 19$
	600°C	$16{,}7 - 0{,}12 \cdot t_{\mathrm{ins,0,n}}$
	700°C	$23{,}3 - 0{,}135 \cdot t_{\mathrm{ins,0,n}}$
	800°C	$33 - 0{,}21 \cdot t_{\mathrm{ins,0,n}}$
	$t_{prot,i}$ **correction time** Δt_i	
	400°C	$5{,}7 - 0{,}07 \cdot t_{\mathrm{prot,0,i}}$ if $t_{\mathrm{prot,0,i}} < 30$ $3{,}6 - 0{,}025 \cdot t_{\mathrm{prot,0,i}}$ if $t_{\mathrm{prot,0,i}} \geq 30$
	600°C	$27{,}6 - 0{,}49 \cdot t_{\mathrm{prot,0,i}}$ if $t_{\mathrm{prot,0,i}} < 30$ $17 - 0{,}13 \cdot t_{\mathrm{prot,0,i}}$ if $t_{\mathrm{prot,0,i}} \geq 30$
	700°C	$34 - 0{,}38 \cdot t_{\mathrm{prot,0,i}}$ if $t_{\mathrm{prot,0,i}} < 46$ $22 - 0{,}13 \cdot t_{\mathrm{prot,0,i}}$ if $t_{\mathrm{prot,0,i}} \geq 46$
	800°C	$32 - 0{,}195 \cdot t_{\mathrm{prot,0,i}}$
Mineral wool	400°C	$4{,}6 - 0{,}38 \cdot t_{\mathrm{prot,0,i}}$ if $t_{\mathrm{prot,0,i}} < 8$ $2 - 0{,}05 \cdot t_{\mathrm{prot,0,i}}$ if $t_{\mathrm{prot,0,i}} \geq 8$
	600°C	$33 - 3{,}04 \cdot t_{\mathrm{prot,0,i}}$ if $t_{\mathrm{prot,0,i}} < 8$ $10{,}5 - 0{,}34 \cdot t_{\mathrm{prot,0,i}}$ if $t_{\mathrm{prot,0,i}} \geq 8$
	700°C	$27 - 1{,}33 \cdot t_{\mathrm{prot,0,i}}$ if $t_{\mathrm{prot,0,i}} < 12$ $16 - 0{,}42 \cdot t_{\mathrm{prot,0,i}}$ if $t_{\mathrm{prot,0,i}} \geq 12$
	800°C	$22 - 0{,}63 \cdot t_{\mathrm{prot,0,i}}$

7.3. Verification by full scale test (calculation example)

In this chapter the equations developed in chapters 7.1 and 7.2 are used to calculate the fire resistance of structures and the results compared with the data from some full scale tests. For other materials the formulas used are from the European technical guideline Fire Safety in Timber Buildings [6].

***Protect F* test 1**

The first test with *Protect F* was conducted in The Building Test Centre in the UK on February 6th 1995 [26]. It was a vertical structure with timber studs (45x100 mm), covered on both sides by one layer of *Protect F*. The cavities were completely filled with glass wool (ρ=18.75 kg/m³). The test duration was 93 minutes and the average temperature rise on the unexposed side was 415°C.

Two heat transfer paths are possible in this structure – through insulation or through the timber members. In the following a comparison is made for the path through insulation as there was not adequate thermocouple data for the other path.

<u>Calculated fire resistance</u>

Layer 1 – gypsum plasterboard *Protect F* (15.4 mm)

$$t_{\mathrm{prot,0,1}} = 31\ \mathrm{min}$$

$$k_{\mathrm{pos,exp,1}} = 1{,}0$$

$$k_{\mathrm{pos,unexp,1}} = 0{,}609$$

$$k_{j,1} = 1{,}0$$

$$t_{\mathrm{prot,1}} = \left(t_{\mathrm{prot,0,1}} \cdot k_{\mathrm{pos,exp,1}} \cdot k_{\mathrm{pos,unexp,1}} + \Delta t_1\right) \cdot k_{\mathrm{j,1}} = (31 \cdot 1{,}0 \cdot 0{,}609 + 0) \cdot 1{,}0 = 18{,}9\ \mathrm{min}$$

Layer 2 – glass wool insulation (100 mm, ρ=18.75 kg/m³)

$$t_{\mathrm{prot,0,2}} = (0{,}0007 \cdot \rho_2 + 0{,}046) \cdot h_2 + 13 = 18{,}9\ \mathrm{min} < 30$$

$$k_{\mathrm{pos,exp,2}} = (0{,}001 \cdot \rho_2 + 0{,}27) \cdot \left(\frac{t_{\mathrm{prot,0,2}}}{\sum t_{\mathrm{prot,i-1}}}\right)^{0{,}75-0{,}002\cdot\rho_2} = 0{,}29$$

$k_{\mathrm{pos,unexp},2} = 1{,}0$

$\Delta t_2 = 16{,}5 - 0{,}47 \cdot t_{\mathrm{prot},0,2} = 7{,}6\ \mathrm{min}$ (assuming fall-off at 700°C)

$k_{j,2} = 1{,}0$

$$t_{\mathrm{prot},2} = \left(t_{\mathrm{prot},0,2} \cdot k_{\mathrm{pos,exp},2} \cdot k_{\mathrm{pos,unexp},2} + \Delta t_2\right) \cdot k_{\mathrm{j},1} = (18{,}9 \cdot 0{,}29 \cdot 1 + 7{,}6) \cdot 1{,}0$$
$$= 13{,}1\ \mathrm{min}$$

Layer 3 (last layer) - gypsum plasterboard *Protect F* (15.4 mm)

$t_{\mathrm{ins},0,3} = 20\ \mathrm{min}$

$$k_{\mathrm{pos,exp},3} = 1{,}7 \cdot \left(\sum_{\mathrm{p}=1}^{\mathrm{p}=\mathrm{n}-1} t_{\mathrm{prot,p}}\right)^{-0{,}35} = 0{,}51$$

$k_{j,3} = 1{,}0$

$$t_{\mathrm{ins},3} = \left(t_{\mathrm{ins},0,3} \cdot k_{\mathrm{pos,exp},3} + \Delta t_3\right) \cdot k_{\mathrm{j},3} = (20 \cdot 0{,}51 + 0) \cdot 1{,}0 = 10{,}1\ \mathrm{min}$$

Total fire resistance of the structure:

$$t_{\mathrm{ins}} = \sum_{\mathrm{i}=1}^{\mathrm{i}=\mathrm{n}-1} t_{\mathrm{prot,i}} + t_{\mathrm{ins,n}} = 18{,}9 + 13{,}1 + 10{,}1 = 42{,}1\ \mathrm{min}$$

Comparison of calculated fire resistance and test results is presented in Table 7.3.

Table 7.3 – Results of calculated and tested fire resistances of [26]

Layer no	Material	t_{ins} [min]	
		Calculated	Tested
1	*Protect F*	18,9	25
2	Glass wool	32,0	73
3	*Protect F*	42,1	83

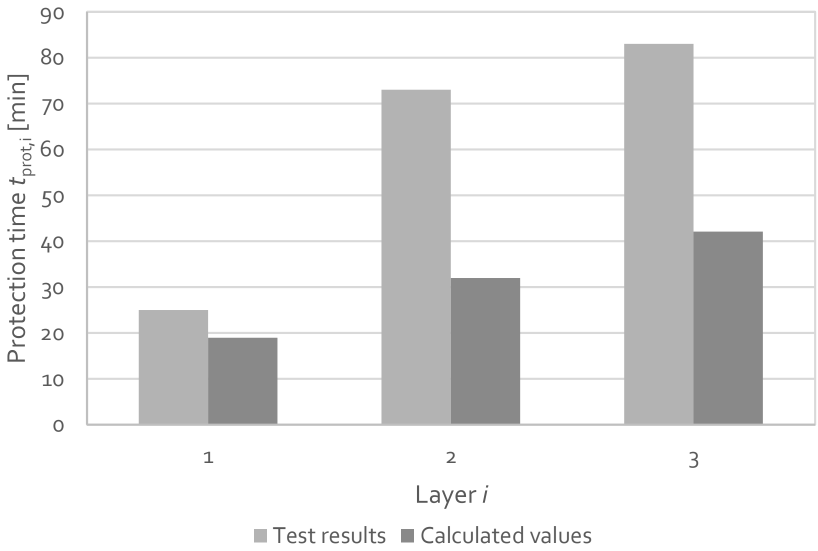

Figure 7.38 – Comparison of protection times from fire tests and calculations

***Protect F* test 2**

The second test [27] was conducted with a vertical structure comprising of steel studs (150 mm) and protected on both sides by two layers of *Protect F* boards (2x15,4 mm). The cavities were filled with glass wool batts (1x100 mm, ρ=15.76 kg/m^3 and 1x50 mm, ρ=20.56 kg/m^3). The test was terminated at 156 minutes. Insulation requirement failure happened at 147 minutes. The heat transfer path chosen for calculation is through insulation.

<u>Calculated fire resistance</u>

Layer 1 – gypsum plasterboard *Protect F* (15.4 mm)

$t_{\text{prot,0,1}} = 31 \text{ min}$

$k_{\text{pos,exp,1}} = 1{,}0$

$k_{\text{pos,unexp,1}} = 1{,}0$

$k_{j,1} = 1{,}0$

$$t_{\text{prot,1}} = \left(t_{\text{prot,0,1}} \cdot k_{\text{pos,exp,1}} \cdot k_{\text{pos,unexp,1}} + \Delta t_1\right) \cdot k_{\text{j,1}} = (31 \cdot 1{,}0 \cdot 1{,}0 + 0) \cdot 1{,}0$$
$$= 31{,}0 \text{ min}$$

Layer 2 - gypsum plasterboard *Protect F* (15.4 mm)

$t_{\text{prot,0,2}} = 31 \text{ min}$

$k_{\text{pos,exp,2}} = 0{,}5 \cdot \sqrt{\frac{t_{\text{prot,0,2}}}{\sum t_{\text{prot,i-1}}}} = 0{,}5$

$k_{\text{pos,unexp,2}} = 0{,}609$

$\Delta t_2 = 33 - 0{,}2 \cdot t_{\text{prot,0,2}} = 26{,}8 \text{ min}$ (assuming fall-off at 800°C)

$k_{j,2} = 1{,}0$

$$t_{\text{prot,2}} = \left(t_{\text{prot,0,2}} \cdot k_{\text{pos,exp,2}} \cdot k_{\text{pos,unexp,2}} + \Delta t_2\right) \cdot k_{\text{j,3}} = (31 \cdot 0{,}5 \cdot 0{,}609 + 26{,}8) \cdot 1{,}0 = 36{,}2 \text{ min}$$

Layer 3 – glass wool (100 mm, ρ=15.76 kg/m³)

$t_{\text{prot,0,3}} = (0{,}0007 \cdot \rho_3 + 0{,}046) \cdot h_3 + 13 = 18{,}7 \text{ min}$

$$k_{\text{pos,exp,3}} = (0{,}001 \cdot \rho_3 + 0{,}27) \cdot \left(\frac{t_{\text{prot,0,3}}}{\sum t_{\text{prot,i-1}}}\right)^{0{,}75-0{,}002 \cdot \rho_3} = 0{,}11$$

$$k_{\text{pos,unexp,3}} = 0{,}01 \cdot h_3 - \frac{h_3^2}{30000} + \rho_3^{0{,}09} - 1{,}3 = 0{,}65$$

$\Delta t_3 = 23 - 0{,}7 \cdot t_{\text{prot,0,3}} = 9{,}9 \text{ min}$ (assuming fall-off at 800°C)

$k_{j,3} = 1{,}0$

$$t_{\text{prot,3}} = \left(t_{\text{prot,0,3}} \cdot k_{\text{pos,exp,3}} \cdot k_{\text{pos,unexp,3}} + \Delta t_3\right) \cdot k_{\text{j,3}} = (18{,}7 \cdot 0{,}11 \cdot 0{,}65 + 9{,}9) \cdot 1{,}0 = 11{,}3 \text{ min}$$

Layer 4 – glass wool (50 mm, ρ=20.56 kg/m³)

$t_{\text{prot,0,4}} = (0{,}0007 \cdot \rho_4 + 0{,}046) \cdot h_4 + 13 = 16{,}0 \text{ min}$

$$k_{\text{pos,exp,4}} = (0{,}001 \cdot \rho_4 + 0{,}27) \cdot \left(\frac{t_{\text{prot,0,4}}}{\sum t_{\text{prot,i-1}}}\right)^{0{,}75-0{,}002 \cdot \rho_4} = 0{,}09$$

$k_{\text{pos,unexp,4}} = 1{,}0$

$k_{j,4} = 1{,}0$

$$t_{\mathrm{prot},4} = \left(t_{\mathrm{prot},0,4} \cdot k_{\mathrm{pos,exp},4} \cdot k_{\mathrm{pos,unexp},4} + \Delta t_4\right) \cdot k_{\mathrm{j},4} = (16{,}0 \cdot 0{,}09 \cdot 1{,}0 + 0) \cdot 1{,}0$$
$$= 1{,}5 \text{ min}$$

Layer 5 - gypsum plasterboard *Protect F* (15.4 mm)

$$t_{\mathrm{prot},0,5} = 31 \text{ min}$$

$$k_{\mathrm{pos,exp},5} = 0{,}5 \cdot \sqrt{\frac{t_{\mathrm{prot},0,5}}{\sum t_{\mathrm{prot,i-1}}}} = 0{,}31$$

$$k_{\mathrm{pos,unexp},5} = 1{,}0$$

$$k_{j,5} = 1{,}0$$

$$t_{\mathrm{prot},5} = \left(t_{\mathrm{prot},0,5} \cdot k_{\mathrm{pos,exp},5} \cdot k_{\mathrm{pos,unexp},5} + \Delta t_5\right) \cdot k_{\mathrm{j},5} = (31 \cdot 0{,}31 \cdot 1{,}0 + 0) \cdot 1{,}0$$
$$= 9{,}6 \text{ min}$$

Layer 6 (last layer) - gypsum plasterboard *Protect F* (15.4 mm)

$$t_{\mathrm{ins},0,6} = 20 \text{ min}$$

$$k_{\mathrm{pos,exp},6} = 1{,}7 \cdot \left(\sum_{\mathrm{p=1}}^{\mathrm{p=n-1}} t_{\mathrm{prot,p}}\right)^{-0{,}35} = 0{,}35$$

$\Delta t_6 = 18 - 0{,}13 \cdot t_{\mathrm{ins},0,6} = 15{,}4 \text{ min}$ (assuming fall-off at 600°C)

$$k_{j,6} = 1{,}0$$

$$t_{\mathrm{ins},6} = \left(t_{\mathrm{ins},0,6} \cdot k_{\mathrm{pos,exp},6} + \Delta t_6\right) \cdot k_{\mathrm{j},6} = (20 \cdot 0{,}35 + 15{,}4) \cdot 1{,}0 = 22{,}4 \text{ min}$$

Total fire resistance of the structure:

$$t_{\mathrm{ins}} = \sum_{\mathrm{i=1}}^{\mathrm{i=n-1}} t_{\mathrm{prot,i}} + t_{\mathrm{ins,n}} = 31{,}0 + 36{,}2 + 11{,}3 + 1{,}5 + 9{,}6 + 22{,}6 = 112{,}1 \text{ min}$$

Table 7.4 – Results of calculated and tested fire resistances of [27]

Layer no	Material	t_{ins} [min]	
		Calculated	Tested
1	*Protect F*	31,0	32
2	*Protect F*	67,2	68
3	Glass wool	78,5	
4	Glass wool	80,0	111
5	*Protect F*	89,7	
6	*Protect F*	112,1	147

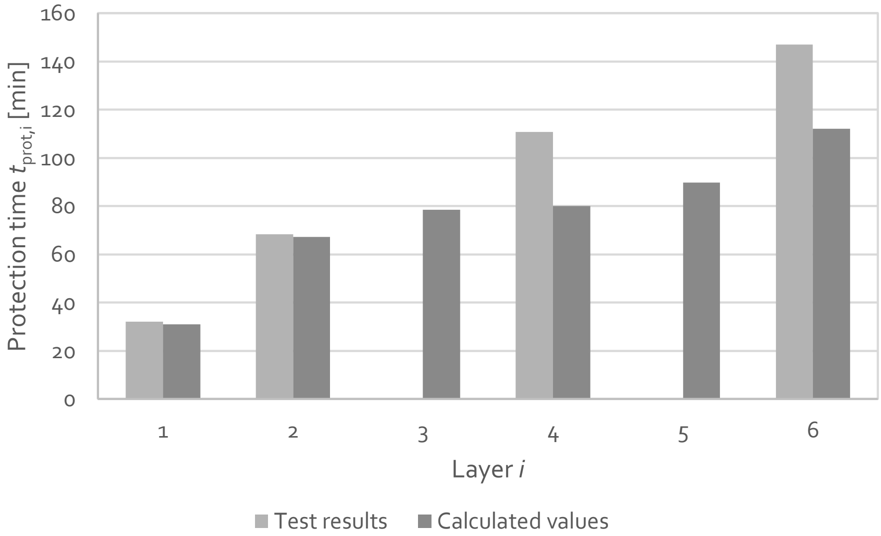

Figure 7.39 – Comparison of protection times from fire tests and calculations

Two test reports were available for *Habito* as well. Both were wall (vertical) structure tests with void cavities and on metal studs.

***Habito* test 1**

The first test [28] with *Habito* had 45 mm voids protected on both sides by one layer of *Habito* board. Test duration was 60 minutes. Insulation requirement failure occurred at 57 minutes.

<u>Calculated fire resistance</u>

Layer 1 – gypsum plasterboard *Habito* (12.5 mm)

$t_{\text{prot,0,1}} = 23 \text{ min}$

$k_{\mathrm{pos,exp,1}} = 1{,}0$

$k_{\mathrm{pos,unexp,1}} = 1{,}0$

$k_{j,1} = 1{,}0$

$$t_{\mathrm{prot,1}} = \left(t_{\mathrm{prot,0,1}} \cdot k_{\mathrm{pos,exp,1}} \cdot k_{\mathrm{pos,unexp,1}} + \Delta t_1\right) \cdot k_{\mathrm{j,1}} = (23 \cdot 1{,}0 \cdot 1{,}0 + 0) \cdot 1{,}0$$
$$= 23{,}0 \text{ min}$$

Layer 2 - gypsum plasterboard *Habito* (12.5 mm)

$t_{\mathrm{ins,0,2}} = 16 \text{ min}$

$$k_{\mathrm{pos,exp,2}} = 1{,}6 \cdot 1{,}64 \cdot \left(\sum_{\mathrm{p=1}}^{\mathrm{p=i-1}} t_{\mathrm{prot,p}}\right)^{-0{,}37} = 0{,}82$$

$k_{j,2} = 1{,}0$

$$t_{\mathrm{ins,2}} = \left(t_{\mathrm{ins,0,2}} \cdot k_{\mathrm{pos,exp,2}} + \Delta t_2\right) \cdot k_{\mathrm{j,2}} = (16 \cdot 0{,}82 + 0) \cdot 1{,}0 = 13{,}2 \text{ min}$$

Total fire resistance of the structure:

$$t_{\mathrm{ins}} = \sum_{\mathrm{i=1}}^{\mathrm{i=n-1}} t_{\mathrm{prot,i}} + t_{\mathrm{ins,n}} = 23{,}0 + 13{,}2 = 36{,}2 \text{ min}$$

Table 7.5 – Results of calculated and tested fire resistances of [28]

Layer no	Material	t_{ins} [min]	
		Calculated	Tested
1	*Habito*	23,0	19
2	*Habito*	36,2	57

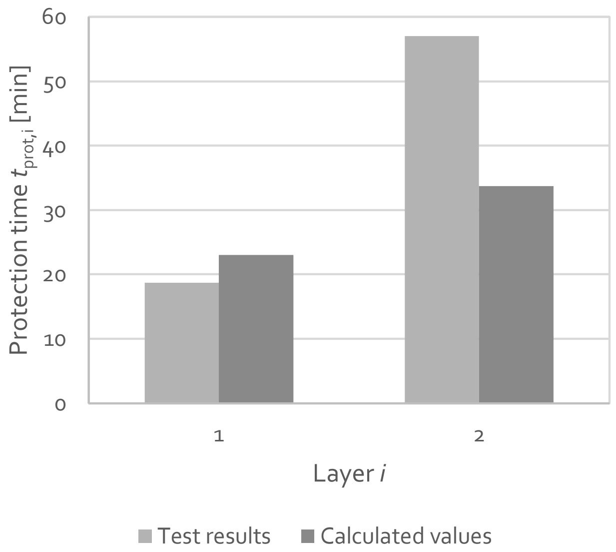

Figure 7.40 – Comparison of protection times from fire tests and calculations

***Protect F* test 1**

The second test with *Habito* [29] had a similar configuration but on the outer surfaces of the *Habito* boards were *Normal* boards with the thickness of 12.5 mm on both sides. The duration of the test was 91 minutes and the maximum temperature on the unexposed side was slightly less than 100°C. The insulation time is therefore even longer.

<u>Calculated fire resistance</u>

Layer 1 – gypsum plasterboard *Normal* (12.5 mm)

$t_{\mathrm{prot,0,1}} = 24{,}1\ \mathrm{min}$

$k_{\mathrm{pos,exp,1}} = 1{,}0$

$k_{\mathrm{pos,unexp,1}} = 1{,}0$

$k_{j,1} = 1{,}0$

$$t_{\mathrm{prot,1}} = \left(t_{\mathrm{prot,0,1}} \cdot k_{\mathrm{pos,exp,1}} \cdot k_{\mathrm{pos,unexp,1}} + \Delta t_1\right) \cdot k_{\mathrm{j,1}} = (23 \cdot 1{,}0 \cdot 1{,}0 + 0) \cdot 1{,}0$$
$$= 24{,}1\ \mathrm{min}$$

Layer 2 – gypsum plasterboard *Habito* (12.5 mm)

$t_{\mathrm{prot,0,2}} = 23\ \mathrm{min}$

$$k_{\mathrm{pos,exp,2}} = 2{,}25 \cdot \left(\sum_{\mathrm{p=1}}^{\mathrm{p=i-1}} t_{\mathrm{prot,p}} \right)^{-0{,}436} = 0{,}56$$

$$k_{\mathrm{pos,unexp,2}} = 1{,}0$$

$$k_{j,2} = 1{,}0$$

$$t_{\mathrm{prot,2}} = \left(t_{\mathrm{prot,0,2}} \cdot k_{\mathrm{pos,exp,2}} \cdot k_{\mathrm{pos,unexp,2}} + \Delta t_2\right) \cdot k_{\mathrm{j,2}} = (23 \cdot 0{,}56 \cdot 1{,}0 + 0) \cdot 1{,}0$$
$$= 12{,}9 \text{ min}$$

Layer 3 – gypsum plasterboard *Habito* (12.5 mm)

$$t_{\mathrm{prot,0,3}} = 23 \text{ min}$$

$$k_{\mathrm{pos,exp,3}} = 1{,}6 \cdot 2{,}25 \cdot \left(\sum_{\mathrm{p=1}}^{\mathrm{p=i-1}} t_{\mathrm{prot,p}} \right)^{-0{,}436} = 0{,}75$$

$$k_{\mathrm{pos,unexp,3}} = 1{,}0$$

$$k_{j,2} = 1{,}0$$

$$t_{\mathrm{prot,3}} = \left(t_{\mathrm{prot,0,3}} \cdot k_{\mathrm{pos,exp,3}} \cdot k_{\mathrm{pos,unexp,3}} + \Delta t_3\right) \cdot k_{\mathrm{j,3}} = (23 \cdot 0{,}75 \cdot 1{,}0 + 0) \cdot 1{,}0$$
$$= 17{,}1 \text{ min}$$

Layer 4 (last layer) – gypsum plasterboard *Normal* (12.5 mm)

$$t_{\mathrm{ins,0,4}} = 12{,}1 \text{ min}$$

$$k_{\mathrm{pos,exp,4}} = 0{,}5 \cdot \sqrt{\frac{t_{\mathrm{prot,0,4}}}{\sum t_{\mathrm{prot,i-1}}}} = 0{,}29$$

$$k_{j,4} = 1{,}0$$

$$t_{\mathrm{ins,4}} = \left(t_{\mathrm{ins,0,4}} \cdot k_{\mathrm{pos,exp,4}} + \Delta t_4\right) \cdot k_{\mathrm{j,4}} = (12{,}1 \cdot 0{,}29 + 0) \cdot 1{,}0 = 5{,}4 \text{ min}$$

Total fire resistance of the structure:

$$t_{\mathrm{ins}} = \sum_{\mathrm{i=1}}^{\mathrm{i=n-1}} t_{\mathrm{prot,i}} + t_{\mathrm{ins,n}} = 24{,}1 + 12{,}9 + 17{,}1 + 5{,}4 = 59{,}6 \text{ min}$$

Table 7.6 – Results of calculated and tested fire resistances of [29]

Layer no	Material	t_{ins} [min]	
		Calculated	Tested
1	*Normal*	24,1	21
2	*Habito*	37,0	39
3	*Habito*	34,1	79
4	*Normal*	59,6	>91

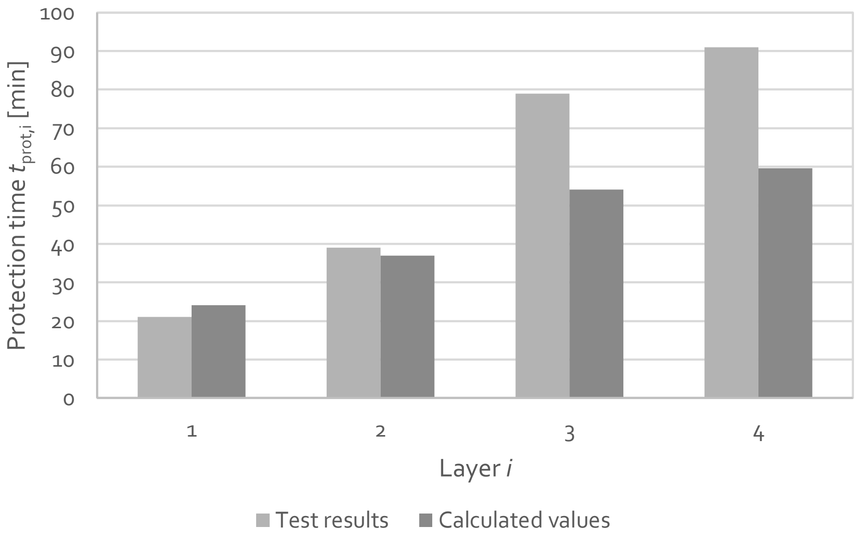

Figure 7.41 – Comparison of protection times from fire tests and calculations

The equations provided safe results in all the checked cases.

8. Conclusions

As gypsum plays an important role in the fire protection of timber structures, new information on the topic is always much needed. In the making of this thesis, the knowledge in the field has been increased with design equations for two commercially available gypsum plasterboard products – Gyproc Protect F and Gyproc Habito.

Another important outcome is the development of the calibration procedure of input parameters for thermal simulations. This is an area of study that should be popularised even further.

It can be seen from the results of this thesis that fairly accurate thermal simulations are possible. Computer simulations seems to be an underutilised tool, even though they are a less expensive and much more versatile calculation method. The reliability of the simulation results depends heavily on the applicability of the thermal parameters. As described at length in the previous chapters, it is not only a matter of finding these parameters experimentally, but also their suitability for the restrictions of the software currently available to the user. Determining the thermal parameters was one of the great challenges in this work.

The development of the design equations is based on the fundamental work from the PhD thesis of Vanessa Schleifer who specified the system of methodical computer simulations. The same configurations were simulated in this thesis. The obtained equations yielded safe results when compared to suitable full scale tests.

9. Resümee

Puit on inimkonna ajaloo jooksul ilmselt kõige rohkem kasutust leidnud ehitusmaterjal. Viimastel aastatel on puitu hakatud taasavastama. Üks suurimaid väljakutseid puitmajade ehitamisel on tulepüsivusnõuete täitmine, milleks tänapäeval on mitmeid võimalusi alates puidu impregneerimisest ja mittepõlevate materjalidega katmisest kuni sprinkleriteni. Levinuim kaitse on puitkonstruktsioonide eraldamine võimalikest tulekolletest kaitsvate materjalikihtidega.

Euroopas kehtivad standardid lubavad kasutada nii katseid kui heakskiidetud arvutusmeetodeid puitkonstruktsioonide tulepüsivuse projekteerimisel. Tulekatsed on aga kallid ja töömahukad, mistõttu tuleks arendada teoreetilisi meetodeid. Üks sobiv alternatiiv tulekatsetele on termiliste simulatsioonide kasutamine, mille lähteandmeteks on materjalide termilised omadused. Käesolevas töös on esitatud nende omaduste leidmise meetod.

Euroopa tehniline juhend *Fire Safety in Timber Buildings* kirjeldab täiustatud komponentide liitmise meetodit, mis põhineb Vanessa Schleiferi doktoritööl. Tegemist on Euroopa standardis EN 1995-1-2 kirjeldatud meetodi täiendusega, mis võimaldab arvutada laiema valiku konstruktsioonide tulepüsivust. Hetkel on käsiraamatus esitatud üldised valemid materjalitüüpidele.

Käesolev töö käsitleb kahte konkreetset kipsplaati, Gyproc Protect F ja Gyproc Habito, mis on mõlemad Saint-Gobain Gyproc'i tooted. Gyproc Protect F on standardi EN 520 järgne F-tüüpi kipsplaat paksusega 15,4 mm. Seda kasutatakse kõrgete tulepüsivusnõuetega hoonete karkasside jäigastava elemendina. Habito on eriti tugeva koostisega kartongkattega kipsplaat paksusega 12,5 mm, mida kasutatakse suurt kulumis- ja löögikindlust nõudvates konstruktsioonides näiteks vineeri või OSB-plaadi asemel.

Perioodil detsember 2015 kuni aprill 2016 teostati Rootsis SP tehniliste uuringute instituudis neli tulekatset. Samu katsekehasid simuleeriti programmiga SAFIR. Kuna esialgsed tulemused ei olnud rahuldavad, ilmnes vajadus kohandada termilisi omadusi.

Termiliste omaduste leidmiseks iteratiivse lähenemise meetodil, koostas autor vastava koodi programmiga MATLAB. Iga tsükli käigus muudeti ühte väärtust ja kontrolliti seeläbi saadud simuleeritud temperatuuri tõusu kõverat tulekatse tulemustega. Termilised omadused, mille tulemusel saadud simuleeritud graafikud kattusid reaalsete katsetulemustega, võib lugeda efektiivseteks. Leitud termiliste omaduste efektiivväärtused olid sisendiks valemite tuletamisele. Valemitega saadud tulepüsivusaegu võrreldi täismõõdus tulekatsete tulemustega, mis kinnitasid arvutuste turvalisust.

Kalibreerimise meetodit kontrolliti vabalt valitud teist tüüpi materjalil, milleks oli tselluloosil põhinev isolatsioonimaterjal. Tulemust võib pidada edukaks, arvestades, et arvutisimulatsioonid ei suuda kirjeldada mittehomogeensete materjalide käitumist tuleolukorras.

Töö tulemuseks on kahe uue materjali lisamine puitkonstruktsioonide tulepüsivuse täiustatud komponentide liitmise meetodisse. Autor loodab, et töö aitab ka tulevikus kaasa uute materjalide lisamisele ning seeläbi suurendab teadmisi puitkonstruktsioonide tulepüsivuse projekteerimisest.

10. References

[1] B. Östman and D. Rydholm, "National fire regulations in relation to the use of wood in European and some other countries," Trätek, Stockholm, Sweden, 2002.

[2] *Eurocode 5: Design of timber structures - Part 1-2: General - Structural fire design*, CEN, 2004.

[3] A. D. Ariyanayagam and M. Mahendran, "Development of realistic design fire time-temperature curves for the testing of cold-formed steel wall systems," *Frontiers of Structural and Civil Engineering*, vol. 8, no. 4, pp. 427-447, 2014.

[4] *Eurocode 1: Actions on structures - Part 1-2: General actions - Actions on structures exposed to fire*, CEN, 2002.

[5] V. Schleifer, *Zum Verhalten von raumabschliessenden mehrschichtigen Holzbauteilen im Brandfall*, Zürich, Switzerland, 2009.

[6] Östman B. et al, Fire safety in timber buildings. Technical guideline for Europe, Stockholm, Sweden: SP Technical Research Institute of Sweden, 2010.

[7] "Using gypsum board for walls and ceilings Section I - Gypsum Association," [Online]. Available: https://www.gypsum.org/technical/using-gypsum-board-for-walls-and-ceilings/using-gypsum-board-for-walls-and-ceilings-section-i/. [Accessed 10 May 2016].

[8] "How drywall is made," [Online]. Available: http://www.madehow.com/Volume-2/Drywall.html. [Accessed 10 May 2016].

[9] *EN 520 Gypsum plasterboards - Definitions, requirements and test methods*, CEN, 2005.

[10] D. Kontogeorgos and M. Founti, "Gypsum board reaction kinetics at elevated temperatures," *Thermochimica Acta*, vol. 529, pp. 6-13, 2012.

[11] G. Thomas, "Thermal properties of gypsum plasterboard at high temperatures," *Fire and materials*, vol. 26, no. 1, pp. 37-45, 2002.

[12] "Plaadid / Tooted / Gyproc ee," [Online]. Available: http://www.gyproc.ee/tooted/43/plaadid. [Accessed 9 May 2016].

[13] K. G. Wakili, "Four types of gypsum plaster boards and their thermophysical properties under fire condition," *Journal of Fire Sciences*, vol. 27, pp. 27-43, 2009.

[14] N. Benichou, M. A. Sultan, C. MacCallum and J. Hum, "Thermal properties of wood, gypsum and insulation at elevated temperatures," National Research Council Canada, 2001.

[15] G. K. Semitelos, I. D. Mandilaras, D. A. Kontogeorgos and M. A. Founti, "Simplified correlations of gypsum board thermal properties for simulation tools," *Fire and materials*, vol. 40, no. 2, pp. 229-245, 2014.

[16] D. Lazaro, E. Puente, M. Lazaro, P. G. Lazaro and J. Pena, "Thermal modelling of gypsum plasterboard assemblies exposed to standard fire tests," *Fire and materials*, vol. 40, no. 4, pp. 568-585, 2015.

[17] SP Technical Research Institute of Sweden, "SP Report no 5P08165. Model scale fire test of 4 gypsum plasterboards of Gyproc," 2015.

[18] SP Technical Research Institute of Sweden, "SP Report no 5P08165-03. Model scale fire tests of 4 gypsum plasterboards of Gyproc and stone wool," 2016.

[19] SP Technical Research Institute of Sweden, "SP Report no 5P08165-04. Model scale fire tests of 2 gypsum plasterboards of Gyproc," 2016.

[20] *ISO 834-1:1999 Fire-resistance tests - Elements of building construction - Part 1: General requirements*, International Organization for Standardisation, 1999.

[21] "Sciences Appliquées- SAFIR," [Online]. Available: http://www.facsa.ulg.ac.be/cms/c_1584029/en/safir. [Accessed 13 April 2016].

[22] J. M. Franssen, *User's manual for SAFIR 2013b2*, Liège, Belgium: University of Liège Department ArGEnCO Service Structural Engineering, 2012.

[23] *SAFIR Technical documentation*, 2011.

[24] A. Just and M. Tiso, "Behaviour of insulation materials in timber frame assemblies exposed to fire," in *WCTE*, 2016.

[25] A. Just, Structural fire design of timber frame assemblies insulated by glass wool and covered by gypsum plasterboards, Tallinn, Estonia: TUT Press, 2010.

[26] The Building Test Centre, "Report Number BTC 5400F," 1995.

[27] The Building Test Centre, "Report number BTC 11977F," 2002.

[28] SP Technical Research Institute of Sweden, "SP Report number 4P07239," 2014.

[29] SP Technical Research Institute of Sweden, "SP Report number 4P08585," 2015.

Appendix A

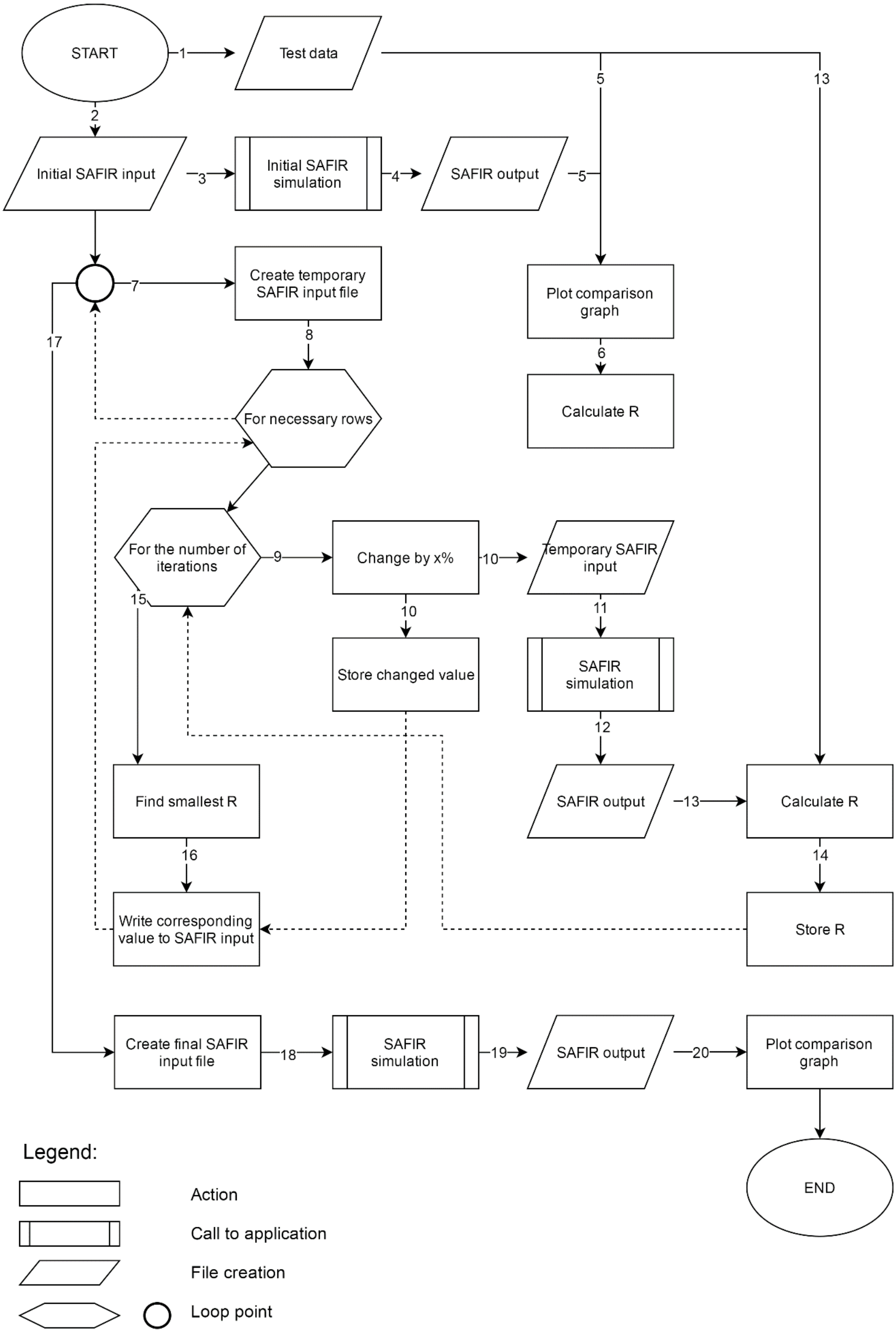

R is the residual sum of squares